MODIFICATION OF STYRENE-METHYL METH ACRYLATE COPOLYMER IN THE PRESENCE OF PRISTINE AND MODIFIED GRAPHENE BY USING MICROWAVE IRRADIATION

BY

Mukarram Zubair

A Thesis Presented to the
DEANSHIP OF GRADUATE STUDIES

KING FAHD UNIVERSITY OF PETROLEUM & MINERALS

DHAHRAN, SAUDI ARABIA

In Partial Fulfillment of the
Requirements for the Degree of

MASTER OF SCIENCE

In

CHEMICAL ENGINEERING

December, 2013

KING FAHD UNIVERSITY OF PETROLEUM AND MINERALS

DHAHRAN 31261, SAUDI ARABIA

DEANSHIP OF GRADUATE STUDIES

This thesis, written by Mukarram Zubair under the direction of his thesis advisor and approved by his thesis committee, has been presented to and accepted by the Dean of Graduate Studies, in partial fulfillment of the requirements for the degree of **MASTER OF SCIENCE IN CHEMICAL ENGINEERING**.

Thesis Committee

Dr. Mamdouh A Al-Harthi
(Thesis Advisor)

Dr. Abdulhadi Al-Juhani
(Member)

Mozahar Hossain

Dr. M.Mozahar Hossain
(Member)

Dr. Usamah Al-Mubaiyadh
(Department Chairman)

Dr. Salam A. Zummo
Dean of Graduate Studies
Date: 30/12/13

Dedication

To my beloved parents, wife, daughter, sisters and brother

ACKNOWLEDGMENTS

Thanks to Almighty Allah who gave me the courage to complete this work successfully.

I would like thanks to my parents, sisters and my wife for their moral support in completing the graduate program.

I am very much thankful and grateful to my thesis advisor, Dr. Mamdouh A Al-Harthi, for his excellent cooperation, encouragement and technical guidance throughout my research work.

Special gratitude to my committee members Dr. M. Mozahar Hussain and Dr. Abdulhadi Al-Juhani for their useful suggestions, reviews and comments.

Thanks to all my colleagues, especially Dr. Jobin Jose for his very useful cooperation especially in journal paper write-up.

Finally, I would like to thank all my friends specially Mr. Shahid M Bashir for his encouragement and moral support during graduation program.

TABLE OF CONTENTS

LIST OF TABLES

LIST OF FIGURES

LIST OF SCHEMES

ABSTRACT

Full Name : Mukarram Zubair

Thesis Title : Modification of styrene methyl methacrylate copolymer in the presence of pristine and modified graphene by using microwave irradiation

Major Field : Chemical Engineering

Date of Degree : December 2013

Poly(styrene-co-methyl meth acrylate)/graphene and poly(styrene-co-methyl meth acrylate)/modified graphene nano composites were prepared via melt blending. The effects of pristine (G) and modified graphene (MG) and microwave irradiation on the properties of styrene-co-methyl meth acrylate (P(S-co-MMA) polymer matrix were studied. Modification of graphene was done by chemical oxidation method using nitric acid. The nanocomposites were irradiated under microwave at different time intervals (5, 10 and 20 minutes) with fixed power of 1000Watt. Compared to pristine graphene, modified graphene showed improved interaction with P(S-co-MMA) polymer after melt mixing and microwave irradiation. The mechanism of formation of covalent bonds and improved interfacial interaction of pristine and modified graphene with P(S-co-MMA) polymer matrix induced by microwave irradiation was attributed to the formation of defects on graphene and free radicals on P(S-co-MMA) polymer chains explained by FT-IR, Raman spectroscopy and XRD studies. There was significant increase in the storage modulus of P(S-co-MMA) polymer after addition of pristine and modified graphene and microwave irradiation. However at higher irradiation duration, degradation of polymer nanocomposites occurred. The DSC results showed a considerable increase in the T_g value of the nanocomposites. The electrical conductivity of the nano composites were also

improved after irradiation. The state of creation of crosslink network and degradation of polymer nanocomposites during irradiation was assisted by SEM. The study provides an alternative, easy and green method to enhance the molecular level interaction and hence to provide a stronger interfacial adhesion between graphene and the P(S-co-MMA) matrix, which significantly changed the final properties of composites.

ملخص الرسالة

الاسم الكامل : مكرم زبير

عنوان الرسالة : تعديل الستايرين كوبوليمر ميتاكريليت الميثيل في وجود الجرافين البكر والمعدل باستخدام أشعة الميكروويف

التخصص: الهندسة الكيميائية

تاريخ الدرجة : نوفمبر 2013

لقد تم تصنيع مركبات متناهية الصغر لكلا من بولي (ستيرين -الميثيل ميث أكريلات) / الجرافين (Poly(styrene-co-methyl meth acrylate)/graphene) و بولي (ستيرين -الميثيل ميث أكريلات) / الجرافين المعدل (poly(styrene-co-methyl meth acrylate)/modified graphene) باستخدام طريقة اذابة المخاليط. ولقد تم دراسة تاثيرات كلا من الجرافين البكر(G) والجرافين المعدل (MG) و أشعة الميكروويف على خصائص نسيج البوليمر ل styrene-co-methyl meth acrylate (P(S-co-MMA) . تم تعديل الجرافين باستخدام طريقة الأكسدة الكيميائية باستخدام حمض النتريك. تم تعريض مركبات البوليمر متناهية الصغر باستخدام اشعة الميكروويف المشع على فترات زمنية مختلفة (5، 10 و 20 دقيقة) مع قوة ثابتة من الطاقة الكهربائية 1000واط .بالمقارنة مع الجرافين البكر. أظهر الجرافين المعدل تحسين الترابط مع بوليمر P (S-co-MMA) بعد ذوبان الخليط و تعريضه الاشعة الميكروويف. آلية تشكيل روابط تساهمية و تحسين التفاعل بينية من الجرافين البكر والمعدل ب P (S-co-MMA) البوليمر الناجمة عن أشعة الميكروويف لتشكيل العيوب على الجرافين والجذور الحرة على P (S-co-MMA) سلاسل البوليمرتم تفسيرها باستخدام مقياس الطيف باستخدام متحول فورييه FT-IR، رامان الطيفي وXRD . وكان هناك زيادة كبيرة في معامل تخزين P (S-co-MMA) البوليمر بعد إضافة الجرافين البكر والمعدل و أشعة الميكروويف. ولكن استخدام مده عالية من الاشعاع تسببت في تدهور مركبات البوليمر المتناهية الصغر. أظهرت النتائج DSC زيادة كبيرة في قيمة درجة حرارة التحول الزجاجي (T_g) ل مركبات البوليمر متناهية الصغر. وتم تحسين الموصلية الكهربائية لمركبات النانو أيضا بعد بعد التعرض للاشعاع. حالة إنشاء الشبك التشعبي وتدهور مركبات البوليمر متناهية الصغر خلال التعرض للاشعاع تم دراسته باستخدام SEM. وتقدم الدراسة طريقة سهلة وبديله وصديقة للبيئة لتعزيز التفاعل المستوى الجزيئي ، وبالتالي لتوفير التصاق بينية أقوى بين الجرافين و P (S-co-MMA) المصفوفة، التي غيرت بشكل كبير خصائص النهائية للمواد المركبة.

CHAPTER 1

INTRODUCTION

1.1 Background

Now a day's polymers are increasingly used for the fabrication of both high tech and consumer products on account of their attractive properties. With little modification they can achieve desirable mechanical, thermal and optical properties with low cost and light weight. This makes them superior over traditional engineering material such as metals. Among low cost commodity polymers polystyrene and poly methyl methacrylate are widely used in industries after polyolefin. They are successfully applied in different fields such as bio materials, protective coatings, microelectronics, tissue engineering, thin film technology, solar technology etc. [Peter et al 2009, Jason and Kristi 2002, Yoshihiko et al 2008, Larry et al 1993]. Polystyrene is a hydrophobic and thermoplastic polymer. It exhibits good optical property, excellent chemical stability. It is preferred to use in the manufacture of products which are in contacts with body fluids such as packaging materials, containers, micro beads and micro plates [Revilla et al 1996, Kawaguchi 2000, Janssen and Riosa 1989]. Poly methyl methacrylate is a low cost thermoplastic polymer. It possesses excellent properties such as high transparency, ease to structure, resistant to weather [Dorranian et al]. In addition it attains good mechanical and thermal properties [Kaniappanand Latha 2011].

For the success of polymeric materials in various applications, special properties such as chemical structure, wettability, hardness, crystallanity, lubricity, roughness, optical property, crosslinking density, and high mechanical and thermal properties are prerequisite. Different physical and chemical treatment methods are available to modify these materials and make them successful in different fields.

Nano composites, especially carbon nano materials, revealed remarkable improved properties, at very low loading content, when incorporated in to the polymer matrix. In particular graphene and its polymer composites have attracted tremendous applications in modern science and technology [Stankovich et al 2006, Si and Samulski 2008, Geim and Macdonald 2007]. Graphene is regarded as the "thinnest material" in the universe. It is a single layer sp^2-hybridized carbon atom arranged in two dimensional densely packed in a honey comb crystal lattice illustrated in Figure 1.1. [Graphene research centre online].

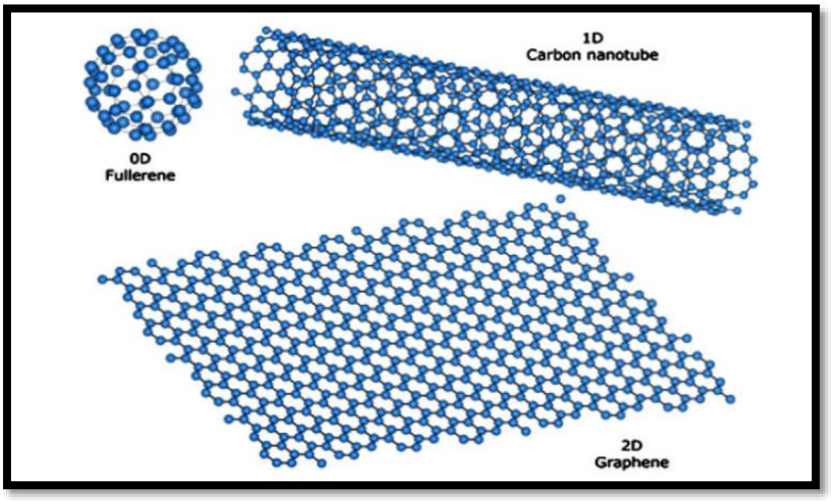

Figure 1-1: Structure of Fullerene, Carbon nano tube and Graphene

Graphene unveils superior properties such as high surface, high tensile strength and aspect ratio, excellent thermal, electrical and mechanical properties, and low coefficient of thermal expansion [Dreyer et al 2010, Wang et al 2009, Blake et al 2008, Rodolfo and Amadeo 2009].These unique properties makes graphene more demanding in different technology fields such as conducting films [Kim et al 2009, Li et al 2008], sensors [Geim and Novoselov 2007, Robinson et al 2008], super capacitors [Stoller et al 2008], nano electronics [Eda et al 2008], batteries [Yoo et al 2008] and bio medicals. [Xu et al 2008]. Table 1.1 [XG Science Online] shows the typical physical properties of grapheme.

Table 1-1: Typical properties of Graphene Nano platelets

Property	**Typical Value Parallel to surface**	**Typical Value Perpendicular to surface**	**Unit of Measure**
Density	2.2	2.2	gram/cc
Carbon Content	>99.5	>99.5	percent
Thermal Conductivity	3000	6	Watt/meter-K
Thermal Expansion	4-6 x 10^{-6}	0.5-1 x 10^{-6}	m/m/deg-K
Tensile Modulus	1000	Na	GPa
Tensile Strength	5	Na	GPa
Electrical Conductivity	10^{7}	10^{2}	Siemens/meter

In literature, three techniques, in situ polymerization [Hu et al 2010], melt mixing [Zhao et al 2007] and solution mixing [Stankovich et al 2006] are extensively used to produce polymer nanocomposites. Among them, melt mixing is an easy, economical and efficient technique in which high temperature and strong shear forces are used to mix solid polymer and nano fillers. Due to high temperature and shear force, the polymer chains may degrade during melt mixing and generate free radicals [Zhang et al 2006]. These low molecular weight chains (degraded) may provide easy dispersion of nano fillers like graphene and may form covalent bonding with graphene [Wenge at al 2011]. In comparison to the in-situ polymerization and solution mixing, melt mixing is not effective to provide same level of dispersion and strong interaction of nano fillers with polymer matrix [Kim et al 2010]. This may be due to the high surface area of bulk graphene, which may possibly to agglomerate when incorporated in to the polymer matrix [Geng et al 2009, Kuilla 2010].Therefore, in order to succeed maximum improvement in properties of polymer/graphene composites, the most challenging step is to achieve high level of molecular dispersion and interaction between graphene and polymer matrix. Different approaches has been investigated such as use of peroxide during melt mixing [Daneesh et al 2007], functionalization of graphene such as oxidation of graphene [Lerf et al 1998] by adding oxygen functionalities like hydroxyl, carboxylic acid and other organic groups like phenyl isocynate [Stankovich(b) at al 2006], prophyrin[Xu et al 2009] and epoxy groups[Bourlinos et al 2009] and implication of low molecular weight polymer chains [Guozhang et al 2010] to crop higher dispersion and better filler-matrix interfacial adhesion but scientists are still looking for more appropriate method to attain high interaction between graphene and polymer matrix

Modification of polymers and polymer nanocomposites using radiation technique is gaining widespread acceptance and suggested as an alternative of conventional chemical method [Spadaro and Valenza 2000] because of several advantages. Types of radiations used in literature for modification of polymers includes e-beam, microwave, gamma, UV, X-rays, ion beam. These radiations when absorbed in the polymer generate a free radical from the polymer chains. This free radical is responsible for several reactions pathways which lead in the arrangement or formation of new bond structure. The major reactions occur during radiation processing are crosslinking, chain scission (degradation), formation of oxygen based functionalities (oxidation) and grafting (in the presence of monomer) [Gueven 2004].Similarly when radiation absorbed on the surface of graphene, defects form on graphene [Cataldo 2000] which results in changing of properties of graphene [Teweldebrhan and Balandin 2009, Ting et al 2013]. The detail description of radiation chemistry of polymers and graphene is described in chapter 3. Microwave radiation; an electromagnetic radiation with frequency ranges from 300 MHz to 300 GHz. is gaining more acceptances in synthesis and modification of polymer materials. Compared to other radiation techniques, it is an easy, cheap and green technique [Brett and Christopher 2005]. It has capability to provide efficient heat, with very short reaction time and also very simple to process.

In this study the blends of poly (styrene-methyl methacrylate) copolymer with pristine and modified graphene were prepared and exposed to microwave radiation illustrated in Figure 1.2. The effects of pristine and modified graphenes on the chemical structure, surface morphology, mechanical and thermal behavior of styrene-methyl meth acrylate copolymer with and without microwave radiation will be studied.

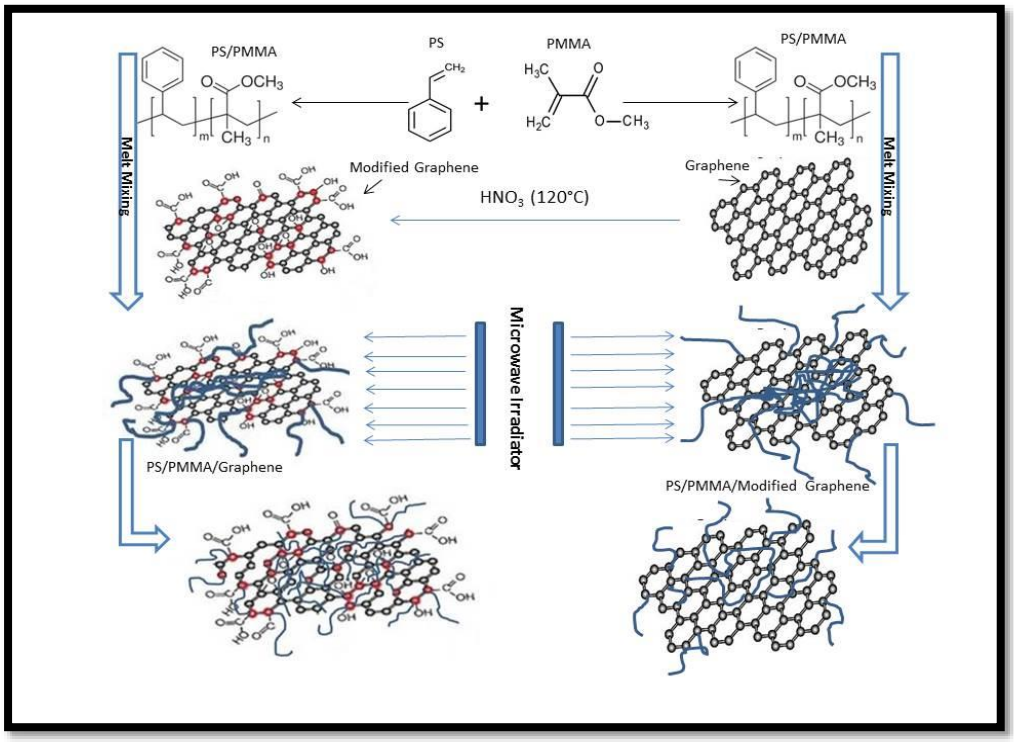

Figure 1-2: Synthesis of P(S-co-MMA) polymer and preparation of P(S-co-MMA) composites with pristine and modified graphene and modification using microwave irradiator.

CHAPTER 2

OBJECTIVES

- Synthesize the Poly (styrene methyl meth acrylate) copolymer using free radical polymerization technique.
- Modification of graphene by chemical oxidation method.
- Blending of Poly(styrene methyl meth acrylate) copolymer with pristine and modified graphene using melt mixing technique.
- Investigate the effects of pristine and modified graphene on the chemical structure, surface morphology, and mechanical and thermal properties of styrene-methyl methacrylate copolymer.
- Modify the structure and physical properties of the polymer nanocomposites using microwave irradiation method.
- Evaluate the influence of operating parameters of microwave radiation on the mechanical and thermal properties of the polymer nanocomposites.

CHAPTER 3

LITERATURE REVIEW

3.1 Radiation

Radiation is the energy in the form of waves or particles comes from different sources and travel through different materials. In general we have two types of electromagnetic radiations, i.e. non-ionizing radiation and ionizing radiation [Encyclopedia of Occupational Health and safety 1998] as shown in Figure 3.1.

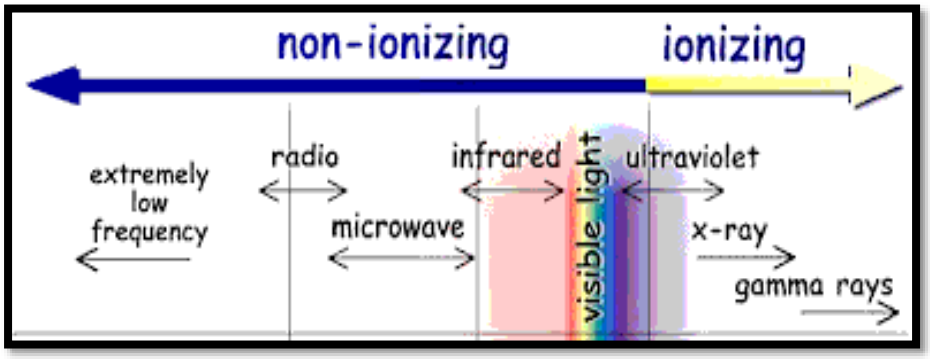

Figure 3-1: EMS of non-ionizing and ionizing

Ionizing radiations are produced by unstable material also termed as radioactive materials. They contain high energy per photon and also termed as high frequency radiations. It includes gamma rays, x-rays, infrared.

Non-ionizing radiation are low frequency radiation and contain low energy per photon. It includes UV, light, visible and microwave and radio waves.

3.2 Microwave Radiation

Microwaves are low energy non-ionizing radiations. It comes in between radio and Infrared radiation, ranges from 300GHz to 300MHz with corresponding wavelength of 1mm to 1m respectively. The energy contain per photon of microwave radiation is between 10^{-4} to 10^{-2} eV as shown in Figure 3.2 [Encyclopedia of Occupational Health and safety 1998.

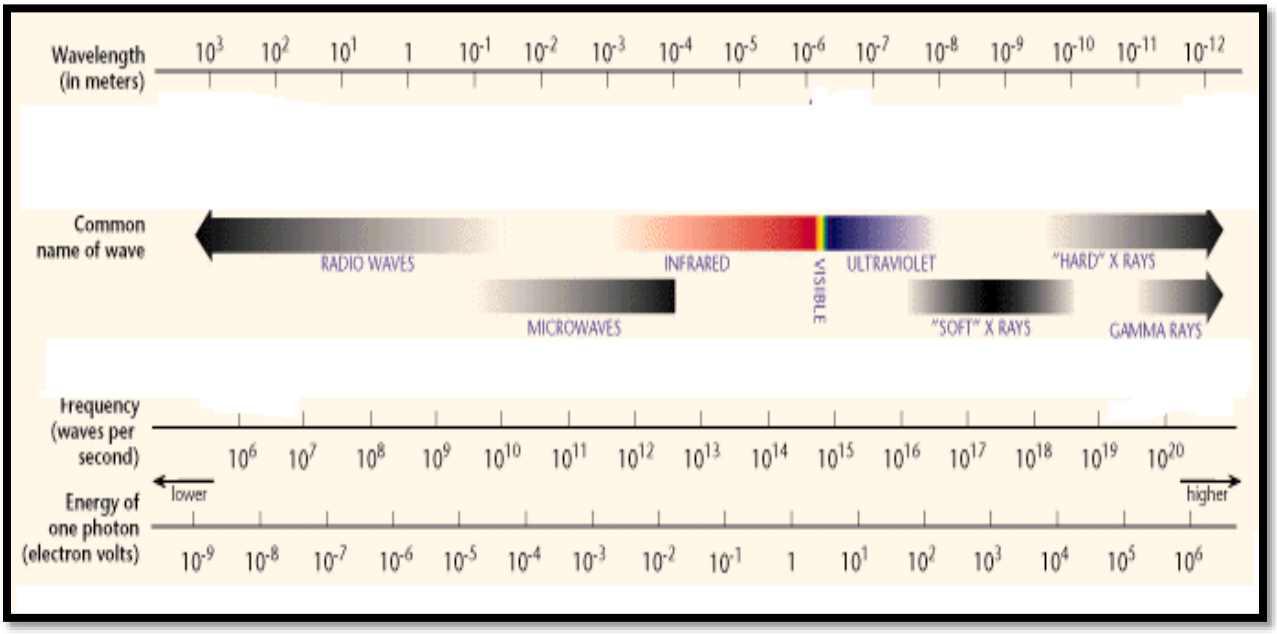

Figure 3-2: Wavelength, frequency and energy of photon of electromagnetic radiation

Commercially microwave radiations are extensively used in telecommunication industry for transmission of information and in different industries, scientific research and medical laboratories for transmission of energy.

3.2.1 Microwave Interaction with polymers

The interaction of microwave with different materials depends on the di-electric properties of that material such as di-electric constant which is the key property for analyzing interaction of microwave with the material and it is defined as "ratio of the electric permeability of the material to the electric permeability of the vacuum"

Polymeric material such as plastic exhibit good di-electric properties, thus consider the best applicant for microwave treatment. Polar polymers contain high dielectric constant than non-polar polymer and therefore have high interaction of microwave radiation. The di-electric constant of some materials are shown in Table 3.1 [Dariusz 2007].

Table 3-1: Di-electric constant of some materials at 20°C

Material	Dielectric constant (ε_r)	Material	Dielectric constant (ε_r)
Vacuum	1	Titanium dioxide	100
Air (1 atm)	1.00059	Water	80
Air (100 atm)	1.0548	Acetonitrile	38
Glass	5–10	Liquid ammonia (−78°)	5
Quartz glass	5	Ethyl alcohol	25
Porcelain	5–6	Benzene	2
Mica	3–6	Carbon tetrachloride	2
Rubber	2–4	Hexane	2
Nylon	3–22	Plexiglass	3
Paper	1–3	Polyvinyl chloride	3
Paraffin	2–3	Polyethylene	2
Soil (dry)	2.5–3	Teflon	2
Wood (dry)	1–3	Polystyrene (foam)	1.05

Another important property to analyze the interaction of microwave radiation with the material is the loss tangent (tan δ) defined as " the ability of any substance to convert microwave energy in to heat energy at a given frequency and temperature". This property is useful for solvent used in microwave treatment. High values of tan δ and ε' are required for fast heating.

$$\tan \delta = \frac{\varepsilon''}{\varepsilon'}(1)$$

where,

ε'= di-electric constant

ε'' = loss factor , efficiency with which the microwave converted in to heat

3.2.2 Microwave Penetration Depth

Penetration depth is defined as "Distance from the material surface where the power absorbed is equal to 1/e of the power absorbed at the material surface". The penetration depth is inversely proportional to the frequency of microwave radiation and also depends on the di-electric properties of the substance. Table 3.2 [Kubel 2005] shows the penetration depth of microwave radiation on different substances.

Table 3-2: Microwave (2.45 GHz) penetration depth (*Dp*) in some common materials

Material	Temperature (°C)	Penetration depth (D_p) (cm)
Water	25	1.4
Water	95	5.7
Ice	−12	1100
Paper, cardboard	25	20-60
Wood	25	8-350
Rubber	25	15-350
Glass	25	35
Porcelain	25	56
Polyvinylchloride	20	210
Epoxy resin (Araldite)	25	4100
Teflon	25	9200
Quartz glass	25	16,000

Penetration depth of substance whose loss tangent is less than 1 can be calculated from the expression below.

$$Dp = \frac{\lambda o\sqrt{\varepsilon'}}{2\varepsilon''} \quad (3.2.1)$$

λ_o= wavelength of radiation.

3.2.3 Microwave Radiator

In our experiment we have used the domestic microwave oven. It consist of two major parts (i) the applicator in which the sample is kept.(ii) the generator which consist of magnetron for producing microwave. Magnetron are vacuum devices consist of anode and cathode. The material of cathode used in domestic microwave magnetron is thorium tungsten with carbonized surface [Tomokatsu 1979]. Figure 3.3 [Dariusz 2007] illustrates the schematic diagram of microwave radiator.

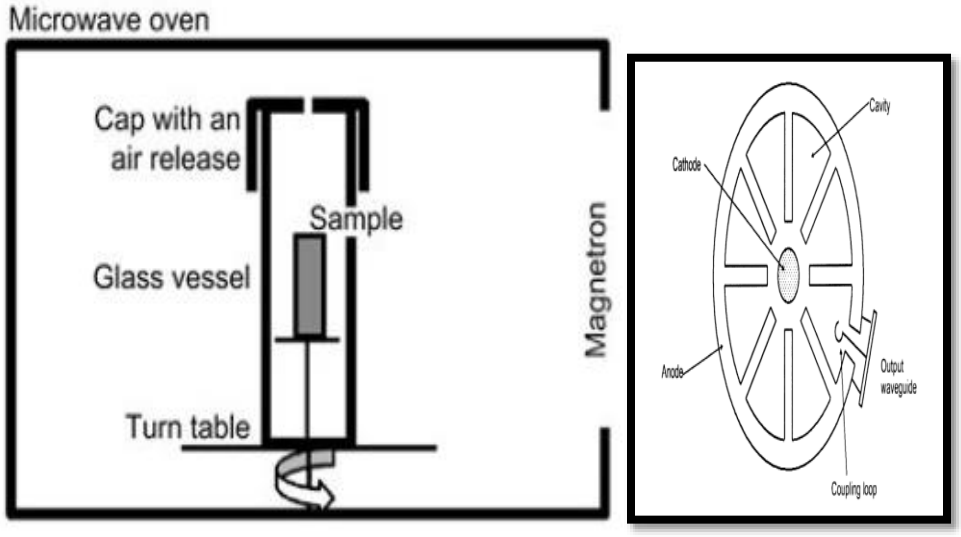

Figure 3-3: (a) Schematic diagram of domestic microwave oven, (b) magnetron of microwave oven

3.2.4 Application of Microwave radiation in modification of polymers

In 2004 Mojtaba.S et al used domestic microwave on polypropylene surface in the presence of $KMnO_4$at 120°C. It was found in the improvement in wet ability, adhesion strength of polypropylene film after irradiation which is due to the oxidation of the polypropylene surface. The author concluded, this is a simple and effective method to modify the surface of polypropylene compared to conventional heating system.

In 2005, Gorin D.A et al studied the effect of microwave radiation on the polymer microcapsules made of poly(sodium styrene sulfonate) (PSS) and poly(allylamino hydrochloride) (PAH) containing inorganic nano particles. The microwave frequencies used were 2.45GHz and 8.208GHz and sample treated at different powers. The SEM graph illustrated that microwave radiation produced partial or complete damage of the microcapsules contain Ag-nano particles. Thus it was concluded that microwave radiation can be used for opening of these microcapsules made of these polymers.

In 2007, D. Di Claudio performed the annealing of TiO_2 film (doped in quartz substrate by sol gel dip). This was performed using microwave irradiation at 2.45 GHz and 600watt power for 10min and conventional heating for 3hrs and 600°C. Results from XRD showed that in both methods formation of antase exhibited. The crystallite size of the film exposed to microwave and conventional heating was 9nm and 15nm respectively. The grain size obtained from AFM was in the range of 10-20nm for microwave exposed film and 20-25nm for conventional heated film. Thus the results proved that in contrast to conventional heating, microwave irradiation has potential to perform annealing of TiO_2 films with reduced time, cost and low energy input.

In 2008, Lim H.R et al irradiated the films of polyurethane using microwave induced argon plasma system at f=2.45GHz and power of 1kW.After irradiation , the author found a significant increase in surface roughness of PU films and decrease in contact angle after treatment of 12.4seconds. This behavior reveals that after irradiation of PU films increase in hydrophilicity occur which makes the PU films desirable for tissue engineering.

In 2009, Ali Khadenhosseni et al succeeded to crosslink PEG, by the formation of microstructure of PEG based acrylate using microwave thermal crosslinking method. The reaction completed in only 10seconds and there was no degradation of polymer observed.

In 2012, Vakce et al investigated the carbonization of wood by using microwave radiation at f=2.45GHz. Microwave irradiation method was found the best pretreatment to form carboneous material such as O-H, CO-OH and C=O on the wood surface compared to other conventional treatment method. After treatment at 3mins the degradation of the wood started.

3.3 Radiation processing of polymers

3.3.1 Chemistry of Radiation

When the polymeric material is exposed to radiation, energy of photon absorbed by the polymer chain and transforms this into valence or binding electron (free polymer radical) by abstracting hydrogen from polymer backbone. This formation of free polymer radical is termed as Initiation.

- **Initiation**

The minimum energy required to open the polymer chain and generate the free polymer radical is 5-10 eV [Czvikovszky 2003]. This polymer free radical then leads to the crosslinking, chain scission, photo oxidation and secondary reactions. [Jan F.Rabek 1996]

$$P\text{-}H \xrightarrow{\quad h\nu \quad} P^{\bullet} + H^{\bullet} \qquad (3.3.1)$$

- **Propagation**

Polymer radical in the presence oxygen readily react with oxygen to form peroxy radical.

$$P^{\bullet} + O_2 \longrightarrow POO^{\bullet} \qquad (3.3.2)$$

The rate of formation of peroxy depends on the structure of the polymer therefore different polymer have different amount of peroxy radical formation.

Peroxy radical abstract hydrogen from the polymer chain and form hydroperoxide with generation of new polymer radical.

$$POO^{\bullet} + PH \longrightarrow POOH + P^{\bullet} \qquad (3.3.3)$$

The hydrogen atom abstruction occur normally from tertiary carbon atom [Jan 1996]

$$POO^{\bullet} + CH_2\text{—}RCH\text{—}CH_2POOH + CH_2RC^{\bullet}CH_2 \qquad (3.3.4)$$

- **Chain Branching**

In chain branching, decomposition of hydroperoxide group occur by radiation. This gives peroxy and hydroxyl radical [Carlsson DJ a,b 1976 and 1969]

$$POOH \xrightarrow{h\nu} PO^{\bullet} + OH^{\bullet} \qquad (3.3.5)$$

These hydroxyl and peroxy radicals abstract hydrogen from the same or nearby chain to form hydroxyl group and generate polymer radical.

$$PO^{\bullet} + PH \longrightarrow POH + P^{\bullet} \qquad (3.3.6)$$

$$HO^{\bullet} + PH \longrightarrow H_2O + P^{\bullet} \qquad (3.3.7)$$

The hydro peroxide and hydroxyl group both form along the polymer chain or on its end but forming at the end is rare. [Jan 1996]

- **Termination**

It is the bimolecular recombination of polymer radical.

$$P^{\bullet} + P^{\bullet} \longrightarrow PP \qquad (3.3.8)$$

$$P^{\bullet} + PO^{\bullet} \longrightarrow POP \qquad (3.3.9)$$

$$P^{\bullet} + POO^{\bullet} \longrightarrow POOP \qquad (3.3.10)$$

$$PO^{\bullet} + POO^{\bullet} \longrightarrow POOOP \qquad (3.3.11)$$

At high pressure of oxygen last two reactions are dominant and at low pressure of oxygen other termination reactions occur.

3.3.2 Radiation Polymer Crosslinking

Crosslinking is a process of forming three dimensional network of polymer chain. Crosslinking of thermoplastic polymer change to thermoset polymer which results in high molecular mass, improved mechanical properties such as tensile strength, impact strength, abrasion resistance etc. and also improved thermal properties which are desirable for different applications [Narkis 1982, Sawatari and Mastuo 1987]. The Figure 3.4 illustrates the crosslinking behavior using radiation.

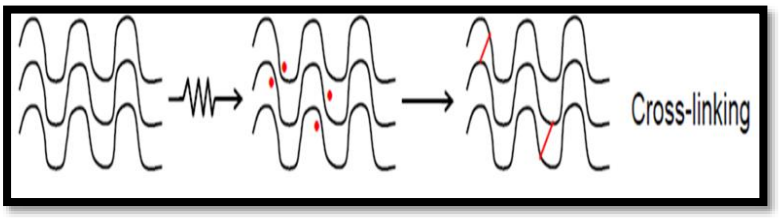

Figure 3-4: Crosslinking behavior using radiation

During irradiation of polymer both crosslinking and chain scission occur simultaneously. The amount of chain scission and crosslinking depend on the chemical structure of the polymer, physical state of the system and most important the radiation conditions (radiation time and power). From the literature it is found that the first three reactions in termination cause crosslinking of the polymer structure [Jan 1996].The Table 3.3 [Nabio 1989] illustrates the number of crosslinking G(x) and chain scission G(s) per 100eV of energy absorbed of some polymers.

Table 3-3: Crosslinking and chain scission of polymer by radiation

Polymer	**G(X)"Crosslinking"**	**G(S)"Chain scission"**
LDPE	1.4	0.8
HDPE	2.1	1.3
Poly methyl methacrylate	-	1.22-3.5
Polystyrene	0.045	<.018
PVC	2.15	-
Poly methyl acrylate	0.55	0.18

3.3.3.1 Improvement of properties by cross linking

Following are the properties of polymer can be enhanced by formation of crosslinking in the polymer structure.

- Increased Tensile Strength and shrink-memory
- Stress Cracking Resistance (ESCR)
- Increased Form Stability and Improved Impact Strength
- Heat Resistance
- Resistance to Abrasion
- Resistance to Solvents
- Reduces Elongation (stretch)

3.3.3.1 Advantages of Radiation Crosslinking

Following are the advantages of radiation crosslinking of polymer over other conventional methods [Lewis 2010, Gueven 2004].

1. Using radiation different types of polymer can cross-linked. However chemical or conventional methods are limited to only few polymers.
2. No addition of additives or catalyst to start the reaction. Initiation starts by generation of polymer free radical due to absorption of heat in the polymer chain.
3. Control of reaction during radiation is easy by controlling the dose of radiation however in chemical crosslinking the control of reaction is very sensitive.
4. In radiation, reaction takes place at room temperature and complete in few seconds/minutes.
5. Low consumption of energy in radiation processing whereas chemical crosslinking is high energy process

6. In radiation processing, no possibility of unwanted residual in products obtained. However in chemical crosslinking there is potential of unwanted residuals in the product due to the presence of additives or catalyst.

3.3.3.1 Parameters of Radiation crosslinking

Radiation crosslinking of polymer mainly depends upon four important parameters [Tamboli et al 2004].

1. **Type of Radiation**

   Different types of radiation contain different energy per photon. The number of free radicals formation also depends upon the energy of photon. Thus different radiation source show different amount of crosslinking behavior.

2. **Nature of Polymer**

   Crosslinking of polymer by radiation method also depend on the chemical structure of the polymer. Different polymer shows different crosslinking when treated with same radiation source and same radiation condition

3. **Physical State of the Reaction**

   Physical state of the reaction also affects the crosslinking after irradiation. For example if polymer is treated in the presence or in absence of oxygen. The treated polymer show different properties with and without oxygen.

3.3.3 Radiation Polymer Degradation

The degradation of polymers attributes to the breakage of long molecular chain of polymer when subjected to high energy. The minimum energy required to break the covalent bond of main carbon chain, typically in the range of 5-10eV [Czvikovszky 2003]. Radiation

technique is widely used in industries to degrade the polymers in an efficient and fast way compared to other conventional methods. Different types of radiations like gamma, electron beam, and microwave are applied. The mechanism of degradation of polymers either by radiation or by other techniques follows the same chain reaction that's includes initiation, propagation and termination. Degradation mechanism of Poly (styrene-co-methyl methacrylate) illustrated by [Gupta et al] in Figure below.

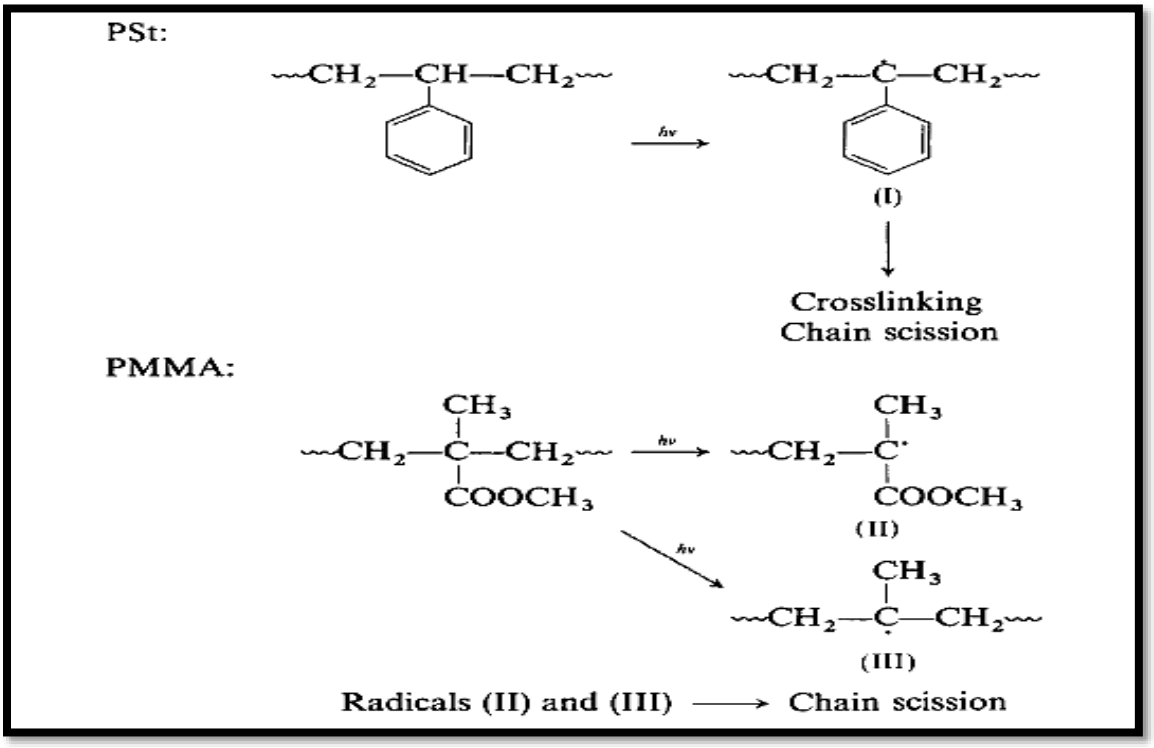

Figure 3-5: Degradation mechanism of Polystyrene and Poly methyl methacrylate

3.3.3.1 Significance of Polymer Degradation

Commodity plastics such as Polyethylene, Polystyrene and Poly methyl methacrylate are abundantly used for food packaging and other service products applications. The rich expenditure of these polymers focused scientists and researchers towards the global environmental destruction caused due to disposal of these polymers. Degradation by radiation technique of these polymer and other environmental concern substances like rubber brings an important discovery to overcome this issue. Below is the brief description of some studies concerning degradation of different materials using radiation technique.

- Degradation of polymers using radiation is an emerging field. It is used for natural polymers such as chitosan , cellulose to achieve the desired molecular weight useful for processing of them for the further application [Czvikovszky 2003]
- Degradation of the polymers particularly recyclable is used to increase its melt index so they can be easily processed for recycling.
- Degradation of medical products such products made of polypropylene, polystyrene, PVC and other polymers using high energy ionization radiations. The degree of degradation depends on the polymer structure[Azhar and Usmani 2003]
- Degradation of tyres and recycle waste tires by using ionizing radiation was extensively studied and reported in literature[Adhikarl et al 2000, Fang et al 2000]

3.4 Polystyrene

3.4.1 Properties

Polystyrene was commercially manufactured in 1938. Now a days, commercially high impact PS and general purpose P-S are used. It is produced from styrene monomer which

is obtained from dehydrogenation of ethyl benzene. The structure of styrene and polystyrene are illustrated in Figure 3.6 [Fried 2003].

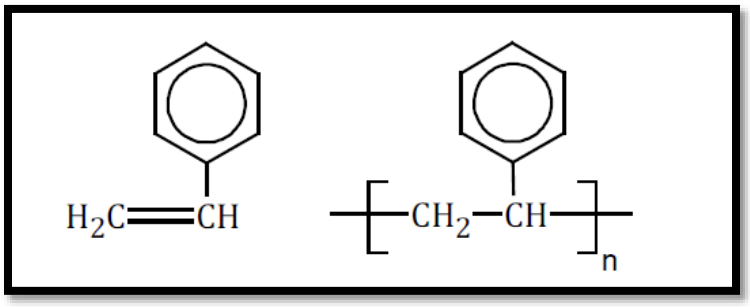

Figure 3-6: Structure of styrene and polystyrene

Polystyrene is a brittle and colorless polymer used usually for packaging material. Its glass transition temperature is at 100^0C and molecular weight of the repeating unit is 104.1g/mole.

Polystyrene is used for various applications i.e. for making rigid materials such as refrigerator, coat hangers, and printer cartridges [Polystyrene fact sheet 2010 (online)]. A derivative of polystyrene such as Styrofoam which is polystyrene foam is also used in protective coating application and also in manufacturing of insulated disposal cups, meat trays and panel insulation [Terry 2004].

3.4.2 Radiation Chemistry of Polystyrene

The presence of phenyl chromophore in each repeat unit of P-S is responsible for excitation by irradiation. The excited phenyl ring transfer the energy to the nearby C-H bond which leads to the formation of alkyl radical through cleavage of hydrogen radical in the polymer backbone.

$$-CH2-CH(Ph)-CH2- \xrightarrow{\quad hv \quad} -CH2-C^{\bullet}(Ph)-CH2- + H^{\bullet} \qquad (3.4.1)$$

Type of radical formed during radiation depends on the wavelength of radiation as it was mentioned above. At wavelength greater than 300 nm we have a formation of hydroxyl groups

$$-CH(Ph)-C^{\bullet}OH-CH(Ph)- \qquad (3.4.2)$$

When the radiation wavelength is above 360nm we have a formation of double bonds. This leads to the formation of allyl-type radicals from alkyl type radical with ration (3:1) respectively.[Kuzina & Mikhailov 2010]

$$-CH2-C^{\bullet}(Ph)-CH=CH(Ph)-CH2- \qquad (3.4.3)$$

All these radicals, in the presence of air, react with oxygen to form peroxy radicals. This leads to the formation of hydro peroxides (according to equation 5 discussed in polymer radiation chemistry). These hydro peroxides further decompose to produce terminal carbonyl group or other unsaturated carbons.

3.4.3 Modification of Polystyrene using Radiation

In 1996, Klaumunzer S et al, bombarded high energy particle (0.3 MeV of ^{1}H, 1.5 MeV of ^{18}O and 0.4and 6.5MeV of ^{40}Ar ions) at room temperature and in vacuum on P-S films

to investigate the crosslinking of PS after bombardment. The chosen ions are from wide range of nuclear and electronic energy loss. The degree of crosslinking (Gx) is determined by measuring weight average mol.weight (Mw) as a function of adsorbed dose (D). Maximum crosslinking formation is obtained from ^{40}Ar bombardment at 0.4 MeV and very low crosslinking was obtained at 6.5MeV. The results also revealed that the momentum transfer collision using nuclear energy are 20 times more effective in forming crosslinking than the ionization energy.

In 2001, Dong. W et al, used radiation method to investigate the mechanical properties and morphology of immiscible blends of polystyrene and nylon 1010. It was found that after irradiation the elastic modulus of blend (25:75) (PS: nylon 1010 showed linear behavior with irradiation dose. This was evident from the TEM photographs because rubber is easily crosslinking type polymer. However the mechanical properties such as tensile strength, elongation at break and energy of fracture at radiation dose above 0.34MGy started to decrease with increasing radiation dose which is due to the breakage of rubber phase. Thus it can be concluded from the results that at low radiation dose (up to 0.34MGy) it can easily form crosslinking structure in the polystyrene chain.

In 2002, Albano. C et al studied the effect of low dose 10-70kGy gamma irradiation on thermal, mechanical and morphology of polystyrene/polypropylene (80:20) blends with and without compatiblize (SBS) at 7-5 wt%. Thermal studies of the treated blend shows no changes in Tg .At low dose 0-10kGy the author found some crosslinking structure of pure PP but at high value of dose greater than 10kGy, chain scission occur due to melting of PP. In case of pure PS film, it was found very stable against radiation and almost no change in mechanical as well as thermal properties at high radiation dose 10-70kGy.

In 2004, Halnei Kaczmarek studied the effect of UV-radiation on the film of PS modified by addition of 1-5% ketone(acetephenone and benzophenone).It was found from the results that presence of ketone in the polymer chain leads to the formation of oxygen based functionalities such as (C=0, COOH and O-C-O) in the polymer chain after irradiation. These functional group formations facilitate the attack of micro- organisms and promote biodegradation of PS-films when exposed to sunlight. Thus it was proved that by addition of small amount of PS-films, we can produce a biodegradable packaging material.

In 2004, Guruvenket.S et al investigated the effect of microwave electron cyclotronresonance (ECR) plasma treated in the presence of oxygen and argon on biomedical grade polystyrene (PS) films. The irradiation has performed at different treatment time and microwave power. After irradiation of PS film in the presence of oxygen and argon the contact angle decreased which mean that the wet ability of the PS films increases. FTIR results reveals that treatment of PS film in the presence of argon showed some absorption of moisture content and treatment in the presence of oxygen showed the formation of several oxygen functionalities(C=O, COOH, ether and OH group).

In 2010, Vessel.A et al , used electordless radiofrequency discharge oxygen plasma to irradiate the biaxally oriented PS sample at 1-50 seconds. Increase in the surface roughness of PS films confirmed by AFM. Formation of functional group C=O, C-O and -CO-O also appear after irradiation. Decrease in contact angle occur which increases the wettability of the polymer film. The more important thing in that research that un-like other plasma treatment –O-CO-O carbonate functional group appear on the PS film which is due to the reaction of phenyl aromatic ring with oxygen.

In 2011, Jaleh. B et al, studied properties of treated PS-TiO_2 nano-composites using argon RF plasma (13.6MHz with 30-120 seconds). The results showed that there is no change in the optical and crystal properties of PS-TiO2 nano composites films after treatment. FTIR results also indicated that oxidation of PS-TiO_2 films occur after irradiation which is due to the reaction of survival radical with oxygen when it is subjected to air.

3.5 Poly methyl methacrylate

3.5.1 Properties

Poly methyl methacrylate is a transparent polymeric material mostly used for optoelectronic industry [F.Ide and Terada 1987] due to its excellent properties such as high transparency, ease to structure, resistant to weather [Bennamare 1988 , Frank et al 1994] and also low cost.

It is thermoplastic polymer and exhibit desirable physical and chemical properties. It exhibit good tensile strength, high rigidity and high temperature resistant. Figure 3.7 [Dorranian et al 2009] shows the structure of the PMMA polymer.

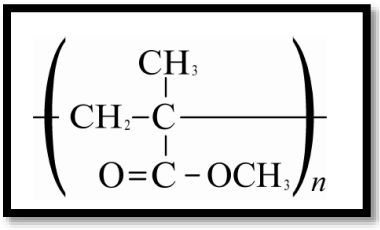

Figure 3-7: Structure of PMMA

3.5.2 Radiation Chemistry of Poly methyl methacrylate

When radiation absorbed on the structure of the PMMA it leads to the generation of free radical as was discussed in radiation chemistry.

In literature,[Aykara and Gueven 1999] the major reactions reported at the time of initiation to produce free radicals are (i) breakage of carbon-carbon bond (ii) breakage of ester side group (iii) breakage of methyl side group. Figure 3.8 [Clegg 1991] shows the free radical formation of PMMA after irradiation.

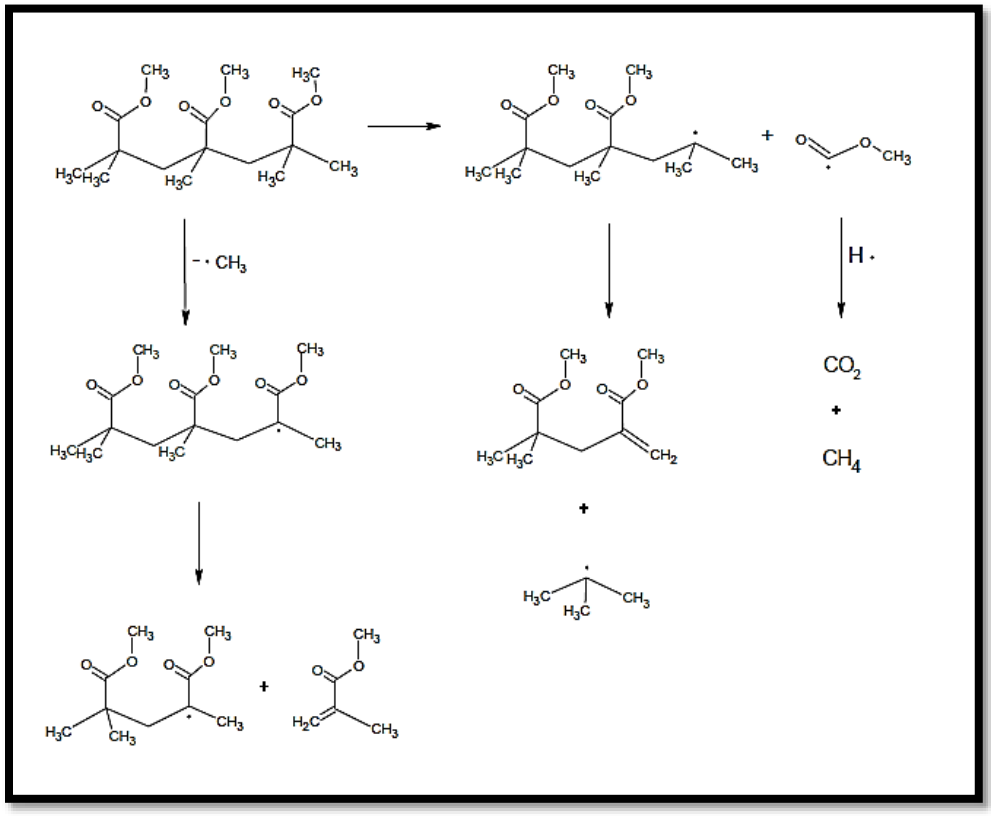

Figure 3-8: Free radical formation and decay in PMMA

In irradiation of PMMA the chain scission rate is very fast. Thus crosslinking of PMMA by irradiation is less observed {G(s) >> 4 G(x)}[Kenneth 2003].After formation of free radical the radiation mechanism is same as discussed early in radiation chemistry.

3.5.3 Modification of Poly methyl methacrylate using Radiation

In 1999, Varad Rajula et al, have used ^{28}Si ion beam 120MeV with influence range of 10^{11} -10^{13} ion/cm^2 to modify the chemical structure of PMMA/PVC blends of different compositions. The authors found from the Infrared spectra that on irradiation with ^{28}Si ion abstraction of Hydrogen, Chlorine, C=O, CH_2 and CH_3 is achieved. In all blends, it is indicated that with increase in fluence range, abstraction of HCl also increased.

In 2001, Lawrence. J et al irradiated biomaterial PMMA using CO_2, Nd:VAG excimer and high power diode laser(HDPL) radiation to investigate the change in wettability after irradiation. It was found that irradiation of PMMA films using CO_2, Nd:VAG excimer showed very small change in contact angle and thus low improvement in wettability. However the interaction Pmma films with laser (HDPL) resulted in the formation of oxygen based functionalities which lead to significant decrease in contact angle and thus remarkably improvement in wettability is achieved.

In 2008, Sakurabayashiused. Y low energy radiation to improve the surface hardness of the Pmma films. The range of the radiation was 500, 700, 1000 V.The author found form the FTIR results that increase in the intensity of C-C bond after irradiation which showed the introduction of crosslinking structure in to the polymer chain. Maximum crosslinking

found at 1000V. The formation of crosslinking is also confirmed by the suppression of invasion of dyeing agent on the treated sample compared to the untreated Pmma film.

In 2009, Lihuaa. Z et al , used Ar-plasma radiation (13.56 MHz radio frequency) to improve the antithtombogenity and reduce UV transmittance of medical grade sample lenses(PMMAintraocular lenses with 3mm radius).The study demonstrated the immobilization of Heparin(Hp) and polyglycol(PEG) on the surface of PMMA film in Ar-plasma atmosphere. The results from the FTIR and XPS confirmed that using Ar-plasma successfully immobilized Hp and PEG on PMMA surface. It also modified PMMA of PEG-PMMA and Hp-PMMA without any change in the morphology of PMMA surface confirmed by SEM. Decrease in UV transmittance and improvement in antithtombogenity is also achieved by using Ar-plasma irradiation confirmed by platelet adhesive experiment.

In 2010, Paramjit. S , investigated the effect of 70Mev C^{5+} ion with influences 3.1 10^{11}, 3.7 10^{12} under vacuum on the optical ,chemical structure of Pmma films.From the results of FTIR and X-rays diffraction, the author concluded that during radiation of Pmma film both crosslinking and degradation reactions occurred. X-rays results showed significant increase in the amorphous nature after irradiation and also about 8% decrease is found in the crystallite size of the irradiated sample.

3.6 Graphene

3.6.1 Brief Introduction

Over the last two decades, the nano science has boomed extensively and the importance of nano technology has attracted increase of significance in the fields such as biomedical, sensors, aircraft, communications, computing and many other applications. These

nanocomposites has gained enormous applications due to their versatile properties but scientist are still researching new materials which are more dimensional stable, exhibit improved physiochemical properties and acquire properties which lacked in the conventional nano- materials.

In this regard, graphene and graphene based polymer composites brings an important discovery in the field of nano-technology and attracted tremendous application in modern science and technology [Stankovich et al 2006,Si y and Samulski 2008, Geim and Macdonald 2007]. Graphene exhibit exceptional mechanical, electrical and thermal properties[Zhu et al 2010, Geim and Novoselov 2007, Compton and Nguyen 2010]. Graphene is regarded as the "thinnest material" in the universe and it is a single layer sp2-hybridized carbon atom arranged in the two dimensional densely packed in a honey comb crystal lattice.

In comparison to the conventional nano-materials (CNT, LDH, Na-MMT etc) it unveiled improved properties such as high surface , high tensile strength and aspect ratio, exceptional thermal and electrical and mechanical properties, great flexibility and transparency and low CTE[Dreyer et al 2010, Wang et al 2009, Blake et al 2008, Rodolfo and Amadeo 2009]. The comparison of the mechanical, thermal and electrical properties of graphene with CNT, steel, plastic rubber and fiber is mentioned in the Table 3.4 [Joong et al 2010]**.**

Table 3-4: Properties of Graphene, CNT, nano sized steel and polymers.

Materials	**Tensile strength**	**Thermal conductivity (W/mk)**	**Electrical conductivity (S/m)**
Graphene	130 $\pm$ 10 GPa	$(4.84+0.44)x10^3$ to $(5.30+0.48)x10^3$	7200
CNT	60-150 GPa	3500	3000-4000
Nano sized steel	1769 MPa	5-6	1.35×10^6
Fiber(Kevlar)	3620 MPa	0.04	Insulator

3.6.2 Discovery and Structure of Graphene

In 1940, graphene was first theoretically established that it is the building block of graphite [Wallace 1947]. It was believed to be composed of benzene rings stripped of their hydrogen. It was considered to be as unstable and not able to be produced at ambient conditions [Landau and Lifshitz 1980,Mermin 1968]. However, in 2004, the 2-D crystalline allotropic form of carbon called graphene was successfully produced by Gein and co-workers from Manchester University [Novoselov et al 2004] by a very simple table top experiment.

Graphene is a single layer sp^2 hybridized carbon atom arranged in 2-D honey comb lattice shown in Figure 3.9 [Graphene research center Online].

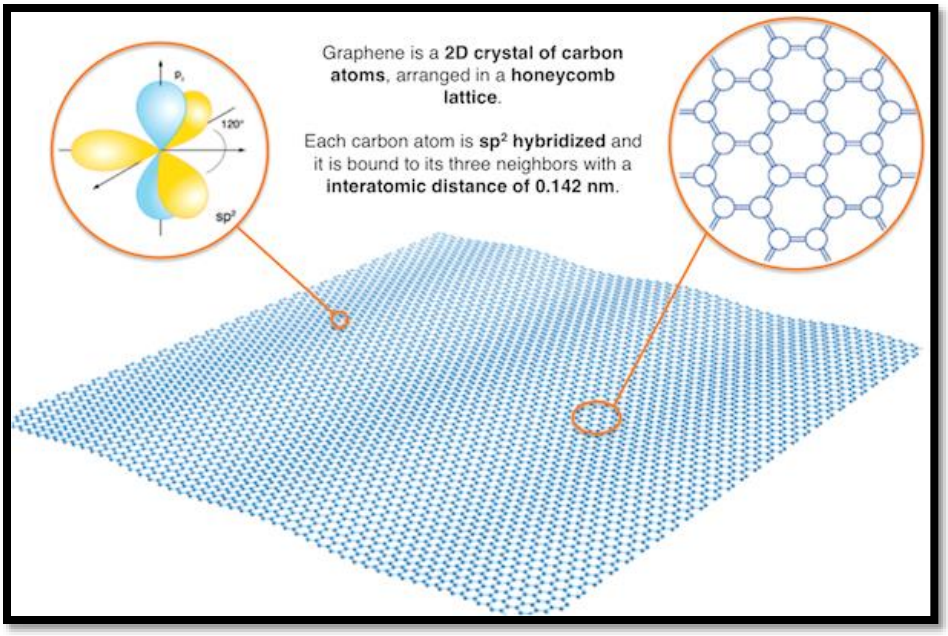

Figure 3-9: Structure of Graphene

The lattice of graphene consists of two interpenetrated sub-triangular lattice. The carbon-carbon bond (sp^2) length is about 1.4 A^o[Reddy et al 2006]. The thickness of graphene layer ranges from 3.5-10 A^o relative to SiO2 substrate [Nemes-Incze et al 2008]. There is also other pseudo sp2 hybridized carbon structure as bi-layer and few layers graphene which acquire some specific properties differ from graphene [Mauricio et al 2010].

3.6.3 Preparation Method of Graphene

There are four methods for synthesis of graphene.

1) First is chemical vapor deposition (CVD) and epitaxial growth [Eizenberg and Blakely 1979]
2) Second one is micro-mechanical exfoliation of graphite , also called ‘peel off’ or scotch

Method [Novoselov et al 2004]

3) Third is the epitaxial growth on electricity insulating surface such as SiC.
4) Reduction of graphene oxide [Berger et al 2006]

Brief advantages and disadvantages of methods used to produce graphene are illustrated in Table 3.5 [Erik et al 2010].

Table 3-5: Advantages and disadvantages of the techniques used to produce graphene.

	Advantages	Disadvantages
Mechanical exfoliation	Low-cost and easy No special equipment needed, SiO_2 thickness is tuned for better contrast	Serendipitous Uneven films Labor intensive (not suitable for large-scale production)
Epitaxial growth	Most even films (of any method) Large scale area	Difficult control of morphology and adsorption energy High-temperature process
Graphene oxide	Straightforward up-scaling Versatile handling of the suspension Rapid process	Fragile stability of the colloidal dispersion Reduction to graphene is only partial

3.6.4 Properties of Graphene

The rapid attraction of graphene in tremendous applications lies in its remarkable mechanical, electrical, thermal properties and other unique properties and availability of range of techniques to synthesize graphene. This happens to matching the short comings of conventional nano-materials as shown in Table 3.4. These features of graphene, principally specific properties have opened a new skyline for the next generation of the nano-composites materials.

1) Mechanical Properties

Graphene and other carbon allotropic form like CNT and diamond exhibit outstanding mechanical properties. The stiffness of graphene calculated by [Lee et al 2008] is of the order of 300-400N/m with breaking strength of 42N/m. Young modulus calculated by [Frank et al 2007] is approximately 0.5-1.0 T Pa. Breaking strength of graphene is around 200 times larger than steel demonstrated by Lee et al 2008.

2) Thermal properties

Graphene exhibit high thermal properties than CNT. Balandin et al in 2008 calculated the thermal conductivity ranging from $(4.84 \pm 0.44)\ 10^3$to $(5.30 \pm 0.48)\ 10^3$W/mk of graphene sheet prepared by mechanical exfoliation method. Recently Cai.W et al(2010) calculated the thermal conductivity around 2.5×10^3 W/mk of graphene prepared by CVD method. A detailed study still needs to be performed to study the thermal properties of pristine graphene and their composites.

3) Electronics

Graphene has remarkably very high electron mobility, large lateral extension and field effect sensitivity compared to CNT. This improved property makes graphene more attractive for the field effect transistor devices [Zhang et al 2005]. Temperature independent of graphene mobility between -10K to 100K, which improves the scattering mechanism caused by graphene defects [Novoselov(b) et al 2004].

4) Reactivity

Surfaces of highly crystalline graphene are not chemically reactive. Interaction with other molecules appeared via physical adsorption ($\pi - \pi$ interactions). To improve the chemical

reactivity of the graphene several chemical groups such as carboxyl COOH, carbonyl COH, hydrogenated C-H and amine NH_2 can be moored at the edge of the graphene. A fully developed hydrogenated graphene sheets called as Graphene was predicted by Sofo J.O et al and produced by Novoslov (c) et al and co-workers.

3.6.5 Radiation Chemistry of Graphene

Radiation mechanism of graphene follows the amorphization route proposed by Ferrari and Robertson in 2000. When radiation absorbed on the surface of graphene it transform the crystalline structure into nano-crystalline and then to amorphous phase due to excitation and disruption of the phonons. The minimum energy required to damage the carbon atoms on the surface of nano structure ranges from 15-90 KeV [Ritter el al 2006]. These high kinetic energy ejected electrons after irradiation of graphene may responsible to form intestinal atoms and defects in graphene [Cataldo 2000] illustrated in Figure 3.10 [Ting et al 2013]. This deformation of crystal lattice of graphene or formation of defects after irradiation results in the modification in the properties of graphene. [Teweldebrhan and Balandin 2009, Ting et al 2013].

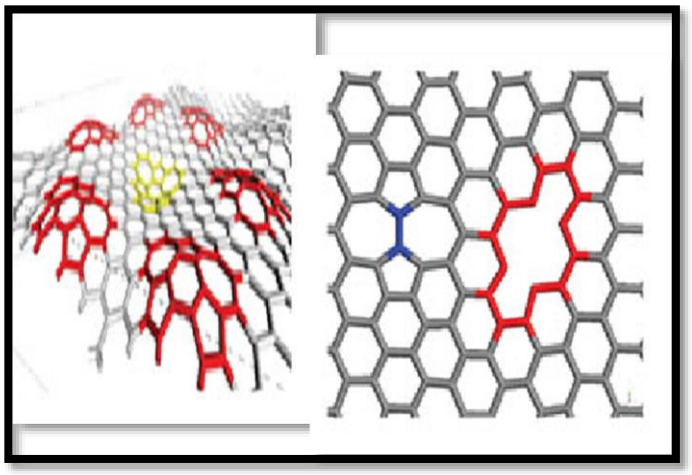

Figure 3-10: Formation of defects/disorder produced after irradaition

The theory of amorphization of graphene upon exposure to radiation proposed by Ferrari and Robertson consist of three steps.

- Crystalline graphite changes into nano crystalline (nc) graphite.
- (Nc) graphite evolves mainly into sp^2 amorphous carbon.
- Sp^2 amorphous carbon transform completely into tetrahedral amorphous carbon.

A Raman spectrum is the best tool to evaluate the defects produced in graphene. In Raman spectra of D-band at peak around 1350 cm^{-1} and G-band at peak around 1575$cm^{-1}$are used to estimate the degree of disorder in graphene structure. Increase in the intensity of ratio of D-band and G-bands illustrates that the crystalline structure changes to nano crystalline structure. When the (nc) crystalline structure mainly transform into amorphous carbon (stage II) decrease in ratio of D-band and G-band is appeared. Figure 3.11 shows the Raman spectra of SLG under electron beam which demonstrates the Stage I and stage II of Ferrari and Robertson theory [Teweldebrhan. D and Balandin.A.A 2009].

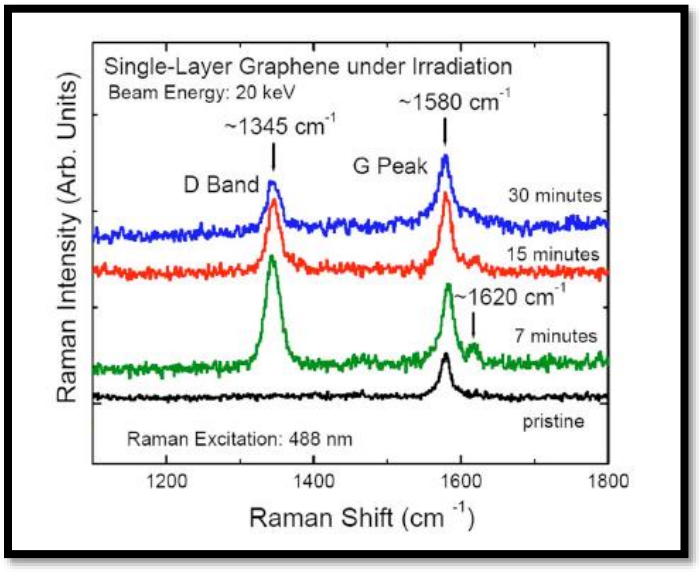

Figure 3-11: Raman spectra of SLG under electron beam irradiation

3.6.6 Functionalization of Graphene

Graphene due to its high surface area, may tends to agglomeration when incorporated into the polymer matrix. In order to reduce the agglomeration of graphene, functionalization of graphene using oxidization methods was performed. Several studies so far done to functionalize graphene [Hummers and Offeman 1958, Shen et al 2009, Yang et al 2009,Cai and Song 2007]. This improves the exfoliation of graphene and dispersed graphene more effectively in the polymer matrix. Functionalized graphene is similar in properties to pristine graphene except a change in structure i.e. a partly damaged carbon atom with some functionality on the surface of it. These functionalities on the surface of graphene reduce the van der Waals forces and increase the distance between the neighbor carbons sheets and thus allow the polymer chains to penetrate more easily. This results in improved dispersion and interaction between graphene and polymeric material. Figure 3.12 [Kannan and Marko 2005] shows the functionalization of graphene performed in our study.

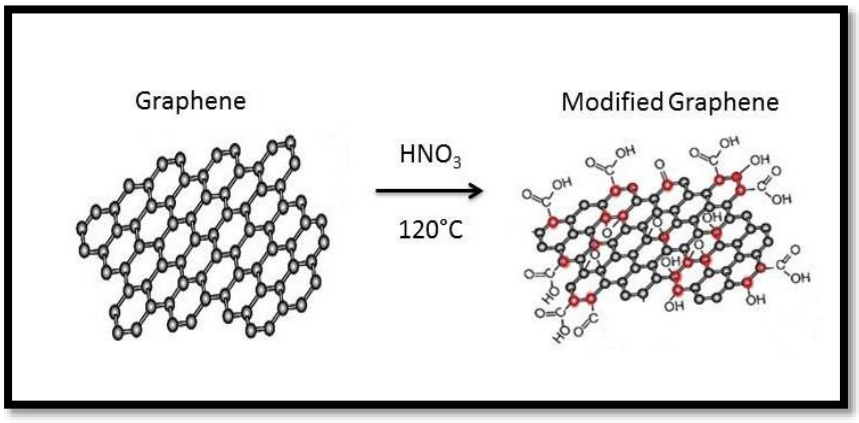

Figure 3-12: Schematic diagram of the oxidation of Graphene using Nitric Acid

CHAPTER 4

METHODOLOGY

4.1 Experimental Procedure

The study is divided in to the following experimental procedure.

- Preparation of Poly(styrene-co-methyl methacrylate) nano composites with pristine and modified graphene.
- Microwave Irradiation of Polymer nano composites.
- Characterization of irradiated and non-irradiated Polymer nano composites using FTIR, Raman, XRD, DSC, DMA and SEM.

4.2 Polymerization of Poly (styrene-co- methyl methacrylate)

Poly (styrene-co-methyl methacrylate) P(S-co-MMA) is produced by free radical polymerization. Benzyl peroxide was used as initiator, 0.1 wt% of total volume of monomers. Reaction took place in round bottom flask equipped with magnetic stirrer at 110 ^{o}C for 5hrs under nitrogen environment (Figure 4.1). After reaction, THF (60ml per 10ml of monomer) was added in to the round bottom flask and kept for 2-4 days to dissolve the product. The dissolved polymer solution is then precipitated in excess amount of methanol and dried in oven at 40^{o}C for at least 24hrs.

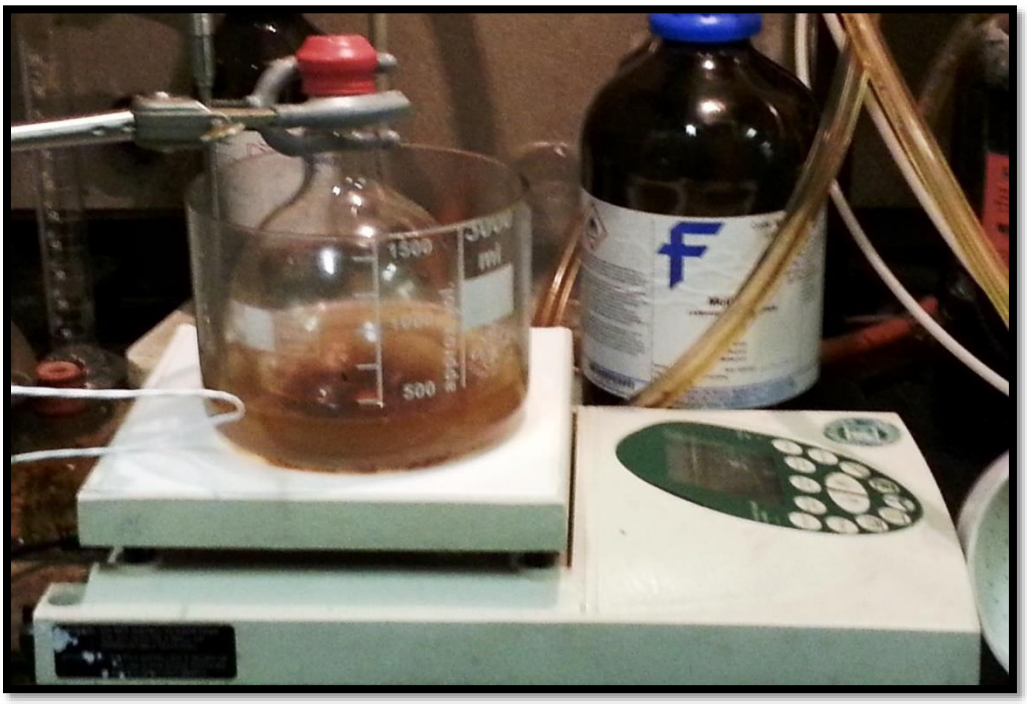

Figure 4-1: Poly (styrene-co-methyl methacrylate) polymerization experimental setup

4.3 Modification of Graphene

Chemical modification of graphene was carried out through thermal oxidation method. First 300ml of concentrated nitric acid (69%, AnalaR grade) was added to 2g of graphene (as-received) in 1000ml round bottom flask. The mixture was refluxed at 120°C for about 48 hours to produce maximum oxidation and then cooled to room temperature. The reaction mixture was diluted with 500 ml of deionized water and vacuum-filtered using 3μm porosity filter paper. The washing operation using deionized water was repeated until the pH became similar to deionized water. The final product was then dried in a vacuum oven at 100°C. Chemical modification of graphene leads to the formation of oxygen based

functionalities (carboxylic, carbonyl and hydroxyl groups) on the defects sites and sides walls of graphene (Figure 4.2) [Kannan and Marko 2005].

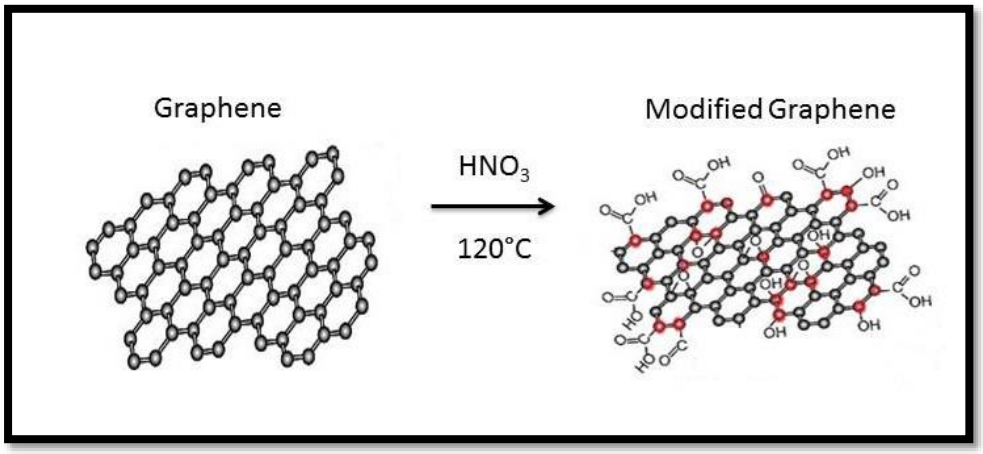

Figure 4-2: Chemical Oxidation of Graphene using Nitric Acid

4.4 Blending of Poly (styrene-methyl methacrylate) with pristine and modified graphene

P(S-co-MMA)/graphene and P(S-co-MMA)/modified graphene nanocomposites were prepared in Brabender Torque Rhemeter and Mini Blender respectively. Different percentage of Graphene(0.1-0.3wt %) was added in P(S-co-MMA) co polymer and mixed in Brabender at 200^{o}C for 10minutes at 60rpm to ensure the homogenous distribution in the matrix. Similar procedure followed for modified graphene (MG).

Figure 4-3: Brabender for melt mixing of polymer and nano filler

4.5 Preparation of Nano composites films

P(S-co-MMA)/graphene and P(S-co-MMA)/modified graphene nano composites films were obtained using laboratory hydraulic carver press, by first pre-heating them at 140°C for 2 minutes and maintain the constant temperature by applying the pressure of 7 tons for another 6minutes. The mold is cold immediately in the water bath up to 8minutes to obtain the plague.

Figure 4-4: Hydraulic Carver press for preparation of sample sheets

4.6 Microwave Irradiation Method

Microwave irradiation was carried out at frequency of 2,450MHZ at fixed power of 1000watt with different treatment time. The irradiation is carried out using domestic microwave oven with internal turnable table.

The detailed procedure is given below

- Sample of dimension (4x10x1mm) were treated at different treatment time at constant power of 1000 watt in the presence of air.

- Irradiation was performed at cycle of 60seconds in the presence of air. After each cycle the sample is then cooled to room temperature, to avoid the effect of heat on the nanocomposites.
- Total irradiation treatment time is 5, 10, 15 and 20 minutes.

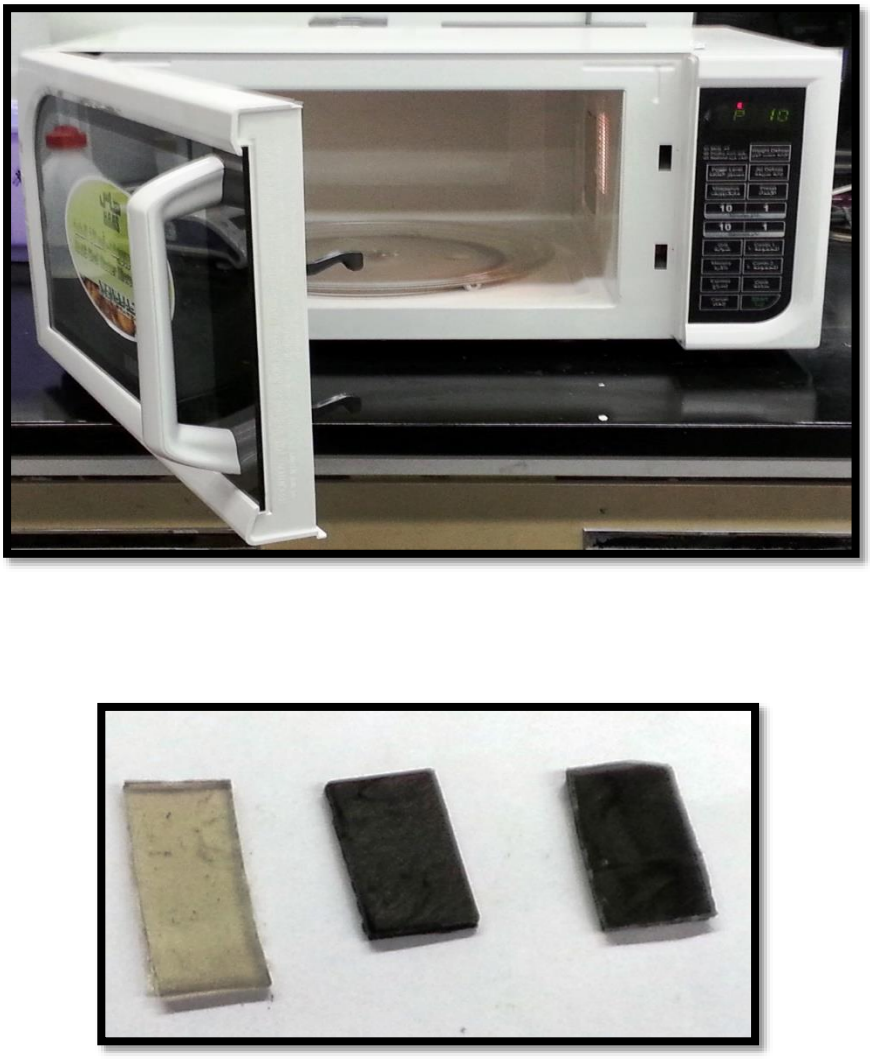

Figure 4-5: Microwave used for Irradiation and Sample films of P(st-mma) and P(st-mma)-Graphene composites

4.7 Characterization of P(S-co-MMA)/Graphene and P(S-co-MMA)/Modified Graphene

The following techniques have been employed to characterization P(S-co-MMA)/graphene and P(S-co-MMA)/modified graphene nanocomposites before and after irradiation.

- Fourier Transform Spectroscopy (FTIR)
- Raman Spectroscopy
- X-ray Diffraction (XRD)
- Scanning Electron Microscopy(SEM)
- Dynamic Mechanical Analysis(DMA)
- Differential Scanning Calorimetry (DSC)

4.7.1 Fourier Transform Spectroscopy (FTIR)

Infrared spectroscopy is (qualitative analysis) usually employed for the identification of different kinds of groups present in a material. In FTIR spectrum, each peak signifies the molecular absorption and transmission. Similar to the fingerprints, there is no other molecular structures yield the same peak in the FTIR spectrum. Moreover, the size of the peaks in the spectrum also represents the magnitude of group present in the material. Here the FTIR spectra are recorded by using Nicolet 6700 spectrometer with resolution of $4cm^{-1}$. To measure the functional group like carbonyl and hydroxyl group after irradiation of samples, the band range of 1700-1725 cm^{-1} and 3000-3450 cm^{-1} respectively are used.

Figure 4-6: FTIR Spectrophometer

4.7.2 Raman Spectroscopy

Raman Spectroscopy is a kind of vibrational spectroscopy. It interaction concerned with the absorption or emission of a phonon. Raman spectroscopy has considered being the first choice for characterization of graphene samples. The interesting features in Raman spectra of pristine graphene are G-band, D-band and 2D-band. G-band is around 1583 cm-^{1} which correspond to the E_{2g} phonon at the center of the Brillouin zone or due to the sp^2 C=C stretching vibrations. The D band (disorder mode) is around 1357 cm^{-1} correspond to the out-plane breathing mode of sp^2 atoms .D band is the indicative of the presence of the defects in graphene and is the best tool to estimate the level of defects arises in graphene. The 2D band at about 2650 cm-1 was used to resolve single layer graphene samples. The

shape, the width, and the position of this peak reveal the electronic band structure which is, in turn, reliant on on the number of layers. In this study the Raman spectra were recorded using Raman Aramis (Horiba Jobin Yvon) instrument with laser power of 0.7 mW and resolution of 473nm.

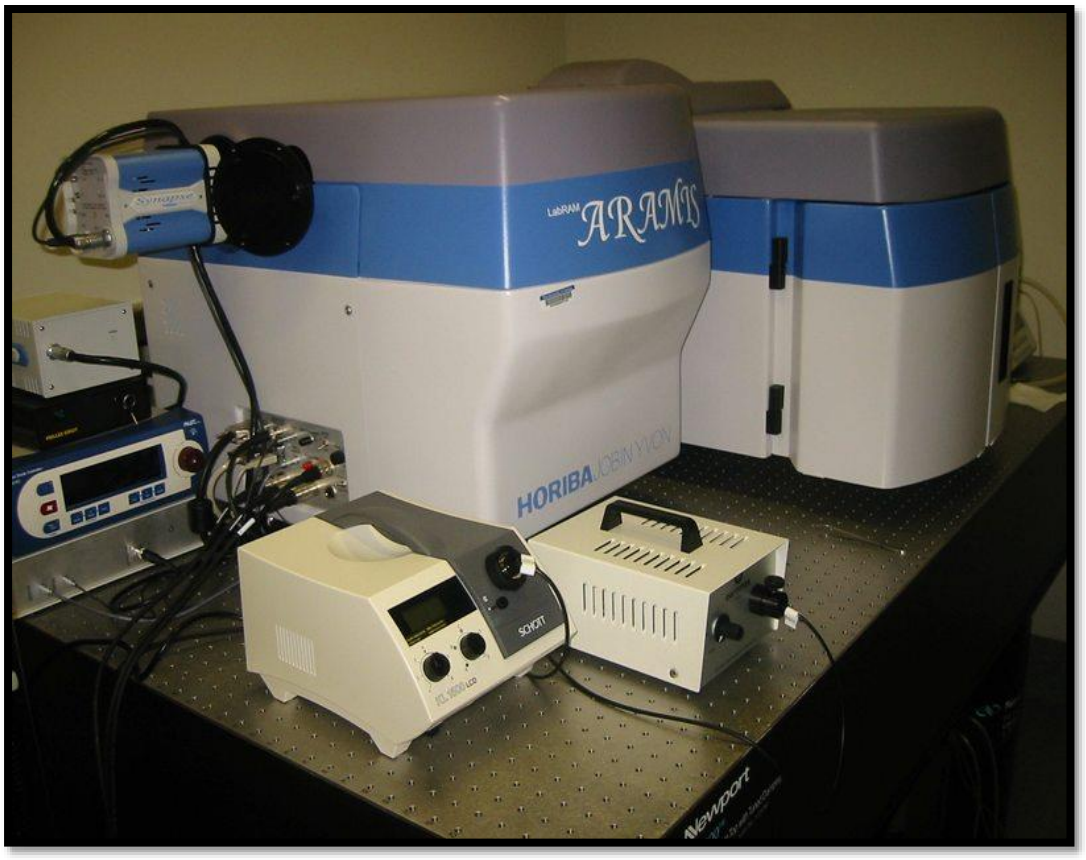

Figure 4-7: Raman Spectrophometer

4.7.3 X-ray Diffraction

X-ray diffraction (XRD) is a powerful tool used to examine various crystalline materials such as metals, polymers and crystals. It has been widely used for crystal structure determination, chemical identification of unidentified samples, lattice size measurement. In this study the

XRD studies were carried out at room temperature using D8 Advance X-Ray Instrument with wavelength of λ = 1.542 Aº and 2ϑ ranges from 20º-70º. The XRD patterns in this study are used to investigate exfoliation of graphene sheets in to the polymer matrix before and after microwave irradiation.

Figure 4-8: X-ray Diffractometer

4.7.4 Scanning Electron Microscopy (SEM)

Scanning electron microscopy a technique is widely used to investigate the morphology of the samples includes catalyst powders, polymers and their composites and the surface of the metals. Usually high magnified images are taken at some specific part of the sample

to be desired. The principle is the focusing of beam of high energy electrons to generate the variety of signals at the solid surface or powder surface. SEM assembly generally includes electron source, electron lenses, detectors and the display units. Prior to taking image samples are put in the holder and are coated with the gold. The reason is that the specimens must be electrically conductive, at least at the surface, and electrically grounded to prevent the accumulation of electrostatic charge at the surface. The electrically conducting material, deposited on the sample is either by low-vacuum sputter coating or by high-vacuum evaporation.JSM-6460LV(Jeol) was used to record SEM images in this study at magnification from 500X to 2500X with a resolution of 3.5nm and a voltage of 15KV.

Figure 4-9: Scanning Electron Microscope (SEM) system

4.7.5 Differential Scanning Calorimetry (DSC)

The glass transition temperature of the samples was determined by using DSC-Q1000, TA instrument. Samples are weighted with ± 0.5 mg accuracy. Heating-cooling-heating procedure is followed to overcome the thermal history. In first and second cycle the heating and cooling is done at a rate of 10^{o}C/min and 5^{o}C/min respectively under nitrogen environment from temperature 35^{o}C to 160^{o}C. In third cycle the heating rate is 10 ^{0}C/min which is then used for analysis of glass transition temperature (Tg).

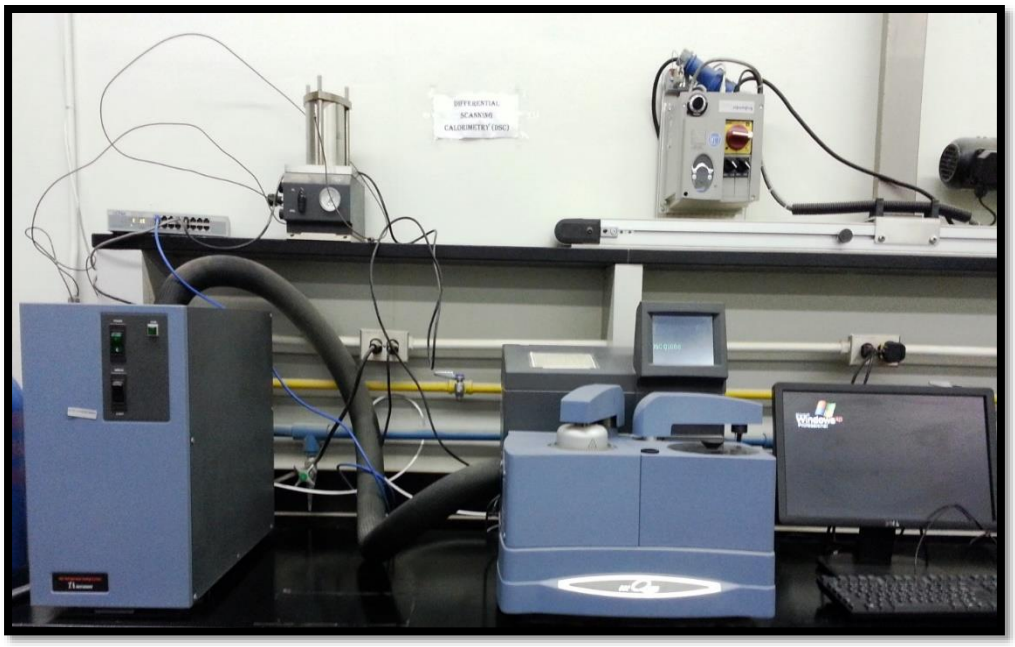

Figure 4-10: Differential Scanning Calorimetry (DSC) Setup

4.7.6 Dynamic Mechanical Analysis (DMA)

DMA is a widely used technique to examine the properties like stress, strain, storage modulus, loss modulus and tan delta of materials as a function of temperature, time, and frequency. In DMA oscillatory force is applied at a fixed frequency to the sample and

describes changes in stiffness and damping. Perkin Elmer DMA Q-800 was used in this study to examine the mechanical properties such storage modulus and tan delta of the samples before and after irradiation. Temperature ranges from 40^{o}C to 160^{o}C in the tension mode at a heating rate of 5^{o}C/min and a frequency of 1Hz. The dynamic mechanical properties are tested under nitrogen environment at a load of 5N with the average sample size 4x10x1 mm.

Figure 4-11: Dynamic Mechanical Analysis (DMA) Setup

4.7.7 Electrical Conductivity

Electrical conductivity was carried out using four probe AIT SR-2000 N/PV machine at a current of 10nA and 2V voltage.

Figure 4-12: Electrical conductivity measurement machine

CHAPTER 5

Modification of P(S-co-MMA)/Graphene Nanocomposites using Microwave Irradiation

The possible mechanism of P(S-co-MMA)/graphene nanocomposites formation via melt blending and the effect of microwave irradiation are shown in Scheme 5.1. Melt blending at high shear and high temperature can lead to attachment of the polymer chains onto the graphene platelets. The irradiation caused free radical formation on polymer chains and surface modification of graphene which eventually leads to better interaction between them.

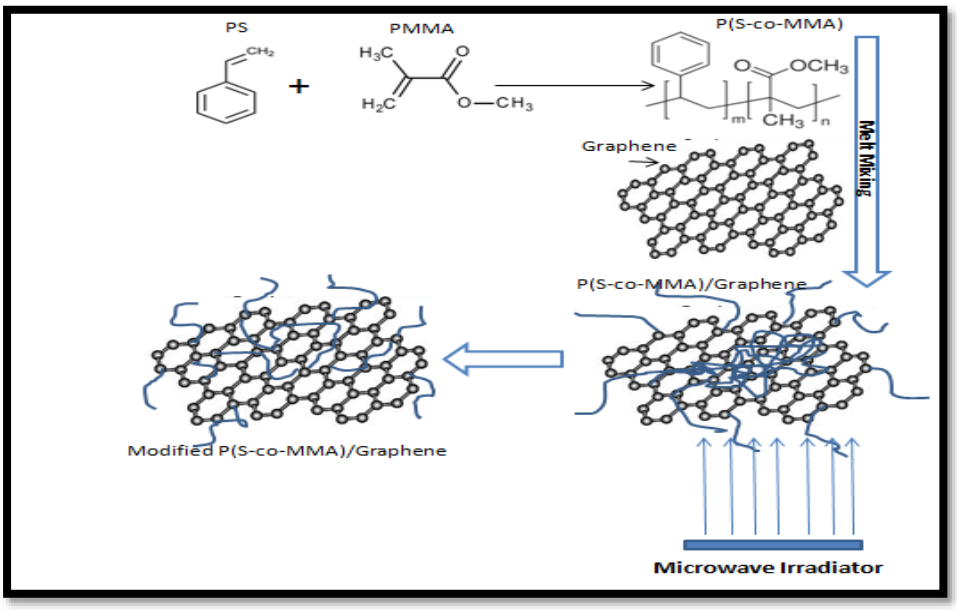

Scheme 5-1 Schematic representation of the improvement of dispersion and interaction between P(S-co-MMA) and graphene after microwave irradiation.

Table 5-1: Composition of P(S-co-MMA) and its composites

Sample Name	Copolymer Composition P(S-co-MMA)	P(S-co-MMA) content (g)	Graphene content (mg)
P(S-co-MMA)	70.6/29.4	40	0
P(S-co-MMA)/G1	70.6/29.4	40	40
P(S-co-MMA)/G3	70.6/29.4	40	120
P(S-co-MMA)/G10	70.6/29.4	40	400

5.1 Copolymer composition

The composition of P(S-co-MMA) calculated by NMR analysis.

- Formula for finding copolymer composition [Neil and Alex 2006]

$$F_{MMA} = \frac{\frac{M}{3}}{\frac{M}{3}+\frac{A}{5}}$$

$$Fs=1-F_{MMA}$$

Where,

F_{MMA} is the molar fraction of methyl methacrylate in co-polymer.

Fs is the molar fraction of styrene in co-polymer

M & A are the integrated areas for the signals designated in the spectra for $0CH_3$ (range 2.5-3.8ppm) of MMA and for aromatic H (range 6.5-7.5ppm) of styrene.

.

Table 5-2: P(S-co-MMA) polymer composition calculated form NMR spectra

Spectra	P(S-co-MMA) wt %	A	M	F_{MMA}	Fs
1	70/30	1	0.25	0.294	0.706

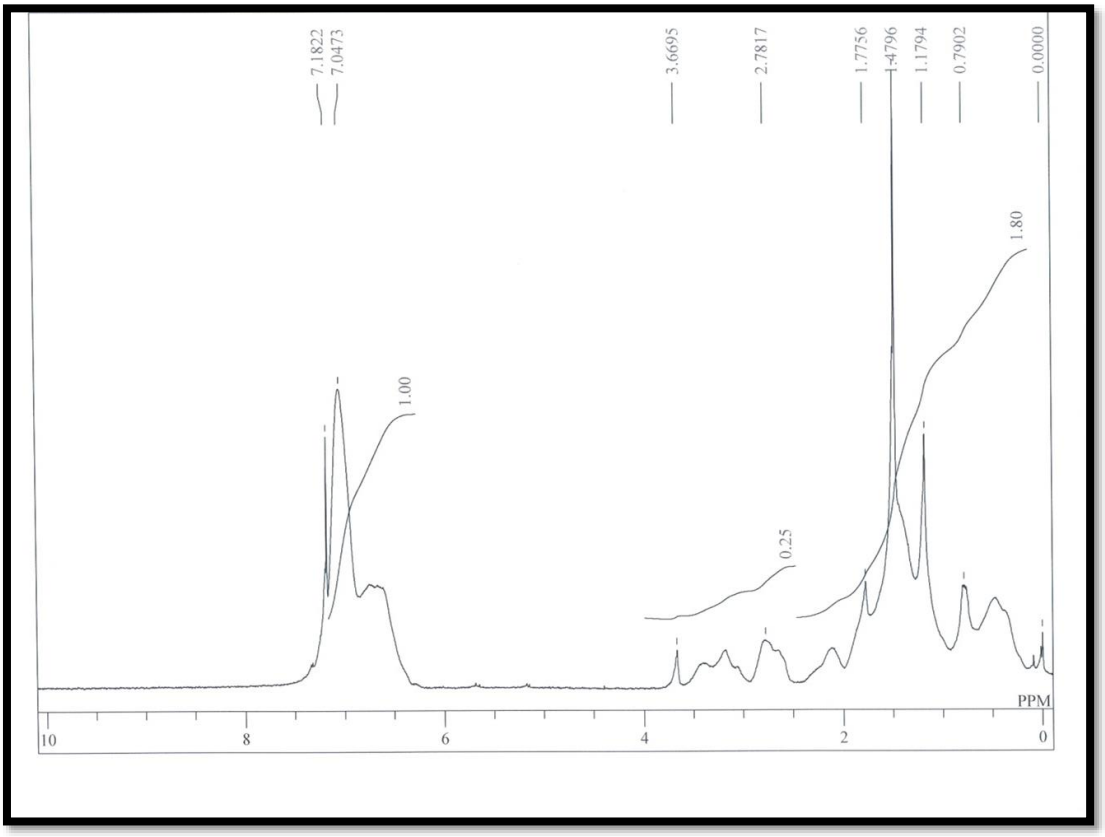

Figure 5-1: NMR spectra of P(S-co-MMA)

5.2 FTIR Analysis

Figure 5.1a and 5.1b shows the FTIR spectra of control P(S-co-MMA), and non-irradiated P(S-co-MMA)/graphene composites, and graphene. Figure 5.2 shows the FTIR spectra of irradiated P(S-co-MMA)/G1 composites. In FTIR spectra's of non-irradiated and irradiated P(S-co-MMA)/graphene composites the trend of bands are almost similar to the control P(S-co-MMA), with an increase or even disappeared in the intensity of the some absorption band after melt mixing and microwave irradiation. In Figure 5.1b, the peak in graphene spectra at 1644 cm^{-1} correspond to the C=C group of graphene. This peak of graphene shifted to lower intensity in the spectra of non-irradiated P(S-co-MMA)/graphene composites (Figure. 5.1a).

In non-irradiated P(S-co-MMA)/G1 and P(S-co-MMA)/G10 , the intensity of carbonyl stretching vibration at peak 1725 cm^{-1} was decreased to low intensity as compared to P(S-co-MMA). This may be due to the reaction of graphene with the methyl acrylate ($COOCH_3$) functionality in polymer matrix [Liang. C et al 1958]. Reduction in intensity of peak at 2917 and 3020 cm^{-1} correspond to the methylene groups was also found in spectra of non-irradiated P(S-co-MMA)/G1 and P(S-co-MMA)/G10 compared to P(S-co-MMA). This showed that the some of the copolymer chains tethered to the surface of graphene after melt mixing.

After irradiation (5 minutes), further decrease in the intensity of absorption band of carbonyl group at peak 1725 cm^{-1} was found in spectra of P(S-co-MMA)/graphene composites. This indicates more grafting of graphene with the methyl acrylate group of copolymer after 5minutes of irradiation.

At 10 minutes of irradiation, an increase in the intensity of carbonyl stretching vibrations at peak 1725cm^{-1} was found in P(S-co-MMA) and P(S-co-MMA)/graphene composites (Figure. 5.2). The enhancement in the absorption band of the carbonyl group after irradiation referred to the photo degradation of methylene group [Joao.C 2002] present in P(S-co-MMA) polymer. This results in the formation of oxygen based functionalities on exposure to microwave radiation.

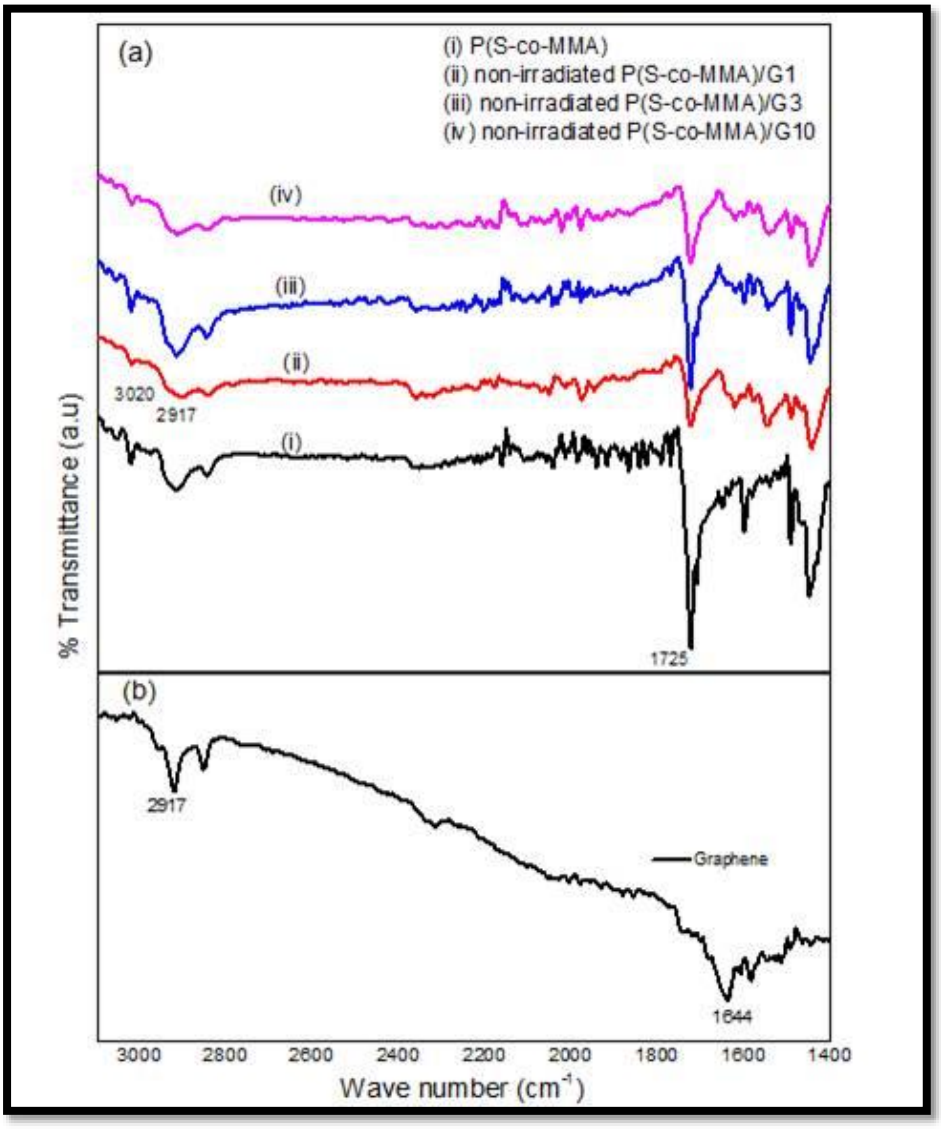

Figure 5-2: FTIR spectra of control P(S-co-MMA), non-irradiated P(S-co-MMA)/graphene composites (a) and graphene (b).

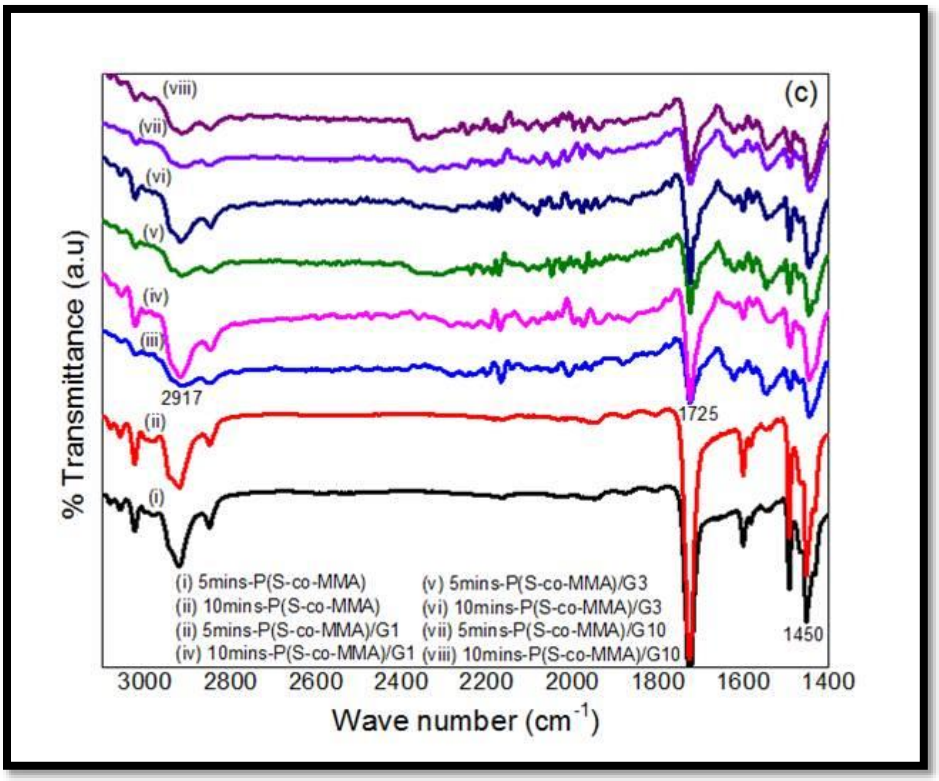

Figure 5-3: FTIR spectra's of irradiated P(S-co-MMA)/graphene composites.

5.3 Raman Analysis

Figure 5.3 shows the Raman spectra of pristine graphene, control P(S-co-MMA), non-irradiated P(S-co-MMA)/G1, and P(S-co-MMA)/G10. Figure 5.4 shows the spectra of 5 minutes irradiated P(S-co-MMA)/G1, and P(S-co-MMA)/G10 composites. The interesting features in Raman spectra of pristine graphene are G-band, D-band and 2D-band. G-band is at 1583 cm^{-1} which correspond to the E_{2g} phonon at the center of the Brillouin zone or due to the sp^2 C=C stretching vibrations [Dresselhaus. M.S et al 1995]. The D band (disorder mode) is at 1357 cm^{-1}corresponds to out-plane breathing mode of sp^2 atoms. D band is the indicative of the presence of the defects in graphene [Thomsen C and Reich S

2000, Ferrari and Robertson 2001] and is the best tool to estimate the level of defects arises in graphene. These defects present on graphene are the potential active sites to form covalent bonding with free radicals of P(S-co-MMA) polymer generated during microwave irradiation. The 2D band at around 2700cm^{-1} is used to examine the quality of graphene.

In Figure 5.3, the very low intensity of D band, and broad peak of 2D band of pristine graphene, indicates its high quality and crystalline nature [Ferrari. A.C et al 2006]. In the case of non-irradiated P(S-co-MMA)/G1 and non-irradiated P(S-co-MMA)/G10 (Figure. 5.3), the 2D band of graphene has fully disappeared and shifted to lower intensity respectively. An increase in the intensity of D band (~1357 cm^{-1}) was also observed in both non-irradiated P(S-co-MMA)/G1 and non-irradiated P(S-co-MMA)/G10. This significant decrease of the 2D band with an increase in D band intensity of non-irradiated P(S-co-MMA)/G1 indicates the formation of disorder in graphene [Patole. A.S et al 2010] and this may cause better interaction of polymer chains on the surface of graphene during melt blending. Similar trends have also found by Patole AS et al in 2012. The characteristic peak of control P(S-co-MMA) in Figure 5.3, was also seen in the Raman spectra of non-irradiated P(S-co-MMA)/G1 which was not present in the non-irradiated P(S-co-MMA)/G10 composite. This may be attributed to the fact that the graphene is poorly dispersed and weakly interacted within the polymer matrix in case of P(S-co-MMA)/G10 compared to P(S-co-MMA)/G1.This is further supported by the findings in DMA and SEM as discussed later in this paper.

After 5minutes of irradiation of P(S-co-MMA)/G1 and P(S-co-MMA)/G10 composites, it was found that the intensity level of D band and G band both increased (Fig. 5.4). The increase in the intensity of D band reveals the formation of more disorder in graphene

surface after irradiation. This shows that free radicals were generated by scission of small polymer chains and attached to the defected surface of graphene due to microwave irradiation of composites. Similar trends have also observed by McIntosh et al in 2007, when SWNT was treated with benzoyl peroxide during melt mixing. The I_D/I_G ratio of both non-irradiated P(S-co-MMA)/G1 and non-irradiated P(S-co-MMA)/G10 were significantly changed after irradiation as illustrated in Table 5.3. In addition to this, it was also observed that some characteristic peaks of control P(S-co-MMA) appeared in 5minutes irradiated P(S-co-MMA)/G10 spectra (Figure. 5.4) which was not seen in non-irradiated P(S-co-MMA)/G10. This also confirmed the improvement in interaction between graphene and the P(S-co-MMA) polymer matrix after 5minutes of microwave irradiation.

Table 5-3: ID:IG ratio of P(S-co-MMA)/graphene composite before and after irradiation.

Samples	**D peak(-1357) Intensity**	**G peak(-1583) Intensity**	**I_D/I_G**
Graphene	95.24	863.17	0.11
non-irradiated P(S-co-MMA)/G1	906.7	1125.3	0.76
non-irradiated P(S-co-MMA)/G10	1164.8	2110.2	0.79
5mins-irradiated P(S-co-MMA)/G1	1831.5	2050.1	0.89
5mins-irradiated P(S-co-MMA)/G1	1984.2	2189.7	0.90

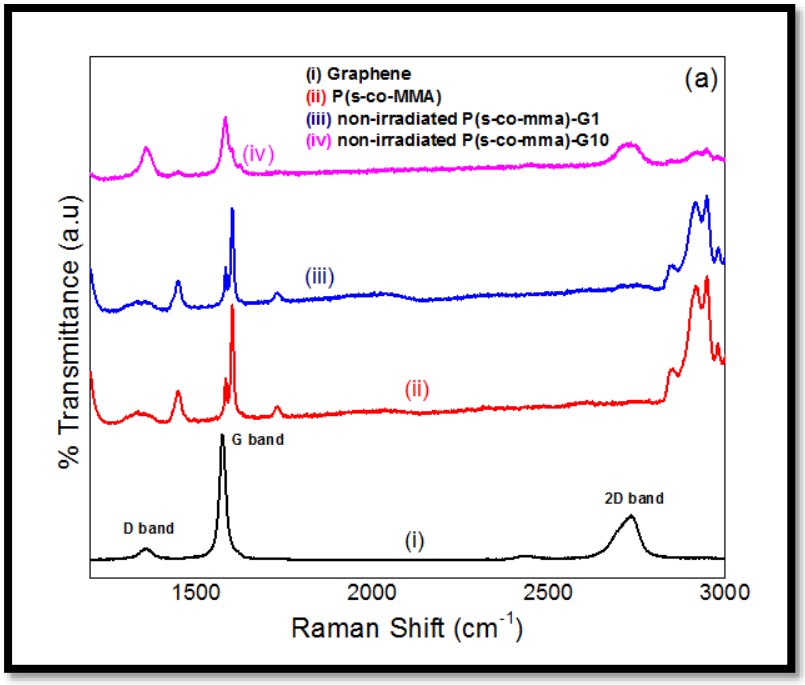

Figure 5-4: Raman spectra of graphene, control P(S-co-MMA) and non-irradiated P(S-co-MMA)/G1, P(S-co-MMA)/G10 composites

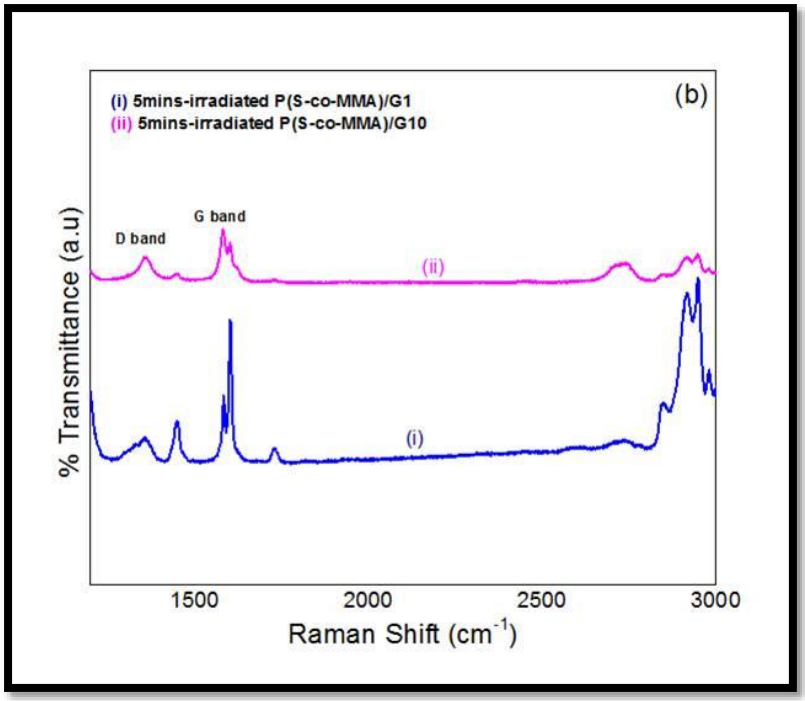

Figure 5-5: Raman spectra of irradiated P(S-co-MMA)/G1 and P(S-co-MMA)/G10 composites

5.4 XRD Analysis

Figure 5.5 displays the XRD patterns of pristine graphene, non-irradiated P(S-co-MMA)/G1, P(S-co-MMA)/G10 and 5 minutes irradiated samples of P(S-co-MMA)/G1, P(S-co-MMA)/G10 respectively. The diffraction peak of pristine graphene was observed at about $2\theta = 26.7°$ [Hua. H et al 2010]. It was found that when graphene was incorporated in P(S-co-MMA) polymer matrix via melt blending, the diffraction peak of graphene in XRD pattern of non-irradiated P(S-co-MMA)/G1and non-irradiated P(S-co-MMA)/G10 increase with the content of graphene (Figure.5.5). After 5minutes of irradiation, the diffraction peak of graphene has almost disappeared and shifted to a low intensity level in the XRD pattern of 5 minutes irradiated P(S-co-MMA)/G1 and 5 minutes irradiated P(S-co-MMA)/G10 composites respectively. This indicates the formation of more disorder in the graphene structure due to microwave irradiation evident from Raman spectra results, which act as active sites and enhanced interaction of graphene with the P(S-co-MMA) polymer matrix [Liang J 2009]. The XRD pattern clearly demonstrates that after 5 minutes of irradiation of the P(S-co-MMA)/G1 composite, the graphene is completely exfoliated in the P(S-co-MMA) polymer matrix as the diffraction peak of graphene has disappeared [Liang J et al 2009, X.S et al 2008] thereby indicating strong interfacial interaction of graphene in the P(S-co-MMA) matrix.

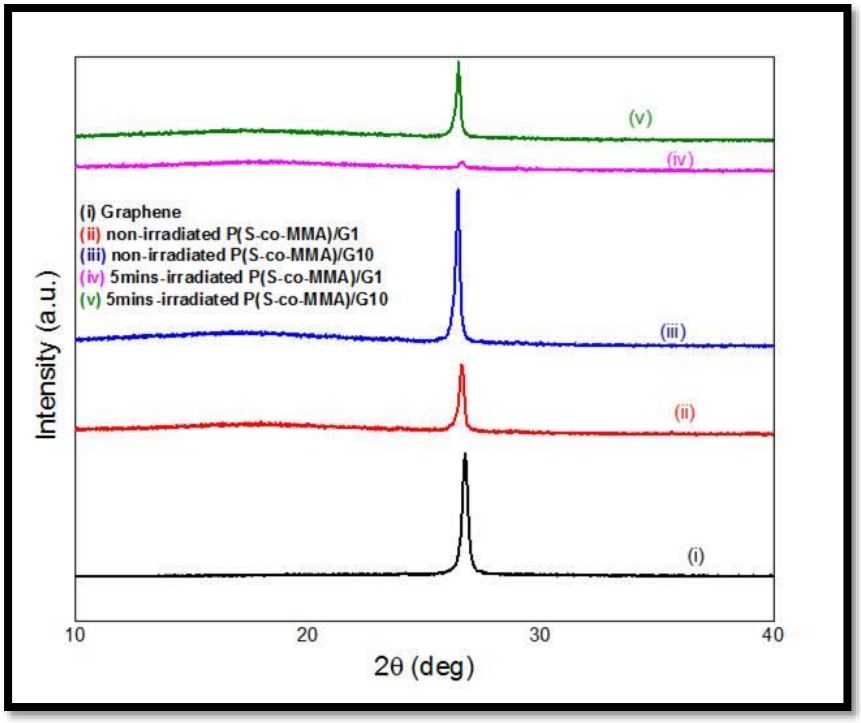

Figure 5-6: XRD patterns of graphene, non-irradiated and irradiated P(S-co-MMA)/G1 and P(S-co-MMA)/G10 composites

5.5 DMA Analysis

The mechanical properties of non-irradiated and irradiated P(S-co-MMA) and P(S-co-MMA)/graphene composites were evaluated by DMA (Table 5.4). Figure 5.4(a-b) showed the storage modulus and tan δ curves of non-irradiated and irradiated P(S-co-MMA) and P(S-co-MMA)/graphene respectively.

At a glassy state (40°C) (Figure. 5.10), the storage modulus of non-irradiated P(S-co-MMA)/G1 and non-irradiated P(S-co-MMA)/G3 composites, increased to higher values compared to the control P(S-co-MMA) polymer. This increase in storage modulus after incorporation of graphene in the P(S-co-MMA) polymer matrix is attributed to the

reinforcing effect of filler on polymer matrix. However, a decrease in the storage modulus, of about 10% was found for non-irradiated P(S-co-MMA)/G10 (Figure. 5.10) with respect to control P(S-co-MMA). This might be due to the plasticization effect of graphene agglomerate on P(S-co-MMA) at higher concentration. Similar kind of behavior was observed by Saladino. M.L et al. when incorporated silica in PMMA matrix.

The tan δ peak position (Figure. 5.10), which is the measure of glass transition temperature (T_g) has shifted from 132°C for control P(S-co-MMA) to a higher temperature of 135°C for the P(S-co-MMA)/graphene composites. This is due to the fact that the graphene platelets restrict the mobility of polymer chains and hence T_g was increased. However, the T_g did not change significantly with increasing concentration of graphene content (from 0.1 to 1 wt %) in P(S-co-MMA) matrix. This attributes to the weak interfacial interaction of graphene with polymer matrix at higher loading content.

At 5minutes of microwave irradiation of P(S-co-MMA), P(S-co-MMA)/graphene composites, the storage modulus reached to high value (Figure 5.7). For example, at 120°C after 5minutes of irradiation of P(S-co-MMA)/G1,the storage modulus was found to increase from 1002MPa to 1215MPa (a 21.25% increase compared to non-irradiated P(S-co-MMA)/G1). Similarly P(S-co-MMA)/G3 and P(S-co-MMA)/G10 composites the storage modulus at 40°C increases from 1452MPa to 1523MPa (5% increase) and from 1308 to 1710 (31% increase) after 5minutes of irradiation. An increase in storage modulus of control P(S-co-MMA) and nanocomposites after 5minutes of microwave exposure may be due to formation of cross linked network and improved polymer-filler interaction induced by microwave irradiation. This is due to the formation of free radicals on polymer chains as well as the defects produced on graphene surface [Giuseppe. C et al 2009], as

observed in FTIR and Raman spectra. This produced a stiffer and stronger polymer graphene nanocomposite. Similar results were also found in the irradiation of carbon nano-fibers [Evora M 2010]. In addition, in Figure 5.7, there is slight change or shift found on the tan δ peak and thereby slight increase in the T_g of the all P(S-co-MMA)/graphene composites after 5minutes of microwave irradiation. Increase in the tan δ peak was also detected after 5 minutes of microwave exposure in P(S-co-MMA)/G1 and P(S-co-MMA)/G10 which may be an indication of restriction in chain mobility of polymer chains, which usually happens due to the existence of graphene nano filler.

However at higher irradiation time, i.e. 10 minutes, the storage modulus of P(S-co-MMA) and all P(S-co-MMA)/graphene nanocomposites started to decrease (10.8%, 6.5%, 11.5% and 20% decrease for non-irradiated P(S-co-MMA) and P(S-co-MMA)/G1, P(S-co-MMA)/G3 and P(S-co-MMA)/G10 nanocomposites respectively). This attributes to the chain scission and photo degradation of the methyl methacrylate in P(S-co-MMA)/graphene composites (confirmed by FTIR spectra). This caused the formation of oxygen based functionalities and thus resulted in the reduction in storage modulus of copolymer and nanocomposites.

Table 5-4: Storage modulus and T_g obtained from DMA of non-irradiated and irradiated P(S-co-MMA) and P(S-co-MMA)/graphene composites.

Sample	**E (MPa) at 40°C**	**E (MPa) at 120°C**	**T_g(°C)**
control P(S-co-MMA)	1367	677	132
non-irradiated P(S-co-MMA)/G1	1663	1102	135
non-irradiated P(S-co-MMA)/G3	1452	906	134
non-irradiated P(S-co-MMA)/G10	1308	1025	135
5mins-irradiated P(S-co-MMA)	1447	820	133
5mins-irradiated P(S-co-MMA)/G1	1567	1215	135
5mins-irradiated P(S-co-MMA)/G3	1523	940	135
5mins-irradiated P(S-co-MMA)/G10	1717	1066	135
10mins-irradiated P(S-co-MMA)	1219	718	132
10mins-irradiated P(S-co-MMA)/G1	1540	1067	134
10mins-irradiated P(S-co-MMA)/G3	1285	740	134
10mins-irradiated P(S-co-MMA)/G10	1037	828	135

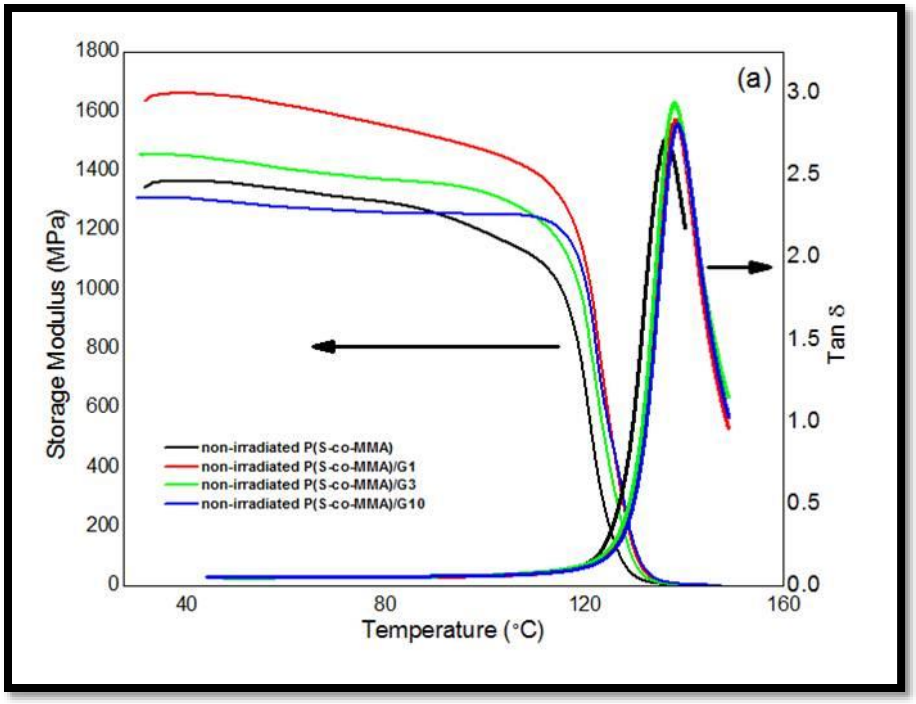

Figure 5-7: Storage modulus and tan δ curve of control P(S-co-MMA) and non-irradiated P(S-co-MMA)/graphene composites.

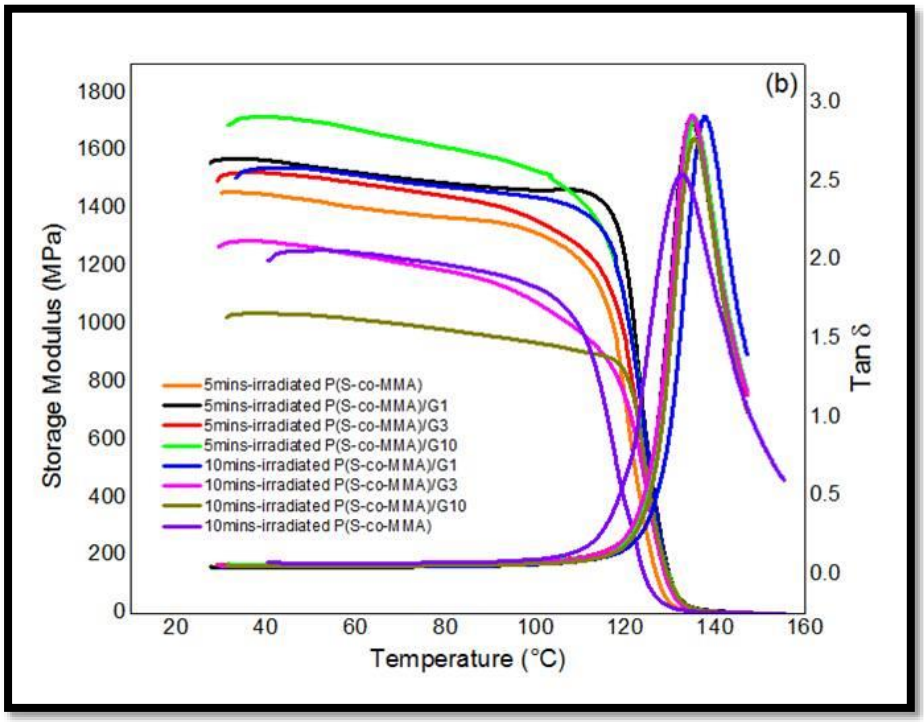

Figure 5-8: Storage modulus and tan δ curve of irradiated P(S-co-MMA) and P(S-co-MMA)/graphene composites

5.6 DSC Analysis

Figure 5.8 shows the glass transition temperature (T_g) of the control P(S-co-MMA), non-irradiated P(S-co-MMA)/graphene composites. Figure 5.9 shows the T_g of irradiated P(S-co-MMA)/graphene composites. These results are the average of three different runs with an average of ± 0.5°C. It was observed in Figure 5.8 that there was an increase of about 2.5°C of temperature in T_g of non-irradiated P(S-co-MMA)/G1, P(S-co-MMA)/G3 and P(S-co-MMA)/G10 compared to control P(S-co-MMA). This indicates that increasing the amount of graphene content on P(S-co-MMA)/graphene has no prominent effect on the glass transition temperature of composites. This is probably due to the agglomeration or weak interfacial linkage of graphene with polymer matrix at higher loading content. After 5 and 10minutes of irradiation, no prominent increase or decrease was observed in the T_g of all P(S-co-MMA)/graphene composites (Figure. 5.9).

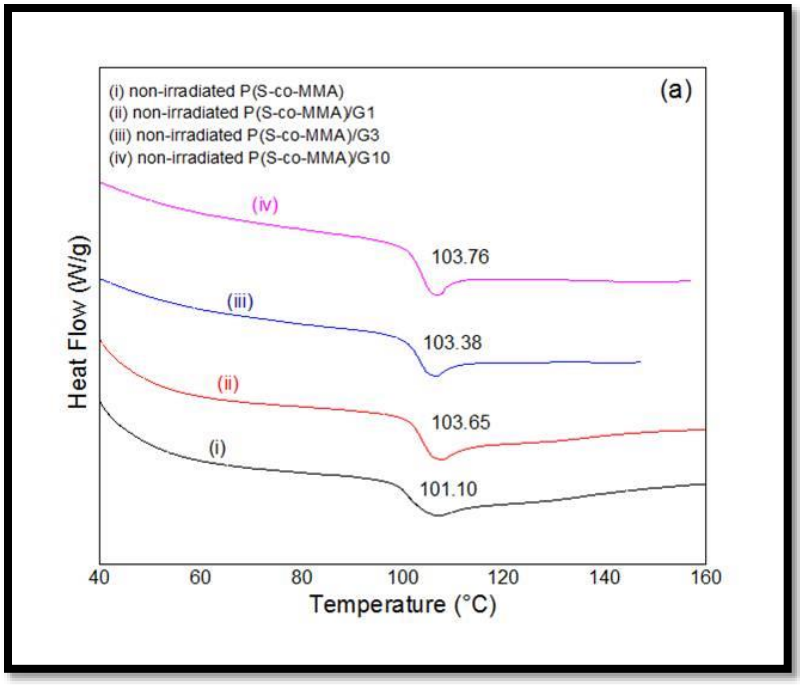

Figure 5-9: Glass transition observed from DSC for control P(S-co-MMA) and non-irradiated P(S-co-MMA)/graphene composites.

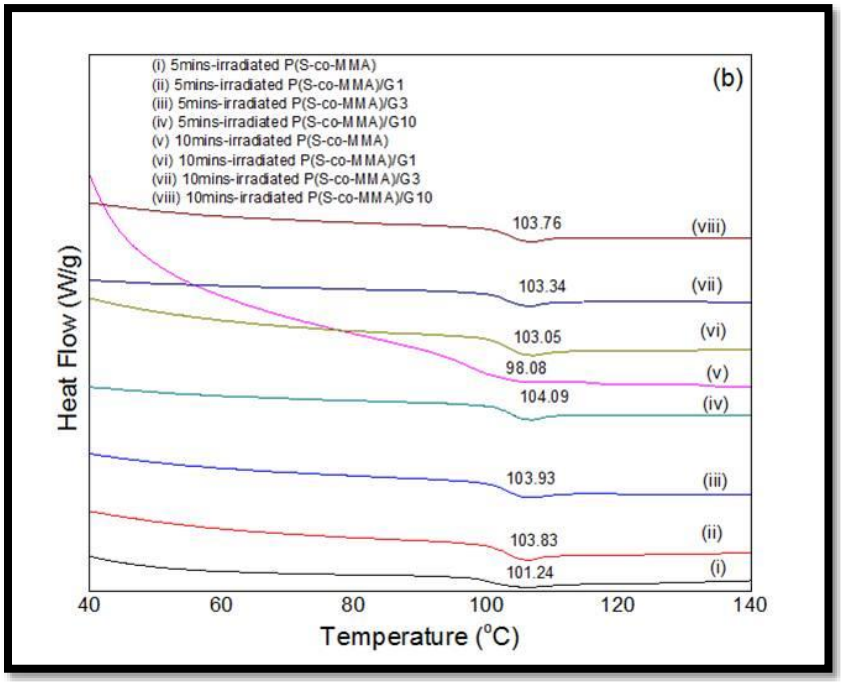

Figure 5-10: Glass transition observed from DSC of irradiated P(S-co-MMA) and P(S-co-MMA)/graphene composites.

5.7 Electrical Conductivity

The electrical conductivity of the P(S-co-MMA)/graphene composites was estimated using a four probe method. The samples P(S-co-MMA)/G1 and P(S-co-MMA)/G10 showed conductivities of $2.01x10^{-6}$ S/cm and 1.2×10^{-4} S/cm respectively which is much higher than control P(S-co-MMA) polymer matrix. The conductivity of P(S-co-MMA)/G10 was found to ascend to 1.38×10^{-3} S/cm after 5minutes of irradiation. This is due to the improved interfacial interaction of graphene in the P(S-co-MMA) polymer matrix after microwave exposure, and finally improved electron conduction.

5.8 SEM Analysis

Figure 5.10 (a-e) shows the SEM images of the non-irradiated, 5minute and 10minute irradiated sample of P(S-co-MMA)/G1 and P(S-co-MMA)/G10 respectively. In Figure 5.10a, the SEM image of non-irradiated P(S-co-MMA)/G1 shows the smooth discrete surface morphology. This can be attributed to the reinforcement effect of graphene in the P(S-co-MMA)/G1 composite. Absence of any agglomerated graphene particle shows the uniform dispersion of graphene. In Figure 5.10b, presence of some fracture and formation of rough surface after 5minutes of irradiation of P(S-co-MMA)/G1 is due to the encapsulation of polymer matrix onto the graphene. This indicates that the enhancement of interfacial interaction between graphene and polymer matrix and results in stronger P(S-co-MMA)/G1 composite. In contrast, a smoother surface of non-irradiated P(S-co-MMA)/G10 is seen in Figure 5.10d. The presence of voids and a smooth surface shows the formation of graphene agglomerates and weak adhesion between graphene and the P(S-co-

MMA) polymer matrix [Na Wang et al 2011]. However, after 5minute of irradiation of P(S-co-MMA)/G10 (Figure.5.10e), the morphology is completely changed to a rough fiber like surface. This demonstrates that the polymer chains adhered to graphene more strongly and formed an interconnecting cross linked network. This confirms that radiation facilitates the improved dispersion and grafting of graphene throughout the P(S-co-MMA)/G10 composites. This cross-linked fiber-like network of 5minutes irradiated P(S-co-MMA)/G10 composites results in improved mechanical properties and higher electrical conductivity which is also confirmed by the DMA and conductivity studies. In Figure 5.10c & 5.10f, at high irradiation time (10minutes) of P(S-co-MMA)/G1 and P(S-co-MMA)/G10 respectively, the surface becomes smoother with some cracks on it. This results in weak interaction and adhesion between the polymer matrix and the dispersed phase of graphene. The SEM image (Figure. 5.10f) also shows the fractured and degraded surface of 10 minutes irradiated P(S-co-MMA)/G10 composite, captured from another part of same sample. This confirms that at high irradiation time (i.e. 10minutes) the P(S-co-MMA) polymer started to degrade. This results in weak P(S-co-MMA)/graphene composite which is corroborated by the DMA studies in the previous section.

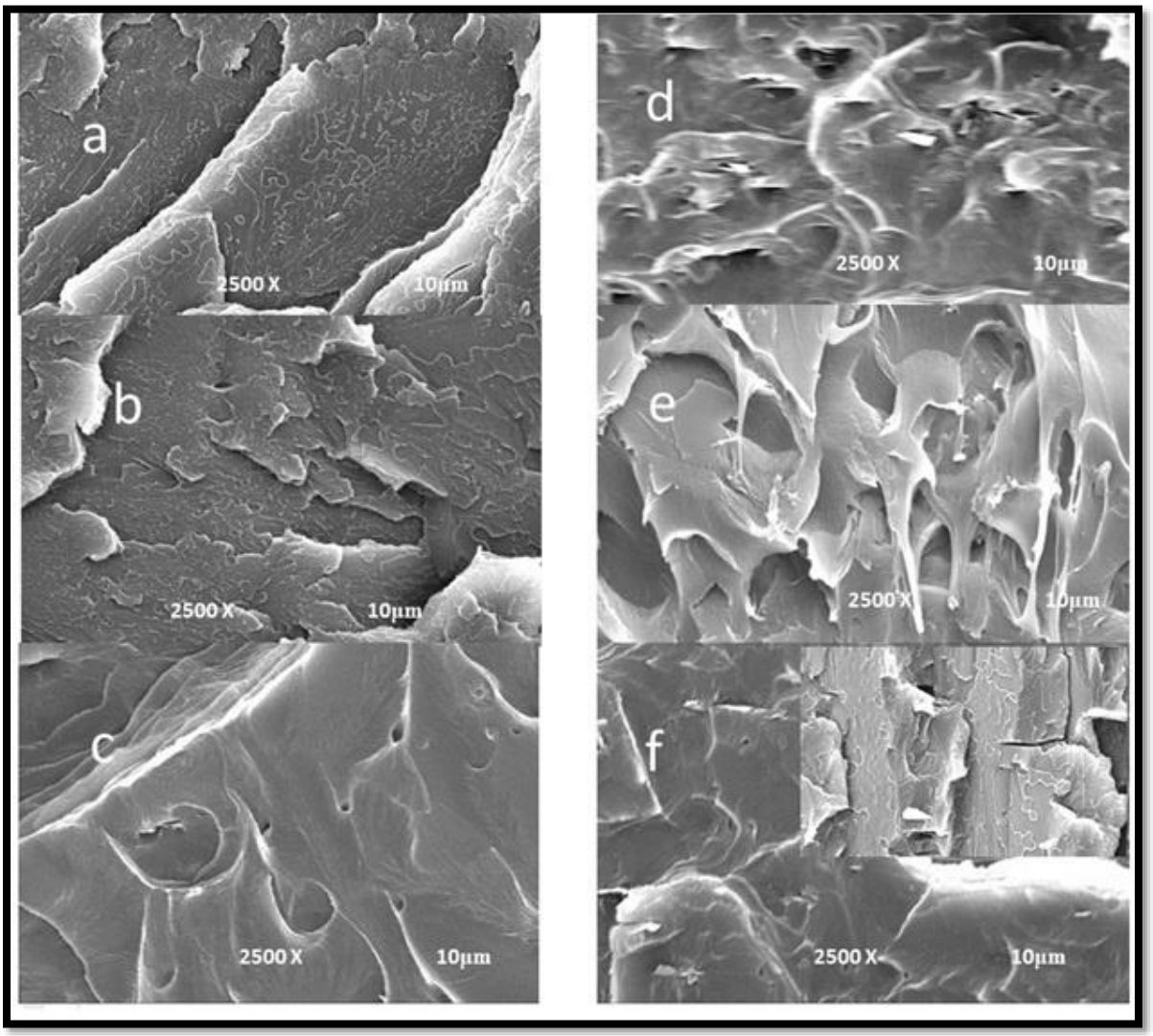

Figure 5-11: SEM images of the non-irradiated, and irradiated samples of P(S-co-MMA)/G1 (a-c), and P(S-co-MMA)/G10 (d-f) composites

CHAPTER 6

Modification of P(S-co-MMA)/Modified Graphene Nanocomposites using Microwave Irradiation

The presence of oxygen groups on the surface of modified graphene not only improved the interfacial interaction with polymer matrix during melt blending but also developed greater influence of microwave irradiation. Therefore, before and after microwave exposure, the P(S-co-MMA)/modified graphene (PMG) compared to P(S-co-MMA)/graphene (PG) nanocomposites, resulted in better improvement of the interfacial interaction between modified graphene and polymer matrices as demonstrated in Scheme 6.1. This assisted to develop cross-linked network and results in enhanced mechanical and thermal properties of PMG nanocomposites.

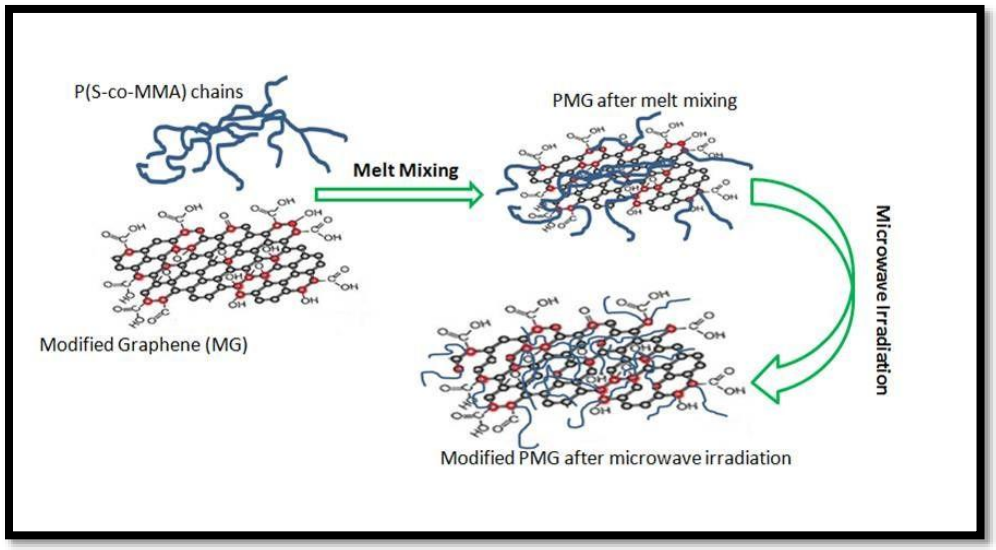

Scheme 6-1 Improvement of interaction between graphene and polymer matrices through chemical oxidation and microwave irradiation.

The composition of P(S-co-MMA) and its composites are given in Table 6.1.

Table 6-1: Composition of P(S-co-MMA) and its composites

Sample Name	Copolymer Composition P(S-co-MMA)*	P(S-co-MMA) content (g)	Graphene/Modified Graphene content (mg)	Irradiation time (minutes)
P(S-co-MMA)	70.6/29.4	6	0/0	0
PG(0)	70.6/29.4	6	6/0	0
PMG(0)	70.6/29.4	6	0/6	0
PG(5)	70.6/29.4	6	6/0	5
PMG(5)	70.6/29.4	6	0/6	5
PG(10)	70.6/29.4	6	6/0	10
PMG(10)	70.6/29.4	6	0/6	10
PG(20)	70.6/29.4	6	6/0	20
PMG(20)	70.6/29.4	6	0/6	20

**Copolymer composition is calculated using Proton-NMR.*

6.1 FTIR Analysis

The structural changes in pristine graphene (G) after chemical oxidation and nanocomposites before and after irradiation were examined using FTIR spectroscopy. In Figure 6.1 for MG spectra, the characteristics vibrations include C-O stretching peak at 1016 and 1102 cm^{-1}, the C-O-C peak at 1260, C=C stretching peak at 1620 cm^{-1} and C-OH peak at 3443cm^{-1} [Silverstein 1981]. The intensity of hydroxyl group in MG is lower than G (Fig. 6.1) which may be due to the reaction of hydroxyl group during chemical oxidation.

In Figure 6.2(b-c), the spectrum of non-irradiated and irradiated PG and PMG nanocomposites retained the similar trend except there was some change in the intensity of

the absorption band of carbonyl groups (C=C) at peak 1725 and 1770 cm^{-1} and aromatic group of styrene (C=C) at peak 1600 cm^{-1} [Silverstein 1981].

For non-irradiated and 10minutes irradiated PG nanocomposites, the C=O absorption band at peak 1725 cm^{-1} decreased to lower intensity as compared to P(S-co-MMA). This attributes to the reaction of epoxy groups of P(S-co-MMA) with the graphene surface after melt mixing and 10minutes irradiation.

In Figure 6.2c, the increasing behavior in the intensity of carbonyl group at peak 1725cm^{-1} of PMG nanocomposites up to 10 minutes irradiation indicates the carbonyl bonding between the oxygen functionalities on the structure of MG and the carbonyl group on the P(S-co-MMA) chains [Huang et al 2012]. In addition, the peak at 1600 cm^{-1} that corresponds to the aromatic vibration of P(S-co-MMA) shifted to lower intensity level in non-irradiated and 10 minutes irradiated PG and PMG nanocomposites. This may be due to the grafting of styrene chains on the graphene and MG surface.

At longer duration of microwave irradiation (20 minutes), an increase in the intensity of C=O group at peak 1725cm^{-1} of PG nanocomposites attributes the photo degradation mechanism of PG nano composite. For 20 minutes irradiated PMG nano composite, the reduction of intensity of C=O group associated with chain scission and breakage of carbonyl bond of modified graphene with P(S-co-MMA). This degradation of nanocomposites caused reduction in storage modulus and glass transition as confirmed below from the DMA, DSC and SEM analysis.

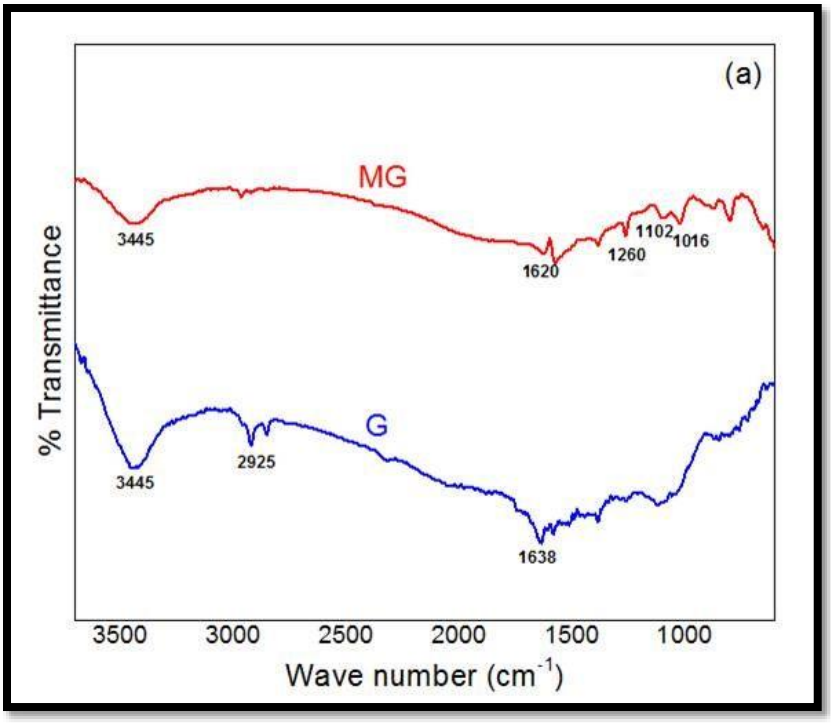

Figure 6-1: FTIR spectra of pristine and modified graphene.

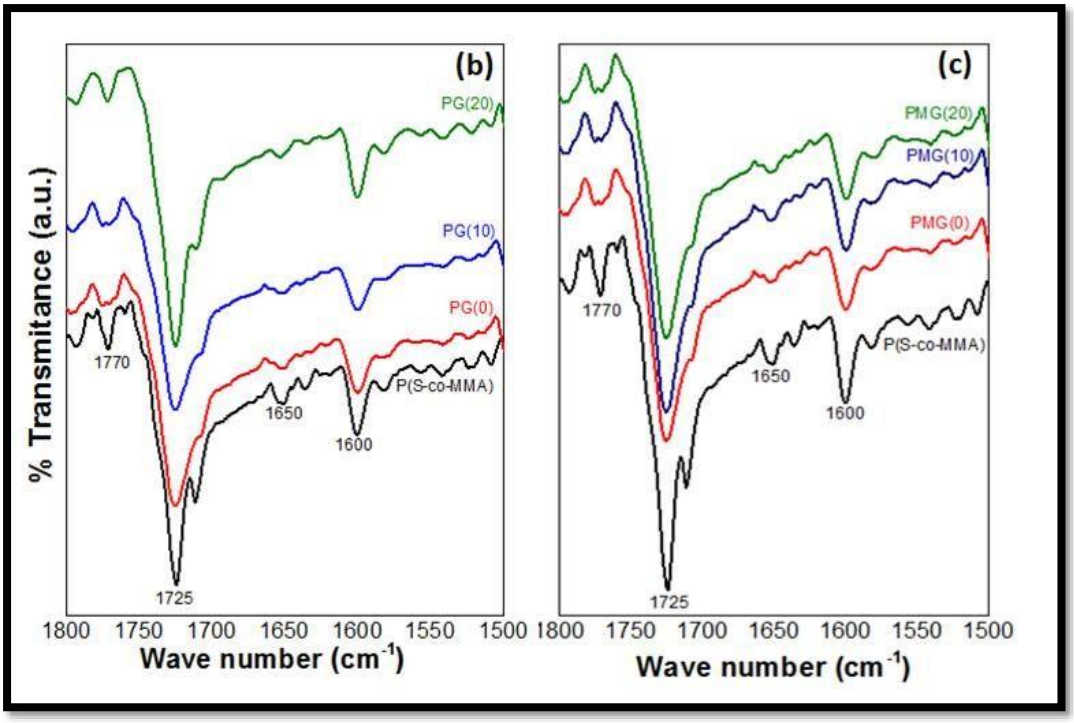

Figure 6-2: FTIR spectra's of control P(S-co-MMA) and non-irradiated and irradiated PG (b), non-irradiated and irradiated PMG (c).

6.2 Raman Analysis

Figure 6.3 and 6.4 shows the assessment of Raman spectra of (a) pristine and modified graphene, (b) non-irradiated and irradiated nanocomposites. The main features of Raman spectra are D-band, G-band, and 2D-band at peaks 1357cm^{-1}, 1583cm^{-1}, and 2700cm^{-1} respectively. The D band (disorder mode) associated to the out-plane breathing mode of sp^2 atoms. D band is the revealing of the existence of the disorder in graphene [Thomsen and Reich 2000, Ferrari and Robertson 2001] and a best tool to evaluate the level of defects appears in graphene. G-band correspond to the E_{2g} phonon at the center of the Brillouin zone or due to the sp^2 C=C stretching vibrations [Rodney et al 2007]. The presence of defects on graphene acted as potential active sites to form covalent bonds with P(S-co-MMA) polymer chains during microwave irradiation. The 2D-band is used to inspect the quality of graphene.

In Raman spectra of modified graphene (Fig. 6.3), reduction in the intensity of G-peak and 2D-peak with respect to pristine graphene was observed. This indicates the breakage of sp^2 C=C bond of graphene which results in the formation of oxygen based functionalities on the surface of graphene. Increase in the ratio of intensity of D band to the intensity of G band (I_D:I_G) of modified graphene compared to pristine graphene as shown in Table 6.2, clearly indicates the oxidation of graphene after modification [Rodney et al 2007].

In Figure 6.4, significant decrease in the intensity of G-peak and 2D-peak in non-irradiated PG and PMG was observed compared to pristine and modified graphene. This may be due to the breakage of pristine and modified graphene structure during the melt blending and leads to the attachment of P(S-co-MMA) chains on pristine and modified graphene surface.

In addition, the I_D:I_G ratio (Table 6.2) which reveals the level of defects, is higher in value of non-irradiated PMG compared to non-irradiated PG nanocomposites. This is due to the better interaction and high grafting of P(S-co-MMA) chain on the surface of modified graphene compared to pristine graphene.

In Raman spectra of 10minutes irradiated PG and PMG nanocomposites (Fig. 6.4), the increase the intensity of D band was observed. This refers to the formation of defects in pristine and modified graphene induced by irradiation. The I_D:I_G ratio of PG and PMG nanocomposites (Table 6.2) increased from 0.52 to 0.96 for PG and from 0.83 to 0.98 for PMG. This increase in the I_D:I_G ratio is associated with formation of disorder in pristine and modified graphene and was explained by Ferrari and Robertson theory [Ferrari and Robertson 2001] (that the crystalline structure of graphene transform to nano crystalline graphene. This structural modification leads to the improvement in interaction and covalent bond formation between P(S-co-MMA) chains with pristine and modified graphene. Moreover the I_D:I_G ratio, of non-irradiated and irradiated PMG is greater than the all PG nanocomposites (Table 6.2). This is attributed to the better interaction of modified graphene with P(S-co-MMA) chains than pristine graphene after melt mixing and microwave irradiation.

The Raman spectra of 20 minutes irradiated PG and PMG nanocomposites (Fig. 6.4) showed further increase in the intensity of D-peak and G-peak. This refers to more defects formation on pristine and modified graphene. The I_D:I_G ratio of 20minutes irradiated of PG and PMG showed the decreasing behavior compared to 10minutes irradiated PG and PMG nanocomposites. It means that at 20minutes of irradiation, the pristine and modified graphene structure start to transform from nano crystalline structure to amorphous phase

enlightened by Ferrari and Robertson. The formation of amorphous structure of pristine and modified graphene at 20minutes of irradiation may outcomes weakening the interfacial interaction with P(S-co-MMA) chains and hence resulted in reduction in mechanical and thermal properties of the nanocomposites as discussed later in this article. This is also in conformity with the results obtained from DMA and DSC analysis.

Table 6-2: ID:IG ratio of pristine and modified graphene, and non-irradiated and irradiated PG and PMG nanocomposites.

Samples	**D peak(-1357) Intensity**	**G peak(-1583) Intensity**	**I_D/I_G**
Graphene	92.1	863.1	0.11
Modified graphene	939.1	1177.1	0.79
PG(0)	158.7	300.1	0.52
PMG(0)	673.2	802.3	0.83
PG(10)	1413.1	1491.6	0.94
PMG(10)	2091.7	2130.9	0.98
PG(20)	2639.8	2776.8	0.95
PMG(20)	3332.5	3421.6	0.97

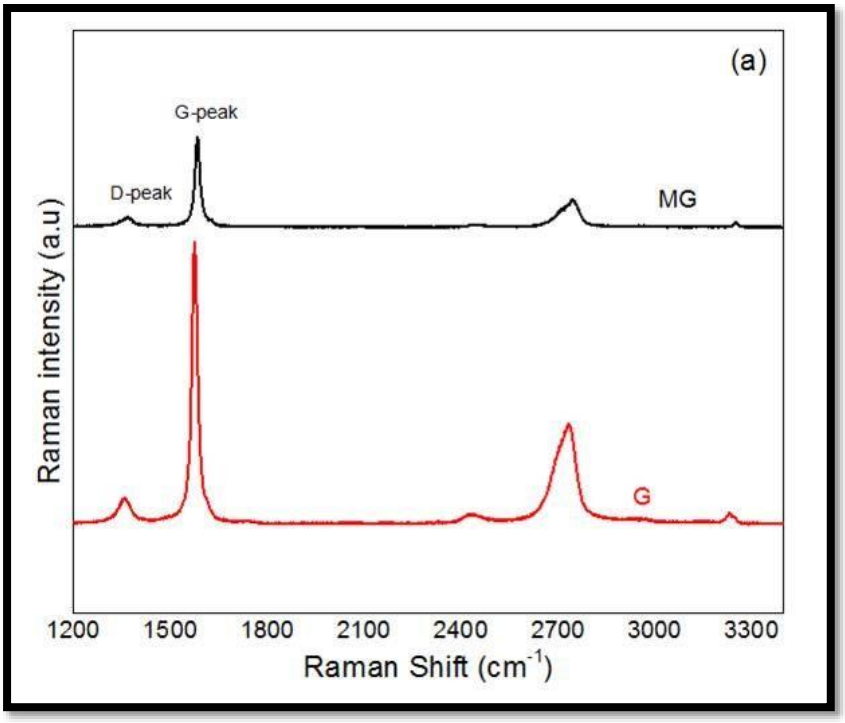

Figure 6-3: Raman spectra of pristine and modified graphene.

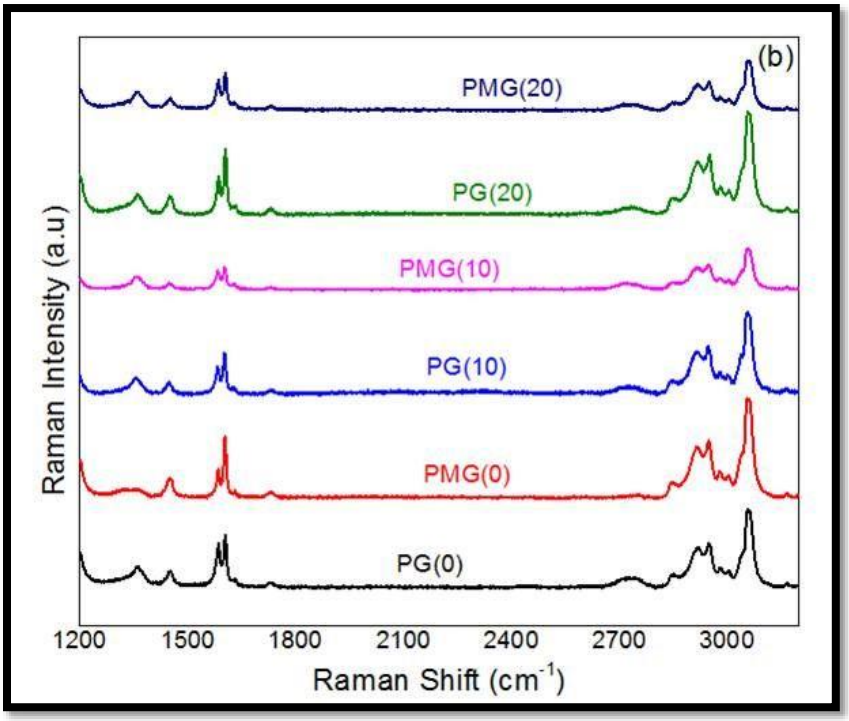

Figure 6-4: Raman spectra of non-irradiated and irradiated PG and PMG.

6.3 XRD Analysis

The changes appeared in the crystal lattice of graphene after modification and dispersion of the nano filler in the polymer matrix were evaluated using XRD patterns. Figure 6.5 display that the diffraction peak of graphene observed at 26.9° and modified graphene diffraction peak at 18.9°. The layer to layer spacing of modified graphene calculated using Bragg's equation is 0.47nm which is slightly higher than the pristine graphene (0.33nm). This refers to the presence of oxygen functionalities and moisture content [Szabo et al 2005]. Reduction of diffraction peak intensity of graphene and modified graphene is observed in the XRD patterns of non-irradiated PG and PMG (Fig. 6.5) respectively. This is attributed to the breakage of graphene and modified graphene structure and leads to the exfoliation in the P(S-co-MMA) polymer matrix after melt blending. The presence of oxygen functionalities (polar groups) on the surface of modified graphene, confirmed by FTIR, enhanced the interaction with microwave irradiation and caused better interaction of modified graphene in P(S-co-MMA) matrix. This caused further reduction of diffraction peak of modified graphene in XRD patterns of 10minutes irradiated–PMG (Fig. 6.6).

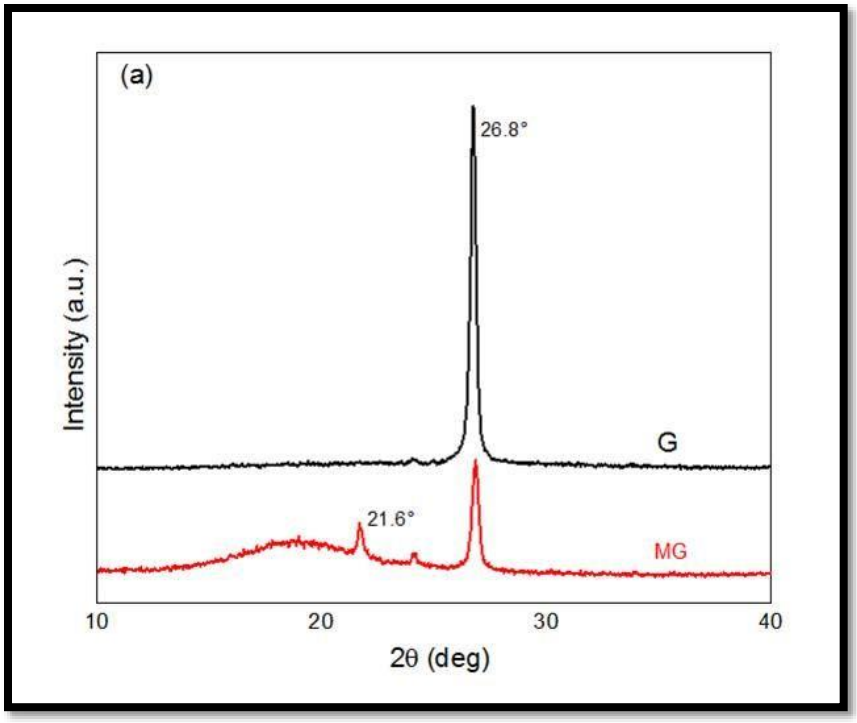

Figure 6-5: X-ray diffraction of pristine and modified graphene.

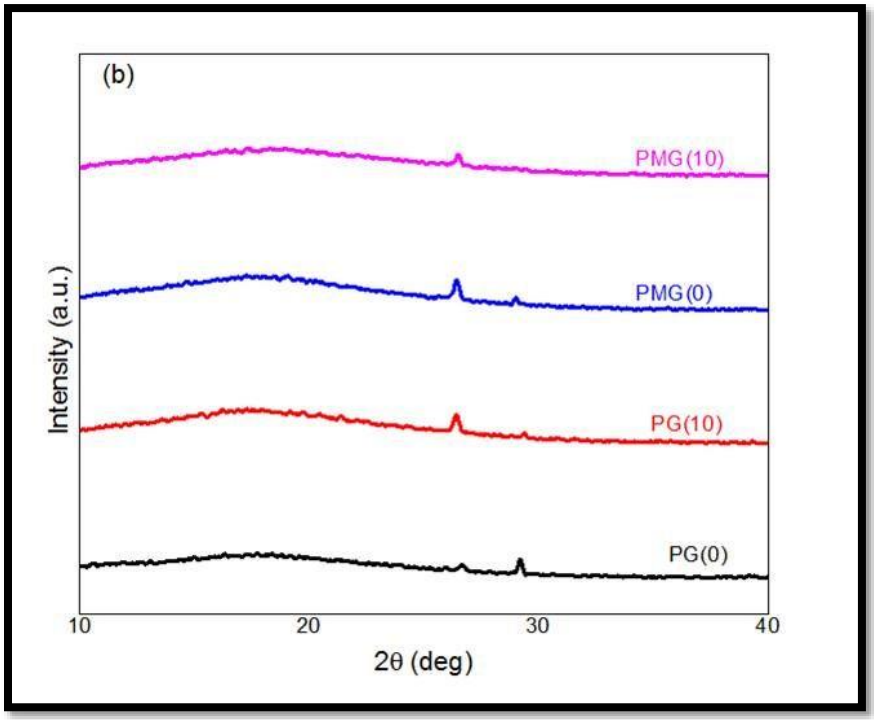

Figure 6-6: X-ray diffraction of non-irradiated and irradiated PG and PMG.

6.4 DMA Analysis

The storage modulus of control P(S-co-MMA), non-irradiated and irradiated PG and PMG nanocomposites were evaluated using DMA (Table 6.3). After the addition of graphene or modified graphene in P(S-co-MMA) polymer matrix via melt blending, the mechanical properties of both PG and PMG nanocomposites enhanced compared to control P(S-co-MMA). For example, incorporation of 0.1 wt% graphene and modified graphene in PG and PMG resulted in an increase of storage modulus (at 40°C) of about 26 % and 38 % respectively compared to control P(S-co-MMA).

Upon exposure to microwave radiation, significant improvement in storage modulus was achieved in both PG and PMG nanocomposites. At 10minutes irradiation of the nanocomposites, the storage modulus (at 40°C) increased from 1462MPa to 1636MPa for PG nanocomposite and from 1603MPa to 2048MPa for PMG nanocomposite. This is about increase of 11.9% and 27.76% of storage modulus after 10 minutes of microwave irradiation (Fig. 6.8) of PG and PMG nanocomposites respectively. This enhancement in storage modulus may refers to the influence of three factors (a) intrinsic mechanical property of graphene and modified graphene (b) improvement in interaction of graphene and modified graphene in P(S-co-MMA) matrix due to structural changes by microwave irradiation which is also proven by Raman results (c) formation of covalent bonds between graphene or modified graphene with P(S-co-MMA) chains. The latter two factors (b and c) are observed stronger in case of modified graphene due to the presence of polar groups on its surface which improved the interaction of modified graphene after microwave

radiation. Therefore it results in more stronger and high storage modulus composite compared to unmodified graphene polymer nanocomposite.

The storage modulus of PG and PMG were reduced (by 23% and 20% with respect to 10 minutes irradiated samples) after a prolonged period of microwave irradiation (20 minutes) (Fig. 6.8). This is attributed to the impact of two factors. (a) Chain scission and photo degradation of the MMA in P(S-co-MMA), which leads the formation of oxygen based functionalities (b) transformation of crystalline phase of graphene and modified graphene into amorphous phase as evident from Raman results. These two factors results in lower interfacial adhesion of graphene or modified graphene with copolymer matrix and thus produces a weak polymer graphene nanocomposites.

Table 6-3: Storage modulus of PG and PMG nanocomposites before and after microwave irradiation.

Sample Name	**MPa (40°C)**	**MPa (100°C)**
control P(S-co-MMA)	1160	996
PG(0)	1462	1165
PMG(0)	1603	1382
PG(5)	1604	1198
PG(10)	1636	1169
PG(20)	1254	1025
PMG(5)	1941	1631
PMG(10)	2048	1660
PMG(20)	1628	1305

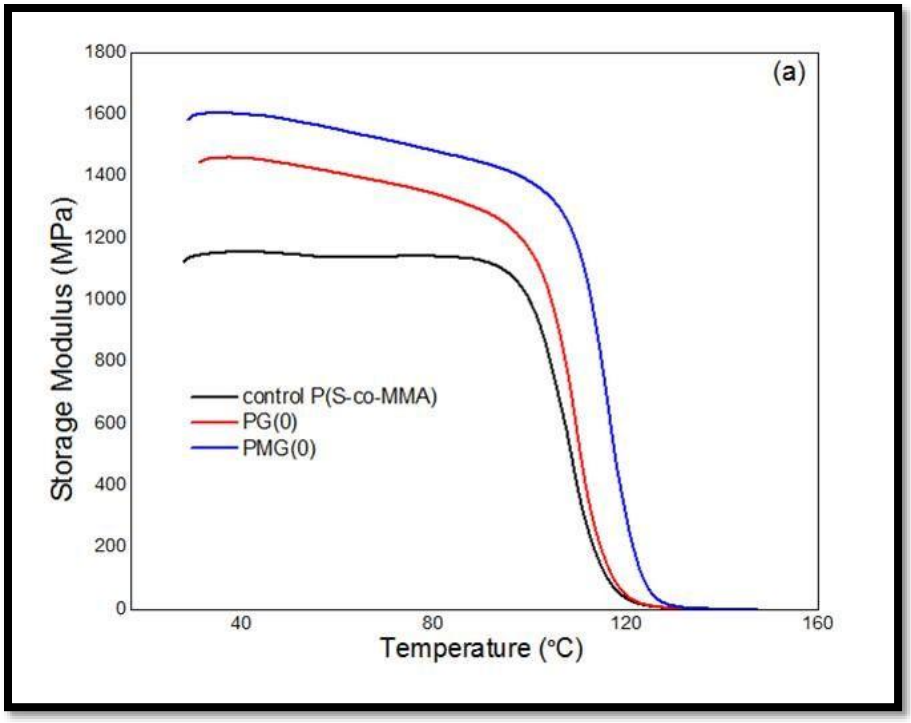

Figure 6-7: Storage modulus of control P(S-co-MMA), and non-irradiated PG and PMG.

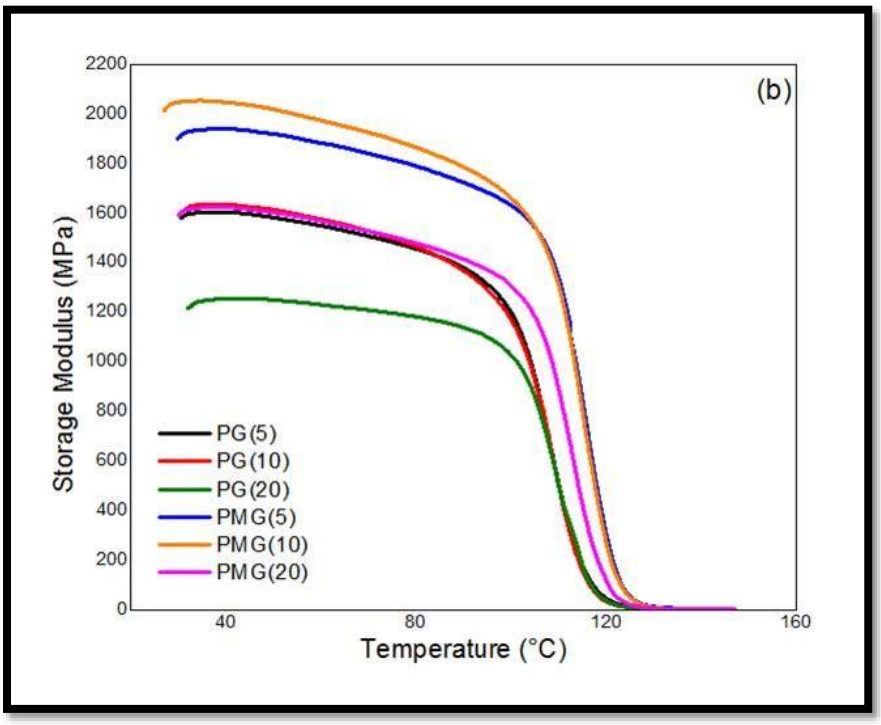

Figure 6-8: Storage modulus of irradiated PG and PMG nanocomposites.

6.5 DSC Analysis

Glass transition temperature is a macroscopic property which is the measure of relaxation behavior of polymer and polymer nano composites. The T_g of graphene based polymer composites, especially non-polar polymer were not significantly tailored compared to the polar polymers. For example, there was an approx 10°C rise of T_g of PS-composite containing 1.5 wt% of nano gold. This represents a significant improvement in T_g of PS-composite [Oh and Green 2009]. Figure 6.9 and 6.10 illustrated that there is increase of 3.2°C and 5.1°C in T_g of the nanocomposites containing 0.1wt % of G and MG respectively. The higher value of T_g of PMG compared to PG composite indicates that modified graphene has better interaction with P(S-co-MMA) matrix due to the presence of oxygen functional groups on the surface of modified graphene. An improvement in the T_g of both PG and PMG was observed on exposure to microwave irradiation up to 10minutes (i.e. increase from 93.21°C to 97.77°C (Fig. 6.9) and from 95.14°C to 100.04°C (Fig. 6.10) of PG and PMG respectively. This indicates a better interaction and covalent bonding between graphene or modified graphene with P(S-co-MMA) matrix. Degradation of PG and PMG nanocomposites produced due to the breakage of polymer chains that created weak interaction between graphene and P(S-co-MMA) matrix. The degradation of polymer nanocomposites outcomes in reduction of T_g value as observed at 20 minutes of irradiation of PG and PGM nanocomposites (Fig. 6.10).

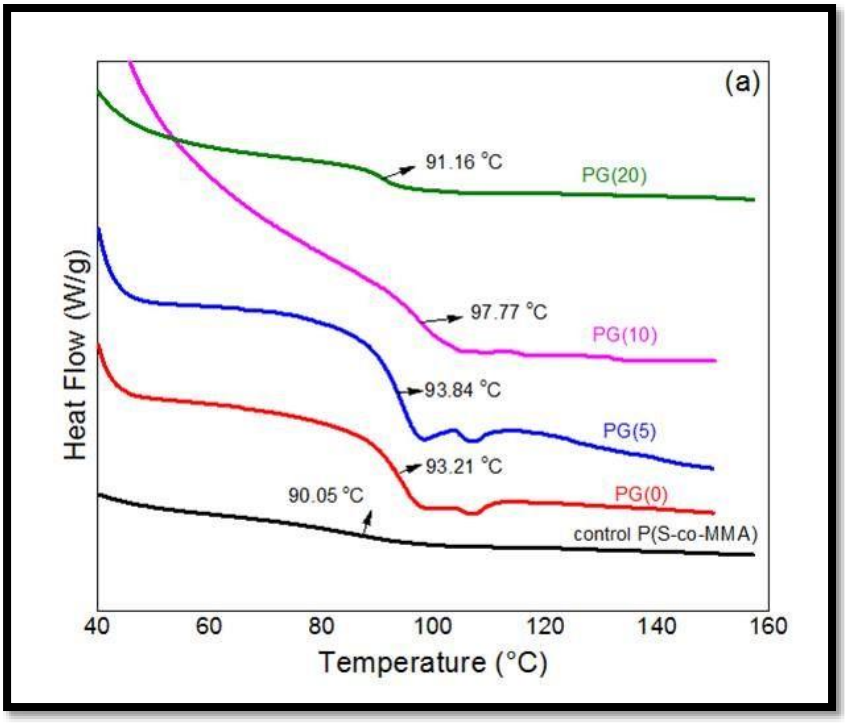

Figure 6-9: Glass transition temperature observed from DSC for control P(S-co-MMA), non-irradiated and irradiated PG.

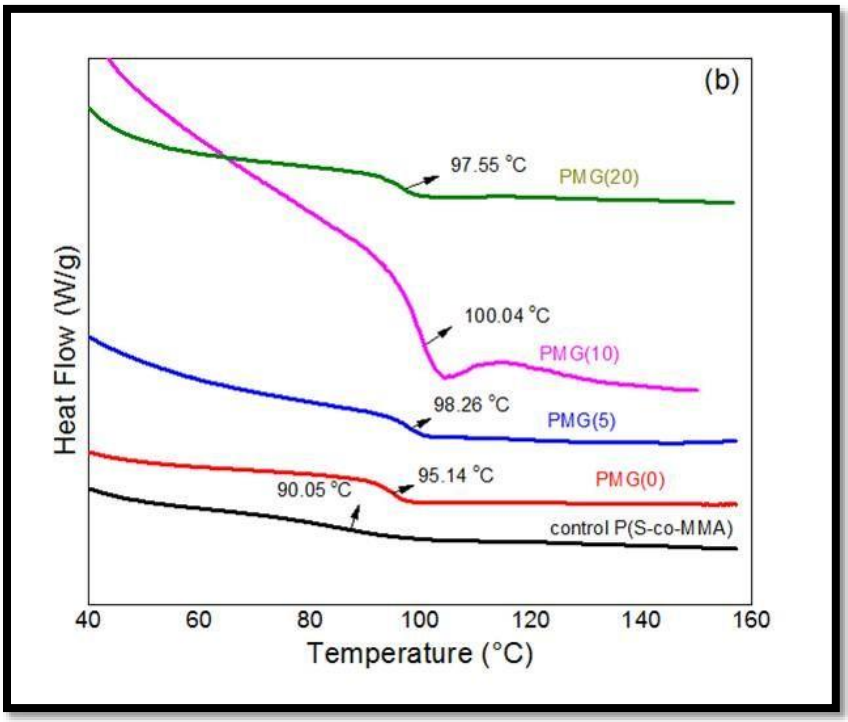

Figure 6-10: Glass transition temperature of non-irradiated and irradiated PMG.

6.6 SEM Analysis

The surface morphology of the irradiated and non-irradiated PG and PMG nanocomposites were evaluated by scanning electron microscope (SEM). The SEM image of non-irradiated PG in Figure 6.12b shows the fractured rough surface with discrete patterns compared to control P(S-co-MMA) (Fig. 6.11). This reveals the reinforcement effect of graphene in the polymer matrix. In contrast, the good interfacial interaction between modified graphene and polymer matrix results a much smoother and continuous surface morphology of PMG composite (Fig. 6.12e) with respect to control P(S-co-MMA) and non-irradiated PG nanocomposite. This attribute to the higher mechanical and thermal properties of PMG nanocomposite compared to PG nanocomposite. The rough surface of PG nanocomposite (Fig. 6.12b) also revealed the low interfacial interaction between graphene and polymer matrix.

The interaction between graphene and polymer matrix was improved on exposure to microwave irradiation for 10minutes (Fig. 6.12c). . This has changed the rough and discrete surface in to smooth and continuous surface that resembles to the non-irradiated PGM nanocomposite (Fig. 6.12e). In Figure 6.12f, the fibrous like cross-linked network structure has appeared on the PGM nanocomposite after 10minutes of irradiation. This fibrous structure strengthened the PGM nanocomposite and thereby increased storage modulus and glass transition as illustrated in Table 6.3.

In Figure 6.12d and 6.12g, breakage of polymer chains caused the formation of voids on the surface of PG and PGM nanocomposites after 20minutes of irradiation. The degradation of polymer chains at high microwave treatment made the nanocomposites

weak and reduced the storage modulus as explained from the DMA results. In addition, Figure 6.12g showed that some fibrous and cross-linked structure still remained in degraded PMG nanocomposite. This restrained the strength and resulted in higher mechanical and thermal property compared to the control P(S-co-MMA).

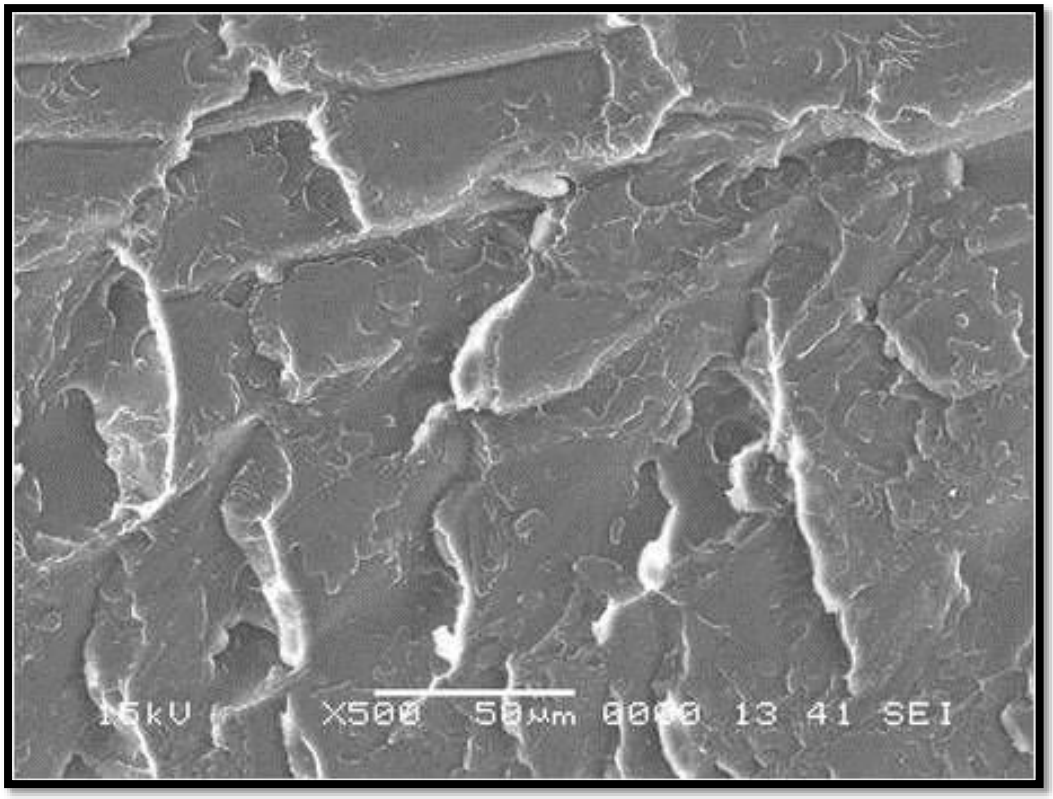

Figure 6-11: SEM images of the control P(S-co-MMA).

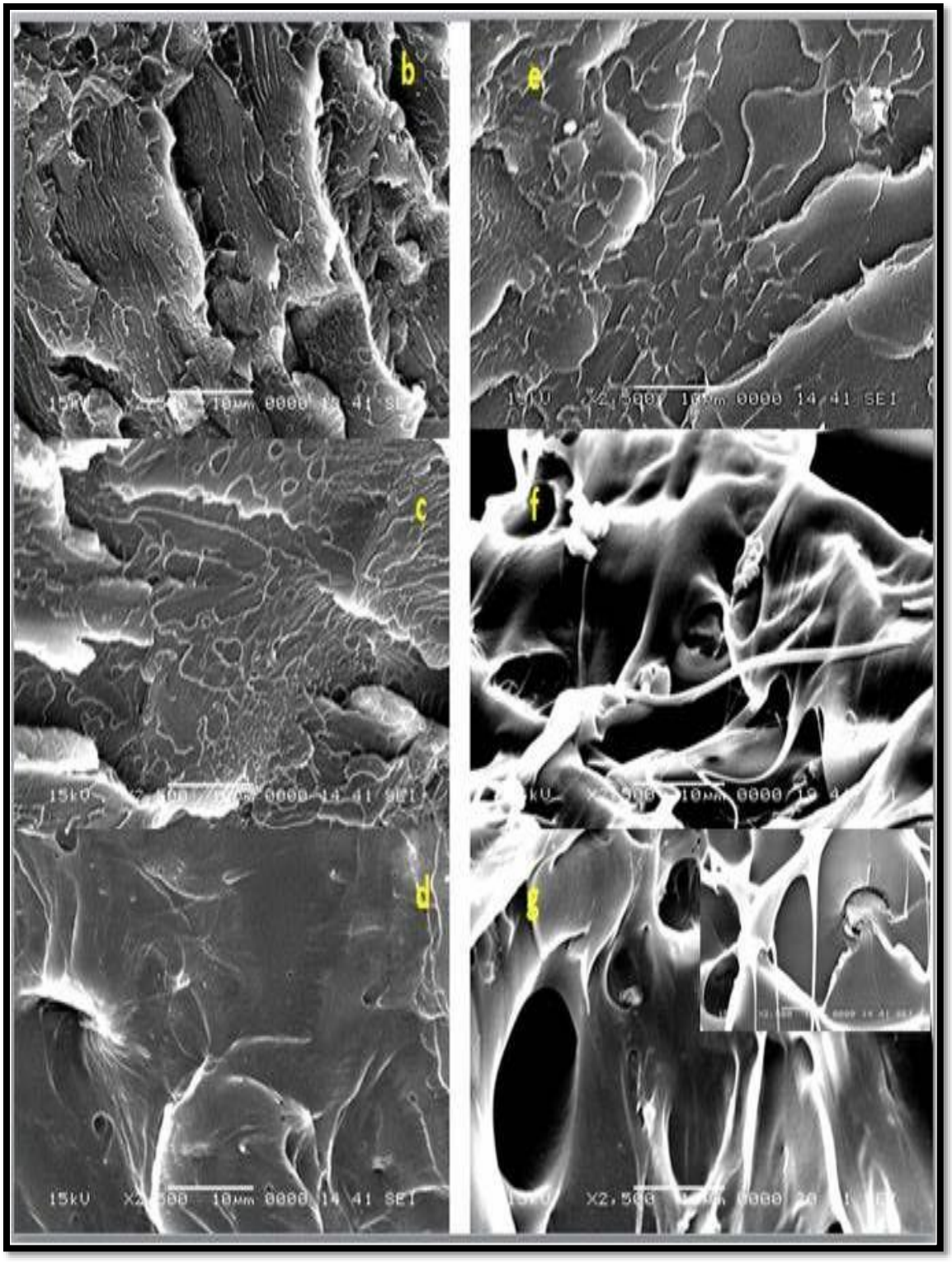

Figure 6-12: SEM images of 0,10 and 20 minutes irradiated samples of PG (b-d), and 0, 10 and 20 minutes irradiated PMG (e-g)

CHAPTER 7

CONCLUSION AND RECOMMENDATIONS

7.1 CONCLUSION

The study provide an novel easy and green method to enhance the molecular level dispersion and hence a stronger interfacial interaction between graphene and P(S-co-MMA matrix, which significantly changed the final properties of nanocomposites. Poly (styrene-co-methyl meth acrylate)/graphene and Poly (styrene-co-methyl meth acrylate)/modified graphene nanocomposites were prepared via melt mixing and the effects of graphene content, modified graphene and microwave irradiation were studied. Modification of graphene was carried out using nitric acid and resultant polymer nanocomposites were exposed to microwave radiation at different time duration to study its effect on the mechanical and thermal properties of the nanocomposites. The mechanism of formation of covalent bonds and changes in chemical structure of of graphene after modification and nanocomposites during melt blending and microwave irradiation were confirmed by FT-IR spectroscopy. Raman spectra were allowed to support the defects formation on graphene induced during modification and microwave irradiation. Investigation of storage modulus by means of DMA, has pointed out that the microwave irradiation up to 5minutes of P(S-co-MMA)/graphene nanocomposites particular for 1wt% graphene composite, is suitable for improving the interfacial interaction between the graphene and host P(S-co-MMA) matrix with significant increase in the storage modulus up to 38%. However modified

graphene develops better interfacial interaction with copolymer matrix and microwave radiation compared to pristine graphene. This resulted in higher dispersion and mechanical properties and better thermal stability of the nanocomposites. Microwave irradiation up to 10minutes of P(S-co-MMA)/modified graphene nano composite results in 27.6% increase of storage modulus which is greater than that of 10minutes irradiated P(S-co-MMA)/graphene nano composite's storage modulus (11.9% increase). The better improvement of properties of PMG compared to PG nano composites after melt blending and microwave irradiation (10minutes) is due to the presence of oxygen based functionalities on the surface of modified graphene.

Conversely at higher irradiation (10minutes for P(S-co-MMA)/graphene and 20minutes for P(S-co-MMA)/modified graphene), the chain scission and photo degradation of the host P(S-co-MMA) polymer chains in polymer nanocomposites leads to reduction in mechanical and thermal properties of the nanocomposites. This is also confirmed from the rough damaged surface as well as appearance of cracks and hole by SEM study.

7.2 RECOMMENDATIONS

The following recommendations can be considered for future work.

- Effects of different parameters of microwave radiation (dose, sample dimension and atmosphere) on the properties of nanocomposites need to be studied.
- Effects of the copolymer composition on the cross-linking and degradation of nanocomposites may be studied.
- More characterizations of the nanocomposites like tensile strength, hardness, molecular weight, weight loss, contact angle etc also required for detailed study.

References

Aahikarl B, DE, D. Maiti. 2000.Reclamation and recycling of waste rubber. Progress in Polymer Science 25: p909-948.

Albano, C. Reyes, J. Ichazo, M. González.2003. Mechanical, thermal and morphological behavior of the polystyrene/polypropylene (80/20) blend, irradiated with γ-rays at low doses (0–70 kGy). Polymer Degradation and Stability: p251–261.

Ali Khademhosseini, Seung Hwan Lee, Won Gu Lee. 2009.Rapid Formation of Acrylated Microstructures by Microwave-Induced Thermal Crosslinking. Macromolecules Rapid Communication: p 1382–1386.

Anjum Q, Singh N.L, A.K. Rakshit, F. Singh, V Ganesan. 2006. Ion beam modification and analysis of organometallics dispersed polymer film. Nuclear Instruments and Methods in Physics Research B: p 244, 235–238.

Archana S. Patole, Shashikant P. Patole, So-Young Jung, JiBeomYoo, JeongHo An, Tae-Ho Kim. 2012. Self assembled graphene/carbon nanotube/polystyrene hybrid nanocomposites by in situ microemulsion polymerization. European Polymer Journal48:p252–259.

Aykara T. CE, O. GuEven. 1999. UV degradation of poly(methyl methacrylate) and its vinyltriethoxysilane containing copolymers. Polymer Degradation and Stability 65: p 225-229.

Azhar A.F and Usmani A.M.2003. Polymer degradation in medical application. Boehringers Mannheim, Indianapolis, Indiana.

Balandin A.A., Ghosh S., W. Bao, I. Calizo, D. Teweldebrhan,F. Miao, C.N. Lau.2008.Superior Thermal Conductivity of Single-Layer Graphene, Nano Letters8:p902.

Bennamare B.Decossas, J.I, GagnardeC ,Vareille J C .1989. Optical Guides in CR 39 Irradiated By Ion Beams, International society for optics and photonics132:p1014.

Berger C, Song Z, Li X, Wu X, Brown N, Naud C.2006.Electronic confinement and coherence in patterned epitaxial graphene. Science312:p1191–1196.

Bibo W, Lei S, Ningning H, Qilong, T., Hongdian,Lu, Yuan H. 2011. Effect of electron beam irradiation on the mechanical and thermal properties of intumescent flame retarded ethylene-vinyl acetate copolymer/organically modified montmorillonite nanocomposites. Radiation Physics and Chemistry 80: p1275–1281.

Blake P, Brimicombe PD, Nair RR, Booth TJ, Jiang D, Schedin F. 2008.Graphene-based liquid crystal device.Nano Letters8: p1704–1708.

Bourlinos, A. B.Gournis, D.Petridis, D.Szabo, T.Szeri, A.Dekany.2003.Graphite oxide: Chemical reduction to graphite and surface modification with primary aliphatic amines and amino acids. Langmuir 19: p6050–6055.

Carlsson DJ, Garton A,Wiles DM. 1976. Macromolecules9: p695.

Carlsson DJ, Wiles DM. 1969. Macromolecules2: p587.

Caterina Soldano, Ather Mahmood, Erik Dujardin.2010.Production, properties and potential of graphene, Carbon 48: p2127–2150.

Cataldo F. 2000.A Raman study on radiation-damaged graphite by γ-rays, Carbon 38:p623.

Clean up Australia Ltd.2010.Polystyrene fact sheet. Royal exchange. NSW: Australia.

Clegg D.W, Collyer A.A.1991.Irradiation effects on Polymer. Applied Science: p383.

Compton OC, Nguyen ST.2010.Graphene oxide, highly reduced graphene oxide, and graphene: versatile building blocks for carbon-based materials. Small 6: p711-723.

Czvikovszky. T.2003.Degradation effects in Polymers. Department of polymer engineering. Hungary.

DaneeshMcIntosh,Valery N. Khabashesku, Enrique V. Barrera. 2007. Benzoyl peroxide initiated in situ functionalization, processing, and mechanical properties of single-walled carbon nanotube-polypropylene composite fibers. J PhysChem111: p1592-1600.

Dariusz Bogdal, Aleksander Prociak.2007.Microwave-Enhanced Polymer Chemistry and Technology.Wiley-Blackwell. Chapter 1: p6-17.

Desalegne, T., and Alexander, B., 2009.Modification of graphene properties due to electron-beam irradiation. AppPhysLett 94, 013101.

Dongnyu. Cai and M. Song. 2007.Preparation of fully exfoliated graphite oxide nanoplatelets in organic solvents. Journal of Material Chemistry 17: p3678–3680.

Dorranian. D, Abedini.Z, A. Hojabri, M. Ghoranneviss.2009.Structural and optical characterization of Pmma surface treated in low power nitrogen and oxygen RF plasmas, Journal of non-oxide glasses 1(3): p217–229.

D.A.Gorin, D.G.Shchukin, A.I.Mikhailov. 2005. Effect of Microwave Radiation on Polymer Microcapsules Containing Inorganic Nanoparticles. Saratov State University, Saratov: Russia.

Di Claudio.D, A.R.Phani, S.Santucci.2007.Enhanced optical properties of sol–gel derived TiO2 films using microwave irradiation. Optical Materials 30: p 279–284.

DOW. Cross-link a variety of material for improved thermal, physical and chemical properties: Online athttp://msdssearch.dow.com/PublishedLiteratureDOWCOM/dh_0045/0901b803800455a5.pdf?filepath=specialtymonomers/pdfs/noreg/503-00002.pdf&fromPage=GetDoc

Dresselhaus, M. S, Dresselhaus, G Saito.1995. Physics of carbonnanotubes.Carbon33: p925.

Dreyer RD, Park S, Bielawski CW, Ruoff RS. 2010. The chemistry of graphene oxide. Chemical Society Reviews 39: p228–40.

Eda, G. Fanchini, M. Chhowalla.2008. Large-area ultrathin films of reduced graphene oxide as a transparent and flexible electronic material, Nature Nanotechnology 3: p270–274.

Eizenberg M, Blakely J.M. 1979.Carbon monolayer phase condensation on Ni(III). Surface Science 82:p228–36.

Evora, Maria Cecilia. 2010. Effect of electron beam radiation on the Surface and bulk morphology of carbon nano fibers. ProQuest Dissertations and Theses: University of Dayton.

Fang, Y.Zhan, M.Wang. 2001. The status of recycling of waste rubber. Materials and Design 22:p123.

Ferrari A.C, Robertson J.2000. Interpretation of Raman spectra of disordered and amorphous carbon. Physical Review B 61: p14095-14107.

Ferrari AC, Robertson J. 2001. Resonant raman spectroscopy of disordered, amorphous, and diamond like carbon. Phys Rev B64(7): p075414.

Ferrari AC, Meyer JC, Scardaci V, Casiraghi C, Lazzeri M, Mauri F, Piscanec S, Jiang D, Novoselov KS, Roth S, Geim AK. 2006. Raman spectrum of graphene and graphene layers. Phys Rev Lett97(18): p187401.

Frank W F X, Schosser A, Brunner S, Linke F, StrenpelTh&Eich M.1994.Nonconducting Photopolymers and Applications. International society for optics and photonics1774: p 268.

Frank IW, Tanenbaum DM, Van der Zande AM, McEuen PL. 2007.Mechanical properties of suspended graphene sheets. 51st International conference on electron, ion, and photonbeam technology and nanofabrication. American Institute ofPhysics: p. 2558–61.

Fried, J. R. 2003.Polymer science and technology, 2nd edition, Pearson Education; New Jersey.

Ide.F, Terada.H.1987.Optical fiber and Optical material, Kyoritsu publication: p12-13

Geim AK, MacDonald AH. 2007. Graphene: exploring carbon flatland. Physics Today60 (8): p35–41.

Geim AK, Novoselov KS.2007. The rise of graphene.Nature Materials 6: p183-191.

Geng, Y, Wang, S. J, Kim, J.K. J. 2009.Preparation of graphite nano platelets and graphene sheets. Colloid Interface Science 336: p592–598.

Giuseppe Compagnini, FilippoGiannazzo, SushantSonde, Vito Raineri, Emanuele Rimini. 2009. Ion irradiation and defect formation in single layer graphene. Carbon 47: p3201 – 3207.

Graphene research centre, Graphene. Online at http://graphene.nus.edu.sg/content/graphene.

Gueven.O.2004.An overview of current developments in applied radiation chemistry of polymers. Hacettepe University: Turkey.

Gupta.A ,Liang.R, F.D Tsay and J.Moacanin. 1980.Characterization of a Dissociative Excited State in the Solid State: Photochemistry of Poly(methyl methacrylate), Photochemical Processes in Polymeric Systems.Macromolecules13: p1696.

Guozhang Wu, Yuchang Tang, RenxiuWeng.2010.Dispersion of nano-carbon filled polyimide composites using self-degradated low molecular poly(amic acid) as impurity-free dispersant. Polymer Degradation and Stability95:p1449-1455.

Guruvenket, S Rao, G. M Komath, Raichur, A. M. 2004.Plasma surface modification of polystyrene and polyethylene. Applied Surface Science236(1-4): p278–284.

Halina Kaczmarek, Ma_gorzata S wic, catek, AlinaKamin, ska.2004.Modification of polystyrene and poly(vinyl chloride) for the purpose of obtaining packaging materials degradable in the natural environment. Polymer Degradation and Stability 83: p35–45.

Hu, H, Wang X, Wang J, Wan L, Liu F, Zheng H, Chen R, XuC. 2010. Preparation and properties of graphene nanosheets–polystyrene nanocomposites via in situ emulsion polymerization. Chemical. Physics Letters 484:p247–253.

Huang H, Ren, P, Chen, J, Zhanga, W, Ji, X, Li, Z. High barrier graphene oxide nanosheet/poly(vinyl alcohol) nanocomposite films. 2012. Journal of Membrane Science 409– 410: p 156– 163.

Hummers W. S. and Offeman R. E. 1958.Preparation of Graphitic Oxide. Journal of American Chemical Society80:p1339.

Hye, R, Hyun, S, Mi, L. 2008.Surface modification for enhancing behaviors of vascular endothelial cells onto polyurethane films by microwave-induced argon plasma. Surface & Coatings Technology 202.p 5768–5772.

Hyunwoo. K, Ahmed A.A, Christopher W.M, 2010. Graphene/polymer nanocomposites. Macromolecules 43, 6515.

http://orise.orau.gov/reacts/guide/define.htm.Radiation emergency assistance Center, Basics of radiation.

http://www.lbl.gov/MicroWorlds/ALSTool/EMSpec/EMSpec2.html. Electromagnetic spectrum

Jaleh. B, ShayeganiMadad. M, S. Habibi.2011.Evaluation of physico-chemical properties of plasma treated PS–TiO2 nanocomposites film. Surface & Coatings Technology 206: p 947–950.

Jason A. Burdick, Kristi S. Anseth.2002.Photo encapsulation of osteoblasts in injectable RGD-modified PEG hydrogels for bone tissue engineering.Biomaterials23:p 4315–4323.

Janssen W.E, Riosa A.M.1989. Non-specific cell binding characteristics of para-magnetic polystyrene microspheres used for antibody-mediated cell selection. Journal of Immunological Methods 121: p289.

Jeanne M Stellman.1998.Encyclopedia of Occupational Health and safety. Chapter 49.
Jan F. Rabek. 1996. Photo degradation of Polymers (physical characteristics and application). Chapter 3: p60-66.Springer.

Joao Carlos,Miguez Suarez, EloisaBiasotto Mano, ElisabethErmel, Da CostaMonteiro, Maria Ines, Bruno Tavares. 2002. Influence of y-Irradiation on poly(methyl methacrylate).ApplPolymSci85: p886–895.

Kaniappanand .K, S.Latha. 2011.Certain Investigations on the Formulation and Characterization of Polystyrene / Poly(methyl methacrylate) Blends. International Journal of Chemical Technology Research Vol 3. No.2: p 708-717.

Kannan B, Marko B, 2005. Chemically Functionalized Carbon Nano tubes, Small1.180-192.

Kawaguchi H. 2000. Functional polymer microspheres. Progress in Polymer Science 25: p1171.

Kenneth H Heffner.2003.Radiation induced degradation pathways for poly methyl methacrylate and Polystyrene as models for polymer behavior in space environment. PhD Dissertation: p 37. Department of chemical, University of south Florida, USA.

Kim H, Miura Y, Macosko CW. 2010.Graphene/polyurethane nanocomposites for improved gas barrier and electrical conductivity. Chemical Materials 22: p3441-50.

Klaumiinzer. S, Zhu Q.Q, W. Schnabel, G Schumacher.1996.Ion-beam-induced crosslinking of polystyrene still an unsolved puzzle. Nuclear Institute and Methods in Physics Research B 116: p154-158.

K.S. Kim, Y. Zhao, H. Jang, S.Y. Lee, J.M. Kim, K.S. Kim, J.H. Ahn, P. Kim, J.Y.Choi, B.H. Hong. 2009.Large-scale pattern growth of graphene films for stretchable transparent electrodes, Nature 457: p706–710.

Kuzina S. I, Mikhailov A. I. 2010.Chain and Photo-chain Mechanisms of Photo-oxidation of Polymers. High Energy Chemistry 44:p 39–53.

Lawrence J, Li L.2001.Modification of the wettability characteristics of polymethyl methacrylate (PMMA) by means of CO2, Nd:YAG, excimer and high power diode laser radiation. Materials Science and EngineeringA303: p 142–149.

Landau LD, Lifshitz EM. 1980.Statistical physics. Part I. 3rd edition, Pergamon Press:OxfordEngland.

Lewis A Parks.2010.Radiation crosslinking of polymer,Stergenics advanced applications.
Lerf A, He H, Forster M, Klinowski J.1998. Structure of Graphite Oxide Revisited. Journalof Physical Chemistry B102:p4477–4482.

Lee C, Wei X, Kysar JW, Hone J. 2008.Measurement of the elastic properties and intrinsic strength of monolayer graphene. Science 321(5887): p385–388.

Liang. C.Y, Krimm. S.J. 1958. Infrared spectra of high polymers. VI. Polystyrene. Polym. Sci 27: p 241-254.

Liang. J, Yi Huang, Long Zhang, Yan Wang, Yanfeng Ma, TianyinGuo,Yongsheng Chen. 2009. Molecular-level dispersion of graphene into Poly(vinyl alcohol) and effective reinforcement of their nanocomposites. Adv Funct Mater19: p1–6.

Li X.L, G.Y. Zhang, X.D. Bai, X.M. Sun, X.R. Wang, E. Wang, H. Dai.2008. Highly conducting graphene sheets and Langmuir-Blodgett films. Nature Nanotechnology 3:p538–542.

Lihua Zhang, DiWu, Yashao Chen, XiaoliWanga.2009.Surface modification of polymethyl methacrylate intraocular lenses by plasma for improvement of antithrombogenicity and transmittance. Applied Surface Science 255: p 6840–6845.

McIntosh. D, Khabashesku. V.N, Barrera. E.V. 2007. Benzoyl Peroxide Initiated In Situ Composite Fibers. J. Phys. Chem 111: p 1592-1600.

Mermin ND. 1968. Crystalline order in two dimensions. Physical Reviews176: p250–254.

Ming.F, Kaigang.W, Hongbin.L, Yuliang.Y, Steven.N.2009. Covalent polymer functionalization of graphene nanosheets and mechanical properties of composites. J. Mater. Chem19: p7098–7105.

Min. Z.R, Ming. Q.Z, Yong. X.Z, Han, M.Z. Walter R, Friedrich K. 2001.Structure–property relationships of irradiation grafted nano-inorganic particle filled polypropylene composites. Polymer 42: p167–183.

Mojtaba S. Mirabedinia, Hamid Rahimia, Sh. Hamedifara.2004.Microwave irradiation of polypropylene surface: a study on wettability and adhesion. International Journal of Adhesion & Adhesives 24:p163–170.

Mu˜noz-Sandovald,Abraham G. Cano-Márquezd, Jean-Christophe Charlierb, HumbertoTerrones.2008. Graphene and graphite nanoribbons: Morphology, properties, synthesis, defects and applications. Nano Today 5: p351-372.

Nabio S V and Rangwala I J. 1989.Radiation curing of polymeric materials. edited by holes Charles E and kinstie JF, ACS Washington: p 15.

Na Wang, NaGao, Qinghong Fang, Erfan Chen. 2011. Compatibilizing effect of mesoporous fillers on the mechanical properties and morphology of polypropylene and polystyrene blend. Materials and Design32: p1222–1228

Neil T MacManus, Alex Penlidis. 2006. NMR Analysis of Butyl Acrylate /Methyl methacrylate /α-methyl styrene terpolymers. Journal of Applied polymer science 103:p 2093-2098

Narkis M. 1982.Modern Plastics 47.

Nemes-Incze P,Osvatha Z, Kamarasb K, Biro LP. 2008. Anomalies in thickness measurements of graphene and few layer graphite crystals by tapping mode atomic force microscopy. Carbon 46: p1435–1442.

Novoselov KS, Geim AK, Morozov SV, Jiang D, Zhang Y, Dubonos SV.2004.Electric field effect in atomically thin carbon films.Science306: p666–669.

Novoselov KS, Geim AK, Morozov SV, Jiang D, Katsnelson MI, Grigorieva IV. 2005. Two-dimensional gas of massless Diracferm ions in graphene.Nature438 (7065): p197–200.

Novoselov, A.K. Geim, K.S ,D.C. Elias, R.R. Nair, T.M.G. Mohiuddin, S.V. Morozov, P. Blake, M.P. Halsall, A.C. Ferrari, D.W. Boukhvalov, M.I. Katsnelson.2009.Control of Graphene's Properties by Reversible Hydrogenation: Evidence for Graphane. Science 323, p610.

Oh, H.J., Green, P.F., 2009. Polymer chain dynamics and glass transition in a thermal polymer/nanoparticle mixtures. Nat. Mater 8, 139.

Olgun, G., 2004. An overview of current developments in applied radiation chemistry of polymers. Hacettepe University, Turkey.

Paramjit Singh, Rajesh Kumar, H.S Virk, Rajendra Prasad.2010.Modification of optical, chemical and structural response of poly methyl methacrylate polymer by 70MeV carbon ion irradiation. Indian Journal of Pure and Applied Physics 48.p 321-325.

Patole AS, Patole SP, Kang H, Yoo JB, Kim TH, Ahn JH. 2010. A facile approach to the fabrication of graphene/polystyrene nanocomposites by in situ microemulsion polymerization. Journal of Colloid Interface Science 350: p530–537.

Patole. A.S, Patole. S.P, Jung. S.Y, Yoo. J.B, An. J.H, Kim. T.H. 2012. Self assembled graphene/carbon nanotube/polystyrene hybrid nanocomposite by in situ microemulsion polymerization. European Polymer Journal 48: p 252-259

Peter A. George,Bogdan C. Donose, Justin J. Cooper-White.2009.Self-assembling polystyrene-block-poly(ethylene oxide) copolymer surface coatings: Resistance to protein and cell adhesion, Biomaterials 30: p2449-2456.

Reddy CD, Rajendran S, LiewKM. 2006. Equilibrium configuration and continuum elastic properties of finite sized graphene. Nanotechnology 17: p864–870.

Revilla J, A. El-Aissari, P. Carriere, C. Pichot.1996.Adsorption of bovine serum album onto polystyrene latex particles bearing saccharidicmoietics. Journal of Colloids Interface Science 180: p405.

Ritter U, Scharff P, Siegmund C, Dmytrenko O P, Kulish N P, Prylutskyy Y I, Belyi N M, Gubanov V A, Komarova L I, Lizunova S V, Poroshin V G, Shlapatskaya V V, Bernas H. 2006.Radiation damage to multi-walled carbon nanotubes and their Raman vibrational modes,Carbon 44: p2694-2700.

Robinson, F.K. Perkins, E.S. Snow, Z.Q. Wei, P.E. Sheehan.2008.Reduced graphene oxide molecular sensors. Nano Letters8: p 3137–3140.

Rodney S.R, Stankovich S, Dmitriy A.D, Richard D.P, Kevin, A. K, Alfred, K.,Yuanyuan, J, Yue, W, SonBinh, T.N. 2007.Synthesis of graphene-based nanosheets via chemical reduction of exfoliated graphite oxide. Carbon 45: p1558–1565.

Rodney S.R, Sungjin P, 2009. Chemical methods for the production of graphenes. Nat. Nanotechnol 4, 217.

Rodolfo M, Amadeo LVP.2009. Graphene: Surfing ripples towards new devices. Nature Nanotechnology 4: p549–550.

Sakurabayashi.Y, M. Yumoto, T. Iwao.2003.Surface Hardness Improvement of PMMA by Low Energy Ion Irradiation, Department of Electrical and Electronic Engineering, Tokyo, Japan.

Saladino M.L., T.E. Motaug, A.S. Luyt, A. Spinella, G. Nasillo, E. Caponetti, Corrigendum. 2012. The effect of silica nanoparticles on the morphology, mechanical properties and thermal degradation kinetics of PMMA. Polym Degrad Stab 97: p452.

Satyendra, K, Paramjit S, R.G, Sonkawade, Kamlendra A, Rajesh K. 2013. 60 MeV Ni ion induced modifications in nano-CdS/polystyrene composite film. Radiation Physics and Chemistry, In press 2013.

Sawatari Chie and Mastuo M.1987.Cross-Linking Effect of Polyethylene-Polypropylene Blend Films Prepared by Gelation/Crystallization from Solution, Polymer Journal 19(12): p1365.

Shen.J, Y. Hu, M. Shi, X. Lu, C. Qin, C. Li and M. Ye. 2009.Fast and Facile Preparation of Graphene Oxide and Reduced Graphene Oxide Nanoplatelets. Chemistry of Materials 21:p3514–3520.

Silverstein R.M, G.C Bassler, T.C Morrill. Spectrometric Identification of Organic Compounds. 4th Edition. New York: John Wiley and Sons, 1981.

Si Y, Samulski T. 2008.Synthesis of water soluble graphene.Nano Letters 8: p1679–1682.

Sofo J.o, Chaudhari A.S, G.D Barber.2007.Graphane: A two-dimensional hydrocarbon. Physical ReviewB75: p153401.

Spadaro G, Valenza A.2000.Influence of the irradiation parameters on the molecular modifications of an isotactic polypropylene gamma-irradiated under vacuum. Polymer Degradationand Stability67:p 449.

Stankovich S, Dikin DA, Dommett GHB, Kohlhaas KM, ZimneyEJ, Stach EA. 2006.Graphene-based composite materials.Nature442: p 282–286.

Stankovich, S, Piner, R. D, Nguyen, S. T,Ruoff, R. S. 2006.Synthesis and exfoliation of isocyanate-treated graphene oxide nanoplatelets. Carbon 44:p3342–3347

Stoller, S.J. Park, Y.W. Zhu, J.H.An, R.S. Ruoff. 2008. Graphene-based ultracapacitors. Nano Letters 8: p 3498–3502.

Szabo,T., Berkesi,O., Dekany,I., 2005.DRIFT study of deuterium-exchanged graphite oxide, Carbon 43, 3186–3189.

Tapas Kuila, Saswata Bose, ParthaKhnara, Nam Hoon Kim, Joong Hee Lee. 2011. Characterization and properties of in-situ emulsion polymerized poly(methyl methacrylate)/graphene nanocomposites. Composite Part A 42: p1856-1861.

Tamboli S M, S T Mhaske, D D Kale.2004.Crosslinked polyethylene. Indian Journal of Chemical Technology Vol. 11: p 853-864.

Teweldebrhan.D and Balandin A.A.2009.Modification of graphene properties due to electron-beam irradiation.Applied Physics Letters 94.p 013101.

Terry L. Richardson, Erik Lokensgard. 1997.Industrial Plastics: Theory and *Application*, p 473.Delmar Publishers Inc. U.S.A.

Ting, H, Jiangyou L, Minlin Z, Juan J, Xiaohui Y, Zhe L, Lin L. 2013. The effects of low power density CO2 laser irradiation on graphene properties. Applied Surface Science 273: p502– 506.

Tomokatsu Oguru, Mobara.1979.Cathode structure of magnetrons.Hitachi Ltd: US patent.

Thomsen C, Reich S. 2000. Double resonant Raman scattering in graphite. Phys Rev Lett 85(24): p5214–5227.

VaradaRajulu A, Lakshminarayana R, Reddy, K. Mohan Raju.1999.Infrared spectroscopic investigation of poly methyl methacrylate/polyvinyl chloride blend films irradiated by a 28Si ion beam. Nuclear Instrument and Methods in Physics Research B156: p195-200.

Vesel A.2010. Modification of polystyrene with a highly reactive cold oxygen plasma. Surface & Coatings Technology205: p 490–497.

Wang G, Shen X, Wang B, Yao J, Park J. 2009.Synthesis and characterization of hydrophilic and organophilic graphene nanosheets,Carbon47: p1359–64.

Wallace PR. 1947.The band theory of graphite. Physical Review 71.p622–634.

W. Cai, A.L. Moore, Y. Zhu, X. Li, S. Chen, L. Shi, R.S. Ruoff. 2010. Nano Lett. 10:p16451.

Wenfei Donga, Guangxin Chen, WanxiZhanga.2001.Radiation effects on the immiscible polymer blend of nylon1010 and high-impact strength polystyrene (II): mechanical properties and morphology. Radiation Physics and Chemistry60: p 629–635.

Wenge Zheng, Bin Shen, WentaoZhai, Cao Chen, Dingding Lu, and Jing Wang.2011.Melt Blending In situ Enhances the Interaction between Polystyrene and Graphene through π_π Stacking. ACS Applied Materials Interfaces 3.p3103–3109.

XG Science.About x-GnPGraphene Nanoplatelets. Online 30/09/2013 http://xgsciences.us/aboutxgnp.html.

X. S. Du, Z. Z. Yu, A. Dasari, J. Ma, M. S. Mo, Y. Z. Meng, Y. W. 2008. New method to prepare graphite nanocomposites. Mai Chem Mater 20: p2066.

Xu, Y. F, Liu, Z. B, Zhang, X. L, Wang, Y, Tian, J. G, Huang, Y, Ma, Y. F, Zhang, X. Y,Chen, Y. S. 2009.A graphene hybrid material covalently functionalized, limiting property, Advanced Materials 21:p1275-1279.

Yanfei, X., Zhibo, L., Xiaoliang, Z., Yan, W., Jianguo, T., Yi H., Yanfeng, M., Xiaoyan, Z.,Yongsheng, C., 2009.A Graphene Hybrid Material Covalently Functionalized with Porphyrin: Synthesis and Optical Limiting Property. Adv Mater 21,1275–1279.

Y. Xu, H. Bai, G. Lu, C. Li, G. Shi.2008.Flexible graphene films via the filtration of water-solublenoncovalent functionalized graphene sheets.Journal American Chemical Society. 130: p5856–5857.

Yoshihiko Kondo,Hirofumi Yoshikawa, KunioAwaga.2008.Preparation, Photocatalytic Activities and Dye-Sensitized Solar-Cell Performance of Submicron-Scale TiO2 Hollow Spheres.Langmuir24: p547–550.

Yoo.E, Kim.J, E. Hosono, H. Zhou, T. Kudo, I. Honma.2008.Large reversible Li storage of graphene nanosheet families for use in rechargeable lithium ion batteries. Nano Letters 8:p 2277-2282.

Yukie saito and Masatosisato.2012. Carboneous structural changes of wood produced by microwave irradiation. University of Tokyo. Japan.

Y. Yang, J. Wang, J. Zhang, J. Liu, X. Yang and H. Zhao.2009.Exfoliated Graphite Oxide Decorated by PDMAEMA Chains and Polymer Particles. Langmuir 25:p 11808–11814.

Zhang YB, Small JP, Amori MES, Kim P. 2005.Electric field modulation of galvanomagnetic properties of mesoscopic graphite. Physical Review Letters 94(17): p 176803.

Zhao, Y. F, Xiao, M.; Wang, S. J, Ge, X. C, Meng, Y. Z. 2007.Preparation and properties of electrically conductive PPS/expanded graphite nanocomposites. Composite Science Technology 67:p 2528–2534.

Zhang Z, Zhang J, Chen P, Zhang B, He J, Hu-GH. 2006. Enhanced interactions between multi-walled carbon nanotubes and polystyrene induced by melt mixing. Carbon 44(4): p 692-698

Zhu Y, Murali S, Cai W, Li X, Suk JW, Potts JR. 2010.Graphene and Graphene Oxide: Synthesis, Properties, and Applications, Advanced Materials22: p 3906-24.

Vitae

Name	:Mukarram Zubair
Nationality	:Pakistani
Date of Birth	:9/28/1984
Email	:muky22@hotmail.com
Address	:2-k, 8/4 Nazimabad No.2, Karachi, Pakistan
Academic Background	:MSc Applied Chemistry and Chemical Technology